

Doctoral (PhD) Dissertation

CAO TENG

BUDAPEST

2023



Hungarian University of Agriculture and Life Sciences

Faculty of Food Science

Department of Food Process Engineering

Doctoral (PhD)thesis

**CONTINUOUS AND CYCLIC PRODUCTION OF GALACTO-
OLIGOSACCHARIDES BY ULTRAFILTRATION-ASSISTED
ENZYME MEMBRANE REACTORS**

Cao Teng

Buda Campus

2023

The doctoral school:

Name: Doctoral School of Food Sciences

Discipline: Food Science

Head of doctoral school:


Livia Simonné Sarkadi, Professor, DSc
Hungarian University of Agriculture and Life Sciences,
Institute of Food Science and Technology

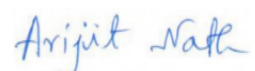
Supervisor(s):

Zoltán Kovács, Professor, PhD
Hungarian University of Agriculture and Life Sciences,
Institute of Food Science and Technology

Arijit Nath, University Research Associate, PhD
Hungarian University of Agriculture and Life Sciences,
Institute of Food Science and Technology

.....
Approval of the Head of Doctoral School


.....
Approval of the Supervisor -
Zoltán Kovács


.....
Approval of the Supervisor –
Arijit Nath

CONTENT

1. INTRODUCTION	7
2. OBJECTIVES TO ACHIEVE.....	10
3. LITERATURE REVIEW	12
3.1. Prebiotics	12
3.2. Galacto-oligosaccharides (GOS).....	12
3.3. Lactose	14
3.4. β -galactosidase	15
3.5. pH and temperature.....	17
3.6. Buffer	17
3.7. Production of GOS.....	18
3.8. UF-EMR utilizing free β -galactosidase	20
3.8.1. <i>Effect of lactose concentration and enzyme activity</i>	21
3.8.2. <i>Effect of characteristics of membrane</i>	24
3.8.3. <i>Effects of membrane module</i>	25
3.8.4. <i>Effects of operation parameters</i>	26
3.9. Mathematical models of trans-glycosylation reaction.....	29
3.9.1. <i>Kinetic models</i>	29
3.9.2. <i>Enzyme inactivation models</i>	37
4. MATERIALS AND METHODS	42
4.1. Materials	42
4.2. Enzyme activity assay	42
4.3. Modelling transgalactosylation reactions.....	42
4.4. STR	43
4.4.1. <i>Enzymatic conversion in batch fashion</i>	43
4.4.2. <i>Evaluation of process curves</i>	44
4.5. Continuous-EMR	44

4.5.1.	<i>Construction of continuous-EMR</i>	44
4.5.2.	<i>Preliminary filtration tests</i>	46
4.5.3.	<i>Short-term enzymatic conversion</i>	47
4.5.4.	<i>Long-term enzymatic conversion</i>	47
4.5.5.	<i>Performance assessment</i>	48
4.6.	<i>Cyclic-EMR</i>	48
4.6.1.	<i>Construction of cyclic-EMR</i>	48
4.6.2.	<i>Enzymatic conversion in cyclic-EMR</i>	50
4.6.3.	<i>Performance assessment</i>	50
4.7.	<i>Membrane regeneration</i>	50
4.8.	<i>HPLC</i>	51
4.9.	<i>Terminology</i>	52
5.	RESULTS AND DISCUSSION	53
5.1.	<i>Modelling transgalactosylation reactions</i>	53
5.1.1.	<i>Kinetic model development</i>	54
5.1.2.	<i>Performance simulation of continuous-EMRs</i>	57
5.1.3.	<i>Accounting for enzyme activity losses</i>	63
5.1.4.	<i>Enzyme inactivation model development</i>	66
5.2.	<i>Performance in STR</i>	67
5.3.	<i>Enzymatic conversion in continuous-EMR</i>	70
5.3.1.	<i>Preliminary filtration experiments</i>	70
5.3.2.	<i>Enzymatic conversion short-term</i>	73
5.3.3.	<i>Enzymatic conversion in long-term</i>	76
5.4.	<i>Cyclic-EMR</i>	80
5.4.1.	<i>Performance assessment in STR</i>	80
5.4.2.	<i>Enzymatic conversion in cyclic-EMR</i>	84
5.4.3.	<i>Quantification of enzyme losses</i>	87
6.	CONCLUSIONS AND RECOMMENDATIONS	90

7.	NEW SCIENTIFIC RESULTS.....	93
8.	SUMMARY	95
9.	PUBLICATIONS.....	97
10.	APPENDICES	98
	A1. References	98
	A2. Additional information	109
11.	ACKNOWLEDGEMENT	112

List of symbols:

F	enzyme activity at initial state ($\text{U}\cdot\text{kg}^{-1}$)
E_0	enzyme activity at initial state ($\text{U}\cdot\text{kg}^{-1}$)
E_1	enzyme activity at intermediate state ($\text{U}\cdot\text{kg}^{-1}$)
E_2	enzyme activity at final state ($\text{U}\cdot\text{kg}^{-1}$)
k_1	deactivation velocity coefficient ($\text{U}\cdot\text{h}^{-1}$)
α_1	the ratio of the specific activity of E_1/E_0
α_2	the ratio of the specific activity of E_2/E_0
y	relative enzyme activity (–)
k_d	enzyme deactivation constant (h^{-1})
t	operational time (h)
C_0	initial concentration of saccharides ($\text{g}\cdot\text{kg}^{-1}$)
$p_1 \times p_2$	initial reaction rate ($\text{g}\cdot\text{kg}^{-1}\cdot\text{h}^{-1}$)
c_b	bulk concentration of retained compounds ($\text{g}\cdot\text{kg}^{-1}$)
c_E	enzyme concentration in reaction liquid ($\text{U}\cdot\text{kg}^{-1}$)
c_L	lactose concentration in feed ($\text{g}\cdot\text{kg}^{-1}$)
c_{lim}	limiting concentration of retained compounds ($\text{g}\cdot\text{kg}^{-1}$)
J_{lim}	permeate flux ($\text{kg}\cdot\text{h}^{-1}\cdot\text{m}^{-2}$)
k	mass transfer coefficient ($\text{kg}\cdot\text{h}^{-1}\cdot\text{m}^{-2}$)
P	biocatalyst productivity ($\text{g}\cdot\text{U}^{-1}\cdot\text{h}^{-1}$)
q	permeate mass flow rate ($\text{kg}\cdot\text{h}^{-1}$)
Y	yield of DP3-6 (w/w%)
V	reaction liquor (L)

Abbreviations:

DP	degree of polymerization
I	inhibitors
EMR	enzymatic membrane reactor
GOS	galacto-oligosachrides
STR	stirred tank reactor
UF	ultrafiltration
GRAS	Generally Recognized As Safe
TMP	transmembrane pressure
MWCO	molecular weight cut off
RMSE	root mean squared error
SSE	sum of squares due to error
ONPG	ortho-Nitrophenyl- β -galactosidase

Greek letters

τ	residence time (h)
--------	--------------------

1. INTRODUCTION

GOS are non-digestible oligosaccharides, consisting of 2–9 units of galactosyl residues with a terminal glucose linked by glycosidic linkages, such as β -(1–2), β -(1–3), β -(1–4), and β -(1–6) (Illanes et al., 2016, Otieno, 2010). GOS belongs to prebiotic family and recognized as GRAS substances that have been widely used in a variety of purposes, including infant formulas, pharmaceuticals, and nutritional products (Lamsal, 2012, Torres et al., 2010). Numerous health benefits associated with the consumption of GOS have been proven. There has been evidence that it modulates the immune system, improves intestinal motility, prevents intestinal infections, promotes calcium absorption and utilization, and displays anticancer and anti-obesity activities. Therefore, GOS provides overall health benefit by combating wide ranges of health risk factors (Fijan, 2014, Kerry et al., 2018, Wan et al., 2019, Wilson and Whelan, 2017).

The mechanism of GOS production is mainly based on a trans-glycosylation reaction, using β -galactosidase to convert lactose into oligosaccharides with different DP. For large-scale production of GOS, lactose is derived from whey or membrane permeate of whey (Paterson, 2022, Pázmándi et al., 2018). Whey is generally considered as a by-product of industrial dairy industry which is considered as environmental pollutant. The reuse of whey may eliminate the environmental problems associated with the discharge of whey in environment and bring an economic boom in food and biopharmaceutical industries (Pires et al., 2021, Rocha and Guerra, 2020). Various sources of β -galactosidases, including bacteria, yeast and fungi, have been demonstrated their potentiality for biosynthesis of GOS (Chen et al., 2008, Pázmándi et al., 2020, Urrutia et al., 2013b). It has been reported that the characteristics of β -galactosidase depend on the source of organism and those impact the quality and quantity of the GOS yield, linkage type, and DP (Gänzle, 2012, Torres et al., 2010). Current sources of β -galactosidase for commercial production of GOS include *Aspergillus oryzae*, *Kluyveromyces lactis* and *Bacillus circulans*. Among them, β -galactosidase from *Bacillus circulans* is widely preferred by producers due to its superior thermal stability and high GOS yield (Chen and Gänzle, 2017, Park and Oh, 2010, Warmerdam et al., 2014).

Enzymatic methods for GOS production include the use of whole-cell biocatalyst (Osman et al., 2010, Yu and O'sullivan, 2014) as well as free (Cao et al., 2020, Das et al., 2011) or immobilized forms of the enzyme (Hackenhaar et al., 2021, Huerta et al., 2011). Conventionally, GOS is mainly produced by batch mode procedure using soluble β -galactosidase in a STR in industry. This operation usually involves further enzyme inactivation and a downstream enzyme removal process to obtain an enzyme-free product. Therefore, waste of expensive enzyme and complicated downstream process are major limiting factors for the production of GOS in conventional industrial process scheme (Scott et al., 2016).

Therefore, reuse of enzyme and simple downstream process for manufacturing of GOS by prolonged way have received lots of attention. Recently, several biosystems, including packed bed reactors (Albayrak and Yang, 2002, Huerta et al., 2011), membrane reactors with free enzymes (Torres and Batista-Viera, 2012, Warmerdam et al., 2014) and immobilized enzymes (Huang et al., 2020, Urrutia et al., 2013a) have grabbed attention for continuous production of GOS. Although the immobilization of biocatalyst has been intensively investigated during the last decade, the industrial application of this approach is currently limited for production of bioactive compounds. It may realize that due to immobilization of β -galactosidase through biochemical route, catalytic triad of enzyme can be affected, which may reduce the catalytic activity of enzyme and influence the production of GOS (Illanes et al., 2016, Kovács et al., 2013). Therefore, attentions have been placed to develop and implement a simpler bioprocess where free enzyme can be used, and the process can provide satisfactory yield in a continuous way for a long time.

The use of ultrafiltration-assisted biocatalytic reactor, also known as enzymatic membrane reactor (EMR), is a promising alternative of traditional STR process. EMRs typically consist of a temperature controlled STR and an external UF membrane assembly, which might be considered as a unique in the platform of process intensification. The biocatalytic reaction is performed in reactor, where the enzyme in the reaction vessel is retained by membrane and saccharide fractions with lower molecular weights pass through the membrane pores. As a result, continuous synthesis of GOS and separation of biocatalyst can be achieved. Several studies have been carried out to

investigate the performance of diverse sources of commercial enzymes for the synthesis of GOS in EMR. These β -galactosidase sources include yeast *Kluyveromyces lactis* (Pocedičová et al., 2010, Ren et al., 2015), fungi *Aspergillus oryzae* (Córdova et al., 2016c, Matella et al., 2006) and bacteria *Bacillus circulans* (Das et al., 2011, Petzelbauer et al., 2002). Majority of experiments were conducted with EMR under short-time (<5h) and laboratory-scale set-up (<4L) to understand the effects of operating parameters on the yield of GOS obtained from EMR utilizing β -galactosidase. Two main factors for the sustainable synthesis of GOS in EMR, such as enzyme inactivation and membrane fouling for long-term operation were not assessed in depth. It has been reported that there was no significant loss of enzyme activity after 96 h of biocatalytic reaction (Ren et al., 2015), while other investigators reported that half-life of β -galactosidase was approximately 7 days (Petzelbauer et al., 2002). These observations of enzyme stability suggest that for GOS production, the free enzyme EMR process has great potential.

There is limited information about the catalytic activity of β -galactosidase from *Bacillus circulans* for the production of GOS in EMR setup. β -galactosidase from *Bacillus circulans*, i.e. Biolacta N5 has been reported to have high transglycosylation activity, relative thermotolerance and provide higher yield of GOS compared to other commercial sources of β -galactosidase (Warmerdam et al., 2014). They reported that half-lives of Biolacta N5 were 29 h, 29 h, and 16 h at temperature 25°C, 40°C, and 60°C, respectively, under 30 % w·w⁻¹ initial concentration of lactose in STR using an ONPG activity assay. Authors also reported that Biolacta N5 has greater stability at higher concentration of lactose (Warmerdam et al., 2013).

The research objective of this study was to investigate the performance of commercially available Biolacta N5 in EMR setup to produce GOS in a batch- and continuous- mode to understand the superior process strategy. The stability of the Biolacta N5 during the production of GOS has also been investigated. Furthermore, a series of deterministic reaction kinetic equations has been developed dedicated to synthesis of GOS from lactose by biocatalytic reaction.

2. OBJECTIVES TO ACHIEVE

The main objective of my investigation was to understand the synthesis of GOS from lactose catalyzed by a commercially available Biolacta N5 from *Bacillus circulans* in ultrafiltration-assisted enzyme membrane reactor (UF-EMR). In order to achieve this aim, a research scheme, combined with both theoretical and experimental aspects has been designed, mentioned herein:

1. In-silico studies were carried out to predict the formation of enzyme-free GOS by EMR, operated with continuous mode. Kinetic equations dedicated to biocatalytic reactions and enzyme stability reported in peer-reviewed literature were adopted for simulation purposes. Subsequently, a mathematical framework was developed to describe GOS formation by EMR, operated with continuous mode. Simulation studies were performed by using numerical software packages.
2. An UF-EMR utilizing free β -galactosidase was developed. It was designed and equipped with necessary control system to operate at a constant product flow. The performance of this EMR was used in experiment, more specifically,
 - a) Preliminary filtration tests with the reaction liquor were performed to characterize the flux behavior of the UF membrane.
 - b) The dependence of TMP and enzyme load in biocatalytic reaction on the permeate flux was experimentally determined.
 - c) A membrane cleaning procedure was proposed, and its efficiency for regenerating the membrane was evaluated.
 - d) A series of short-term experiments were conducted by operating the EMR in continuous fashion, typically for 6–9 h. These tests were performed to determine the steady-state performance of the EMR in terms of yield and productivity. The effect of residence time (τ) and enzyme load on the biocatalytic reaction was investigated under fixed operational parameters, such as temperature, pH of reaction medium, concentration of lactose in feed

and recirculation flowrate.

- e) The catalytic performance of the continuous-EMR was investigated for an extended period of time (over 120 h).
3. A three-step procedure with five cycles for the production of GOS in cyclic-EMR was designed. A comparative analysis between the performance of cyclic-EMR and traditional STR was performed. In the scope of this study, the following tasks were considered.
- a) A series of batch mode investigations were performed with STR. Different known initial concentration of enzyme was considered in biocatalytic reaction. The relationship between the experimental reaction rate and the applied enzyme dose was explored by analyzing the concentration of the individual saccharide over time. Initial reaction rate and enzyme activity were used to understand the correlation among them, and the results were used for calibration purposes.
 - b) Once the initial reaction velocity of each saccharide fraction in cyclic-EMR was determined from the progress curve, the loss of enzyme activity in successive cycles was estimated by using determined correlation and the results from STR.

3. LITERATURE REVIEW

3.1. Prebiotics

The term “Functional Food” was first introduced in Japan in the mid-1980s, which demonstrates a food that can offers wide ranges of physiological benefits; however, its appearance is similar with conventional food and is considered as a part of the regular diet (Hasler and Brown, 2009). The first introduction of prebiotics was in 1995 and it was considered as a member of functional food (Gibson and Roberfroid, 1995). The definition of "prebiotics" has been repeatedly discussed and modified with time. The current widely accepted definition of prebiotics is "a substrate that is selectively utilized by host microorganisms conferring a health benefit" (Gibson et al., 2017). Numerous studies have demonstrated that prebiotics offer wide ranges of health benefits and reduce the risk of several health hazards (Oniszczuk et al., 2021, Schley and Field, 2002, Tuohy et al., 2003). Prebiotics can be classified to five categories, such as oligosaccharide, polysaccharide, phytochemicals, phenolics and polyunsaturated fatty acids (Bamigbade et al., 2022). A wide range of functional oligosaccharides, such as galacto-oligosaccharide (GOS), fructo-oligosaccharide (FOS), xylose oligosaccharide (XOS), pectic oligosaccharide (POS) and inulin, have been used in foods, beverages, pharmaceuticals and animal feeds (Patel and Goyal, 2011, Qiang et al., 2009, Tuohy et al., 2003). According to the online market research by PRECEDENCE RESEARCH, as a result of an increase in health awareness and appreciation offered by prebiotics, their demand is growing year-over-year. It is estimated that the prebiotic market will reach USD 20.78 billion by 2030 (RESEARCH, 2022).

3.2. Galacto-oligosaccharides (GOS)

The wide ranges of beneficial outcomes have catapulted GOS to the forefront of the functional food sector (Macfarlane et al., 2008, Sangwan et al., 2011). GOS was one of the first oligosaccharides, recognized as prebiotic (Gibson and Roberfroid, 1995). It is also known as oligogalactosyllactose, oligogalactose, oligolactose and transgalactooligosaccharide (TOS)

(Gibson et al., 2004). Chain length of GOS varies based on number of carbohydrate monomer. It may contain 1–5 galactose monomers with a terminal glucose residue, associated with glycosidic linkages of β -(1–2), β -(1–3), β -(1–4) and β -(1–6) (Illanes et al., 2016). GOS can be structurally divided into α -GOS and β -GOS. The former mainly occurring naturally in some plants (Dai et al., 2018) and the latter obtained by trans-glycosylation of lactose (Mitmesser and Combs, 2017). GOS as a food ingredient has been commercially used since 1995 in Japan as a member of Foods for Specified Health Uses (FOSHU). GOS were reviewed for safety by the European Commission Scientific Committee on Food (SCF) in 2003 and approved for use in infant formula in the EU (SCF/CS/NUT/IF/65 Final). Further, they are confirmed as GRAS by the US Food and Drug Administration Agency (FDA) in 2008 (Nakakuki, 2002, 2016). GOS is water-soluble, approximately 0.5 times sweeter than sucrose and relatively stable at room temperature. GOS is heat resistant up to temperature 160°C, pH 7.0 for 10 minutes, as well as acid-resistant up to temperature 37°C, pH 2.0 for months. Due to these characteristics, application of GOS in food industry is well-recognized. GOS is considered as an excellent candidate for the fortification of commercial food products (Torres et al., 2010). Furthermore, application of GOS in the formulation of biopharmaceuticals is noteworthy. GOS have the inability to be digested and absorbed in the human upper digestive tract and improve the growth of gut microflora, mainly probiotics (*Lactobacillus* spp. in the small intestine and *Bifidobacterium* spp. in the large intestine) (Gibson et al., 2010). GOS is metabolized to mainly short chain fatty acids (formic acid, acetic acid, propionic acid, butyric acid and valeric acid) and lactic acid, and among them acetate is predominant, followed by proprionate and butyrate (Nath et al., 2016). Consequently, they offer sustainable gastro-intestinal health by reducing the risks of diarrhea, inflammatory bowel diseases (ulcerative colitis and crohn's disease), constipation, colon cancer (Nath et al., 2018a), osteoporosis, diabetes and dyslipidemia in the bloodstream and tissues (Nath et al., 2018b). However, GOS is confirmed as safe, over consumption of them can cause osmotic diarrhea, dehydration, abdominal pain, and vomiting. Doses of GOS is adjusted to 5-20 grams by mouth daily for up to 30 days in adults to ensure 2 to 4 bowel movements per day (Jain et al., 2019).

3.3. Lactose

Currently, pure lactose, whey, milk and permeate of whey or milk are common substrates used in the production of GOS. As compared to pure lactose, whey and milk may provide a lower yield when used as a substrate and need further pretreatments before using as substrates for the production of GOS. Due to the high concentration of lactose in whey and its inexpensive price compared to pure lactose, production cost of GOS from whey can reduce the overall processing cost. In addition to lactose, other components in feedstocks, such as minerals, proteins, fats and dust may also have an impact in the trans-glycosylation reaction (Fischer and Kleinschmidt, 2018). Concentration of lactose is considerable high in liquid byproduct of cheese processing, which may restrict its disposal in aquatic system. Therefore, utilization of whey as a feedstock of the production of GOS not only reduce the processing cost, it has a great impact on valorization of whey and circular economy (Fischer and Kleinschmidt, 2018, Marwaha and Kennedy, 1988).

The initial concentration of lactose is one of the key factors affecting the yield of GOS. It is generally believed that the reaction is favored toward GOS synthesis under higher initial concentration of lactose (Martínez-Villaluenga et al., 2008, Matella et al., 2006). In the enzyme-catalyzed bioconversion of lactose, hydrolysis and trans-glycosylation reactions occur simultaneously. Hydrolysis of lactose produces monosaccharides glucose and galactose, while trans-glycosylation reaction is responsible to produce GOS. Therefore, to increase the yield of GOS, it is necessary to orient biochemical reaction towards the trans-glycosylation reaction. However, lower concentration of lactose (~5%), β -galactosidase has a greater affinity towards water molecule in the reaction solution. As a result, lactose hydrolysis predominates in the reaction solution, producing a large amount of monosaccharides (Das et al., 2011, Warmerdam et al., 2013). As the concentration of monosaccharides in the solution continues to increase, it further inhibits the trans-glycosylation reaction as well as the synthesis of GOS. However, it has been reported that when the concentration of lactose exceeds a certain range (~30% w·w⁻¹), formation of GOS is reduced (Das et al., 2011). The reason for this finding can be attributed by the inhibitory effect of monosaccharides on β -galactosidase. Formation of monosaccharides is increased at high initial

concentration of lactose and those inhibit the activity of β -galactosidase in a competitively manner. It is generally believed that galactose strongly inhibits β -galactosidase from *Kluyveromyces lactis*; whereas, glucose acts as a non-competitive inhibitor in the reaction (Chockchaisawasdee et al., 2005). In contrast, it was reported that glucose acts as a strong inhibitor for the β -galactosidase from *Bacillus circulans* and hinders the formation of GOS. Comparatively, galactose acts as a non-competitive inhibitor with a negligible effect on the synthesis of GOS (Warmerdam et al., 2013).

3.4. β -galactosidase

β -galactosidase, trivially known as lactase (β -d-galactohydrolase, EC 3.2.1.23) plays a critical role in the synthesis of GOS from lactose. It has been reported that the amount of GOS formation from lactose and its degrees of polymerization depend on the initial concentration of lactose in feedstock and the activity of β -galactosidase (Gosling et al., 2010). This is specifically demonstrated by the fact that the structure, type and yield of GOS from lactose depend on the sources of enzymes. β -galactosidase can break the β -1,4 galactosyl bonds of lactose and catalyzes the hydrolysis of terminal non-reducing β -D-galactose residues in β -D-galactoside. Additionally, it catalyzes the trans-glycosylation reaction, which provides a link between the free galactosyl group and other glycosidic receptors through the wide types of glycosidic bonds (β -1,3, β -1,4, or β -1,6) (Warmerdam et al., 2014).

β -galactosidase is derived from various sources, including bacteria, yeast, fungi, plants and the small intestine of young mammals (Rosenberg, 2006). The presence of β -galactosidase has been detected in variety of plants, such as peaches, apricots, tomatoes, etc (Saqib et al., 2017, Smith and Gross, 2000). Wide ranges of microbial consortia, such as yeast (*Kluyveromyces lactis*, *Kluyveromyces fragilis*) (Bosso et al., 2016, Ladero et al., 2002), fungi (*Aspergillus oryzae*, *Aspergillus niger*) (Gennari et al., 2018, Papayannakos et al., 1993) and bacteria (*Bacillus circulans*, *Bifidobacterium bifidum*) (Füreder et al., 2020, Warmerdam et al., 2013) can produce β -galactosidase.

β -galactosidases from bacterial and yeast origins have an optimal pH range of 5-7 and 6-7,

respectively (Saqib et al., 2017). Therefore, they are suitable for the bioconversion of lactose at neutral pH condition, such as sweet cheese whey and skim milk (Boon et al., 2000, Fischer and Kleinschmidt, 2015, Ramana Rao and Dutta, 1978). On the other hand, β -galactosidases sourced from fungi, such as *Aspergillus niger*, *Aspergillus oryzae* and *Sirobasidium magnum* demonstrate an optimal pH range of 3-5. This makes them particularly well-adapted for converting lactose in acidic conditions, such as acid whey. (Haider and Husain, 2007, Roy and Gupta, 2003). Typically, β -galactosidase from yeast is most active at temperature 30-35 °C (Roy and Gupta, 2003). β -galactosidase from bacteria and fungus are often more resistant to heat. For bacterial β -galactosidase, the optimal temperature typically falls between 40-65 °C (Otieno, 2010); whereas, for fungal β -galactosidase, the optimal temperature range is around 50-60 °C (Saqib et al., 2017). In addition, it has been reported that high temperature also promotes the solubility of lactose in water, resulting in higher lactose concentrations (Hunziker and Nissen, 1926). The condition of relatively high concentration of lactose is favorable for GOS synthesis. Therefore, enzymes with high temperature tolerance shall facilitate the synthesis of GOS and have garnered considerable attention in the industrial production of GOS (DeCastro et al., 2018). Depending on the bacterial source, the optimal temperature of β -galactosidase varies. Bacterial β -galactosidase from *Bacillus circulans* is stable up to temperature 65°C (Yan et al., 2021) and for *Thermotoga maritima* it is up to 80°C (Kim et al., 2004a). GOS synthesized using bacterial β -galactosidases are mainly β -1,2, β -1,3, β -1,4 and β -1,6-containing trisaccharide (DP3) (Saqib et al., 2017, Torres et al., 2010). On the other hand, tri- and tetrasaccharides (DP3, DP4) are synthesized primarily by β -1,3, β -1,4 and β -1,6 glycosidic bond when utilizing β -galactosidases from fungal (Roy and Gupta, 2003, Torres et al., 2010). Yeast β -galactosidase converts lactose to GOS containing mainly DP3 and DP4, while also forming non-lactose DP2 (Torres et al., 2010). β -galactosidases from archaea (*Sulfolobus solfataricus*, *Pyrococcus furiosus*) exhibit good heat tolerance with an optimum temperature between 70-95°C and an optimum pH close to neutral. The higher yield with predominant DP3-containing GOS was obtained when β -galactosidase from engineered *Sulfolobus solfataricus* was used (Petzelbauer et al., 2000).

3.5. pH and temperature

The pH and temperature play a pivotal role on the activity of β -galactosidase, and subsequently impacting the ultimate GOS yield. An enzyme can boast maximum activity in the optimal pH and temperature. Substrate lactose can be converted GOS in maximum level under the optimum condition of enzymatic activity and biocatalytic reaction. Optimum pH and temperature of β -galactosidase vary among sources, described in detail in Sect. 3.4. In addition, temperature also affects the solubility of lactose in water. It was already mentioned that the synthesis of GOS is influenced by the maximum concentration of lactose in the reaction medium (Hunziker and Nissen, 1926). Reaction temperature provides activation energy to proceed the reaction forward. Furthermore, enzyme decay with time progress is influenced by reaction temperature. Therefore, effect of temperature on the activity of enzyme is generally described by the Arrhenius equation. It was observed that the half-life of the Biolacta N5 from *Bacillus circulans* decreased from 220 h to 13 h when the temperature was increased from 25°C to 40°C under the same reaction conditions (Warmerdam et al., 2013). Furthermore, the authors observed that Biolacta N5 was more thermally stable at high concentration of lactose at temperature 25°C and 40°C (Warmerdam et al., 2013). Similarly, the half-life of β -galactosidase from *Aspergillus oryzae* in 100 mM phosphate-citrate buffer pH 4.5, decreased from 42 h to 0.8 h when the temperature was increased from 50°C to 60°C (Huerta et al., 2011).

3.6. Buffer

The presence of certain ions in the reaction buffer plays a vital role in the biocatalytic reaction for synthesis of GOS. Phosphate buffer, sodium citrate buffer and sodium hydroxide solution are the commonly used buffers for the production of GOS. It has been reported that sodium, potassium, magnesium and manganese ions are most influential on GOS synthesis. These ions affect GOS synthesis primarily through their effects on the activity of β -galactosidases (Fischer and Kleinschmidt, 2015). Depending on the source of β -galactosidase, these ions have different effects. As example, synthesis of GOS is improved with β -galactosidase from *Aspergillus oryzae* in the

presence of potassium and magnesium ions in citrate buffer (Madani et al., 1999). The activity of β -galactosidases from *Kluyveromyces lactis* (Flores et al., 1996, Plou et al., 2007) and *Kluyveromyces fragilis* (Rosenberg, 2006) are enhanced in the presence of potassium and magnesium ions; while, calcium ion is considered as an inhibitor. β -galactosidase from *Bacillus licheniformis* has activated by magnesium and calcium ions (Akcan, 2011). β -galactosidases from *Bacillus circulans* (Biolacta N5) is positively influenced by cations, including calcium, magnesium, and sodium (Mozaffar et al., 1985).

3.7. Production of GOS

A number of methods are currently known for the production of GOS, including natural extraction, chemical synthesis, hydrolyzed polysaccharides, enzymatic synthesis and microbial fermentation. Enzymatic synthesis of GOS has become the most widely applied method due to its high safety, yield and feasibility to produce in industrial scale (Mei et al., 2022, Weijers et al., 2008). The mechanism of GOS synthesis can be described by either thermodynamically controlled (the equilibrium of reaction towards glycosidic bond formation) or kinetically controlled (formation of glycosidic bond through activated glycosyl donor-enzyme donor complex) phenomena (de Albuquerque et al., 2021). In case of thermodynamically controlled synthesis phenomenon, at high concentration of lactose, a reverse hydrolysis of lactose takes place. According to this concept, a free monosaccharide is combined with a nucleophile, excluding the water activity and transfer the equilibrium towards the formation of GOS (Maksimainen et al., 2012). On the other hand, On the other hand, kinetically controlled synthesis of GOS depends on the nature of enzyme-substrate intermediate. In this case, the activated glycosyl donor, such as lactose (activated glycosyl donor) forms an active glycosyl-enzyme complex, that can be influenced by the water (nucleophile) activity and formation of a new glycosidic bond (Kasche, 1986). The biocatalytic reaction for the formation of GOS from lactose is presented in Figure 1.

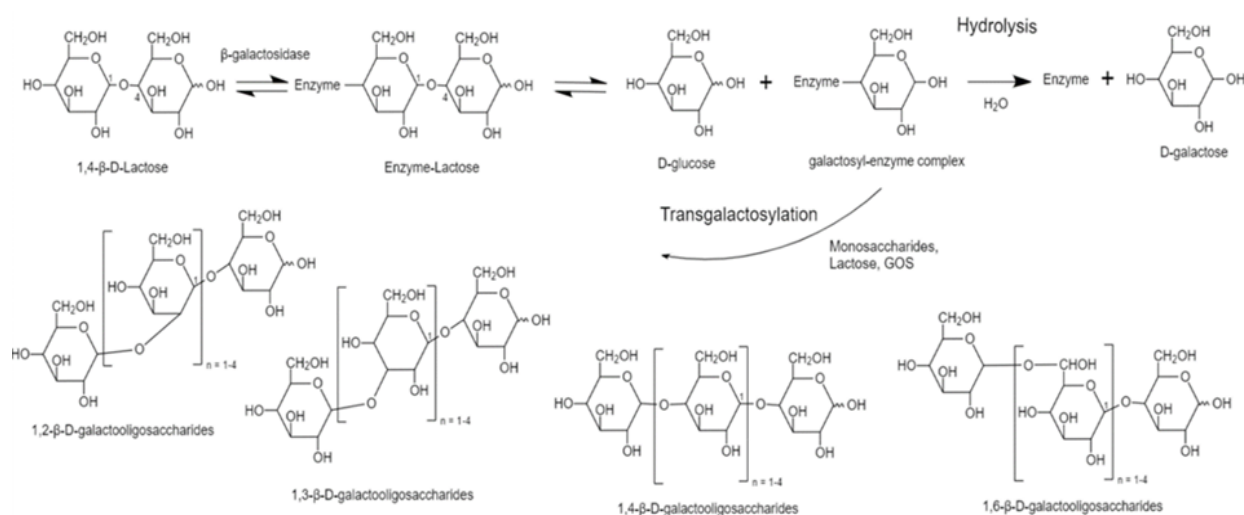


Figure 1. Schematic diagram of the catalytic mechanism of β -galactosidase using lactose a substrate (Torres et al., 2010).

Enzymatic synthesis of GOS is mainly involved by the use of free and immobilized enzymes. A number of reactors were employed for the production of GOS from lactose. Those are stirred tank reactor (STR) (Palai et al., 2012), enzyme immobilized membrane bioreactor (Nath et al., 2013), enzyme immobilized packaged bed bioreactor (PBR) (Sen et al., 2014) and free enzyme membrane bioreactor (Das et al., 2011). The limitations of enzyme-immobilized packed bed reactor include a high pressure drop across the packed bed, slow film and pore diffusions and a complicated scale-up (Sen et al., 2014). The limitations of enzyme-immobilized membrane reactor include a lower catalytic activity due to reduced catalytic triad and lower permeate flux due to formation of concentration polarization on the vicinity of membrane surface and high mass transfer resistance (Nath et al., 2013). STRs are predominantly used for the large-scale industrial production of GOS. In this case, soluble β -galactosidase is added to the lactose solution under optimum temperature and pH settings. The solution is stirred in STR for a period of time and lactose is catalyzed to GOS. When the reaction is complete, the enzyme is inactivated by heating or lowering the pH. Subsequently, GOS is purified by removing by-products, such as enzyme by NF, activated carbon adsorption, ion exchange, etc. A heat treatment is applied prior to evaporation to ensure microbial stability, and at the end of the evaporation process a GOS syrup with a concentration of 40-60% is typically obtained. If a GOS powder is required, further drying is performed (Gosling et al., 2010,

Illanes et al., 2016, Vera et al., 2016).. Flowchart of the production of GOS is depicted in Figure 2.

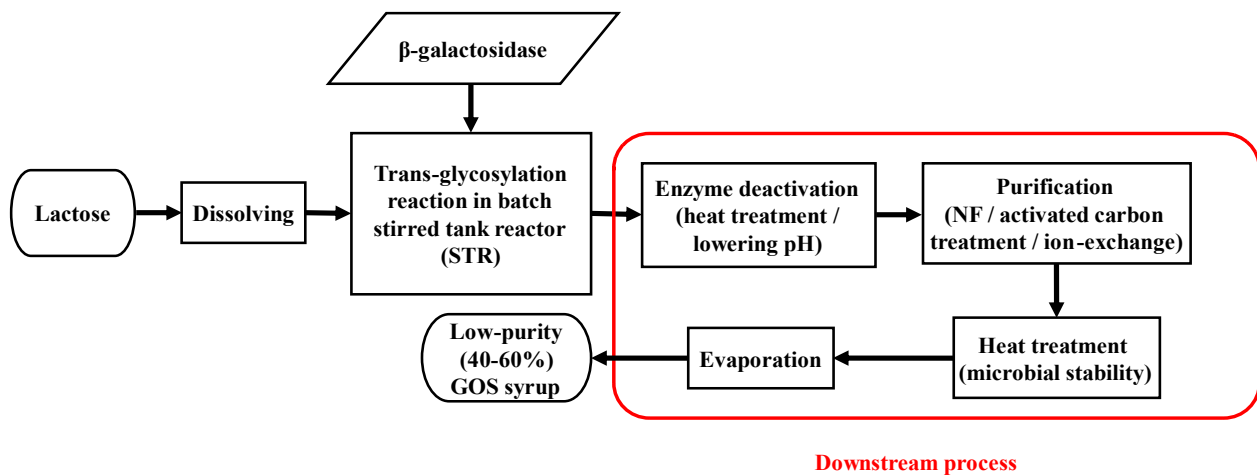


Figure 2. Process flowchart of GOS manufacturing from lactose (self-developed, concept was adopted from Nestlé Nutrition (Gaynor, 2015) and Vitalus Nutrition Inc. (Kampmeyer, 2022)).

However, conventional temperature controlled STR is widely used to produce GOS with industrially acceptable yield. Nevertheless, this setup has been associated with certain drawbacks, such as the high cost of downstream process. It is important to note that the product obtained from STR is a mixture of proteins (enzyme), monosaccharides (glucose and galactose), disaccharides (including non-reacted lactose) as well as GOS. Therefore, subsequent purification and separation steps are necessary to obtain GOS with the desired purity. Therefore, production of GOS by STR incurs additional costs due to the complicated downstream process, which are characterized by the operational complexity and expensive equipment. Furthermore, enzyme expenditure makes up a significant part of total production cost of GOS (Cao et al., 2020).

3.8. UF-EMR utilizing free β -galactosidase

A great attention has been placed to reuse the β -galactosidase for the production of high amount of marketable GOS from lactose. It may belief that this approach may reduce the production cost and increase the production efficiency. Evidence from a number of experimental studies reveal that modification of conventional STR, i.e., implementation of an UF module with STR can

separate β -galactosidase from reaction mixture and reuse the β -galactosidase to achieve GOS in a continuous way. In this UF-EMR setup, in the first step, soluble lactase is inoculated to preincubated substrate (lactose) solution in STR. The process is performed continuously in the mentioned fashion: fresh substrate is continually fed to the bioreactor and enzyme dosed into the reactor to convert lactose. During the filtration process, the enzyme is retained by the UF membrane, and the enzyme-free saccharide mixture is continually collected as permeate in the product tank (Cao et al., 2020). The yield of GOS from UF-EMR is influenced by several factors, including concentration of lactose and pH in reaction medium, formation of monosaccharides, reaction temperature (Gosling et al., 2010, Warmerdam, 2013), residence time (τ) and trans-membrane pressure (TMP) (Córdova et al., 2016c, Czermak et al., 2004, Gonzalez et al., 2009). Until now, two patents have been filed for the production of GOS using the UF-EMR. The patent EP1352967 (Mei et al., 2022) has been granted to Eurodia Industrie (Wissous, France) on “Process for continuous production of galacto-oligosaccharides” (Publication number: EP1352967 B1, Application number: EP20030370016). It describes a process in which a UF-EMR is coupled with a simulated moving bed (SMB) packed with a strong cation-exchange resin. Lactose was separated from GOS by SMB and then lactose was recycled back to the bioreactor. However, due to its reproducibility and geographical limitation (recognized only in European countries), they are not currently widely used. Immediately afterwards, in 2003, the patent “Method for the continuous production of galactosyl-oligosaccharides” (Publication number: PCT/DE2004/002686, Application number: WO2005056810 A1) have been submitted by Transmit Technologie transfer (Giessen, Germany), but not granted because of the similar process was established by Eurodia Industries (Jovanovic-Malinovska et al., 2012). Summarize information about investigations with UF-EMR for GOS production is presented in Table 1 (in A2: Additional information).

3.8.1. Effect of lactose concentration and enzyme activity

Some operating conditions, such as the initial concentration of lactose and concentration of β -galactosidase have effect on the production of GOS. Comparisons between STR and UF-EMR

have been made to elucidate it. It was reported that the production of GOS is proportional to the initial concentration of lactose (generally $< 30\%$ w·w⁻¹) for both STR and UF-EMR (Das et al., 2011). However, high initial concentration of lactose leads to the concentration polarization on membrane surface, which reduces permeate flux and decreases the yield of GOS from UF-EMR (Ren et al., 2015). It has been reported that increase of the concentration of β -galactosidase leads to a rise the yield of GOS. Furthermore, it was found that increase of the concentration of β -galactosidase reduces the process time to get same yield of GOS from same amount of initial concentration of lactose. As example, the maximum yields of GOS was 20% w·w⁻¹ at operation time 0.5 h and 0.25 h, respectively, when the concentrations of β -galactosidase from the *Aspergillus oryzae* was increased from $4.5\text{ g}\cdot\text{L}^{-1}$ to $11.8\text{ g}\cdot\text{L}^{-1}$ within the initial concentration of lactose $270\text{ g}\cdot\text{L}^{-1}$, pH 4.5 and reaction temperature 40°C (Matella et al., 2006). Similar type of results was reported by other investigators. The maximum concentration of GOS was achieved $90\text{ g}\cdot\text{L}^{-1}$ at operation time 4 h and 1 h, respectively when the concentrations of *Kluyveromyces lactis*-driven Maxilact L 2000 was increased from $2.9\text{ U}\cdot\text{mL}^{-1}$ to $8.7\text{ U}\cdot\text{mL}^{-1}$ within initial lactose concentration $340\text{ g}\cdot\text{L}^{-1}$, pH 7 and reaction temperature 40°C (Chockchaisawasdee et al., 2005). During long-term operation, it is often observed that concentration of GOS was decreased after reaching the maximum value (Chockchaisawasdee et al., 2005, González-Delgado et al., 2016, Martínez-Villaluenga et al., 2008). It might be realizing that the concentration of GOS from lactose is increased by the hydrolysis and trans-glycosylation reactions up to a certain period. Under long-term operation, GOS is hydrolyzed to glucose and galactose. The concentrations of monosaccharides (glucose and galactose) continuously increase over time and the monosaccharides further act as inhibitors in trans-glycosylation reaction. Monosaccharides have less influence in trans-glycosylation reaction when it is performed in UF-EMR than STR. This is because of the generated monosaccharides are continuously collected at the permeate with a certain flow rate; whereas, the generated monosaccharides are accumulated in the reaction solution in conventional STR (Das et al., 2011).

According to current literatures, yield of GOS is varied from different sources β -galactosidase in

UF-EMR. In an investigation with UF-EMR, it has been reported that the highest yield of GOS was 60% w·w⁻¹. It was achieved when 0.5% w·v⁻¹ of Biolacta FN5 (β -galactosidase from *Bacillus circulans*) was added to the feedstock where initial lactose concentration was 500 g·L⁻¹, pH 6.6. In that case, low temperature ~24 °C was used in biocatalytic reaction (Das et al., 2011). Although β -galactosidase from *Bacillus circulans* has been reported to have high trans-glycosylation activity (Yan et al., 2021), Biolacta FN5 is not convincing for the synthesis of GOS at low temperature (Gosling et al., 2009). In UF-EMR, the heat-resistant β -galactosidases from *Sulfolobus solfataricus* (Ss β Gly) and *Pyrococcus furiosus* (CelB) were reported to have a maximum GOS yield of 18% w·w⁻¹ from 170 g·L⁻¹ of initial lactose concentration with 0.4 U·mL⁻¹ Ss β Gly and 1.2 U·mL⁻¹ Ss β Gly, respectively. The temperature and pH were maintained 70 °C and 5.5, respectively in biocatalytic reaction (Petzelbauer et al., 2002). Beside the bacterial β -galactosidase, yeast-derived β -galactosidases was widely used in UF-EMR, it has a substantial activity in temperature and pH range of 25-40°C and 6.5-7.5, respectively. The yield of GOS was 30-35% w·w⁻¹ from higher initial concentrations of lactose (300-400 g·L⁻¹) and *Kluyveromyces lactis*-derived β -galactosidase under the optimal reaction temperature and pH in UF-EMR. A GOS yield of 33% w·w⁻¹ was obtained from initial concentration of lactose 300 g·L⁻¹, pH 6.5 and temperature 25°C utilizing *Kluyveromyces lactis*-derived Lactozym Pure 6500L (Ren et al., 2015). Furthermore, the yield of GOS was 35% w·w⁻¹ from initial concentration of lactose 400 g·L⁻¹, pH 7 and temperature 40°C using a β -galactosidase from *Kluyveromyces lactis* (Gonzalez et al., 2009). Low initial concentration of lactose may be responsible for lower yield of GOS. The yield of GOS was 22% w·w⁻¹ from initial concentration of lactose 250 g·L⁻¹ and 8 U·mL⁻¹ Maxilact LX 2000, a β -galactosidase from *Kluyveromyces lactis*. The temperature and pH of the reaction were 40°C and 7.0°C, respectively (Chockchaisawasdee et al., 2005). Under the similar operation conditions, i.e., pH 6.7, and 40 °C, the maximum yield of GOS was 26% w·w⁻¹ from initial concentration of lactose 200 g·L⁻¹ and Maxilact L 2000 (Ebrahimi et al., 2008). Similar results were reported by other investigators. The yield of GOS was much less, such as ~5% w·w⁻¹ from initial concentration of lactose 200 g·L⁻¹ and 6 U·mL⁻¹ Maxilact LX 5000, β -galactosidase from *Kluyveromyces lactis*. In that case, reaction and temperature were pH 6.75 and 37°C, respectively (Pocedičová et al., 2010).

The yield of GOS was 34% w·w⁻¹ with initial concentration of lactose 230 g·L⁻¹ and 32 g·L⁻¹ Maxilact L 2000, pH 7. Reaction temperature was maintained 40°C (Czermak et al., 2004). Fungal-derived β -galactosidases were also used in experiments for GOS production by UF-EMR. The yield of GOS was 30% w·w⁻¹ from initial concentration of lactose 400 g·L⁻¹ and 50 U·g⁻¹ of Enzeco®. The reaction pH and temperature were 4.5 and 50°C, respectively (Córdova et al., 2016c).

3.8.2. Effect of characteristics of membrane

In the UF-EMR process, UF membranes with a suitable MWCO can ensure the retention of enzyme (β -galactosidase) and permeation of saccharides. Membranes which retain 90% of the protein during filtration are considered to have achieved complete protein retention and can be used for enzyme separation. Generally, molecular weight of β -galactosidase is greater than 100 kDa (Schmidt and Stougaard, 2010). Therefore, most researchers have chosen UF membranes with MWCOs between 10 kDa and 50 kDa, which may be considered 99% retention of enzyme. The complete retention of *Kluyveromyces lactis*-driven Maxilact LX 5000 was achieved by a ceramic membrane with MWCO 10 kDa (Gonzalez et al., 2009), polyethersulfone membrane with MWCO 50 kDa (Czermak et al., 2004), and a ceramic UF membranes with MWCOs 30 kDa and 150 kDa (Pocedičová et al., 2010). Similarly, Foda and Lopez-Leiva reported that an enzyme Maxilact L 2000, produced from the same origin of *Kluyveromyces lactis* as Maxilact LX 5000 (molecular mass 135 kDa) was completely retained by a membrane with MWCO 10 kDa (Foda and Lopez-Leiva, 2000). β -galactosidase from the fungus *Aspergillus oryzae* was completely retained by polyethersulphone membranes and ceramic membranes with MWCO of 4 kDa (Matella et al., 2006) and 50 kDa (Córdova et al., 2016c), respectively. Biolacta FN5 from *Bacillus circulans* was completely retained by polyethersulphone UF membrane with MWCO 50 kDa (Das et al., 2011). Heat-resistant bacterial β -galactosidase, such as *Sulfolobus solfataricus* (Ss β Gly) and *Pyrococcus furiosus* (CelB) were completely retained by the spiral wound polyethersulfone (PES) membrane with MWCO 10 kDa. Spiral-wound membranes with MWCO 30 kDa were also used for enzyme

retention in UF-EMR experiments. It was reported that the enzyme activity was decrease by $\sim 2.5\%$ per hour at a permeate flow rate of $40 \text{ mL} \cdot \text{h}^{-1}$, which indicated that the membrane with MWCO 30 kDa was not a perfected choice for the retention of Ss β Gly and CelB (Petzelbauer et al., 2002).

3.8.3. *Effects of membrane module*

Tubular hollow fiber, spiral wound and flat sheet membrane modules are widely used in downstream purification process. Among these modules, hollow fiber and spiral wood membrane modules are widely used due to their characteristics, such as high filling density, relatively high surface area and low capital costs (Cui et al., 2010). Therefore, they are preferred for plant-scale GOS production (Foda and Lopez-Leiva, 2000). Since flat sheet and tubular membrane modules have low filling density and are expensive, they are only used in laboratory-scale filtration operation (Martín, 2016). The majority of the currently known experiments utilizing UF-EMR for GOS production have been conducted at laboratory scale set up (reactor capacity $<4\text{L}$). In most cases, UF tubular membranes, including tubular ceramic membrane (Ebrahimi et al., 2008, Gonzalez et al., 2009, Pocedičová et al., 2010, Córdova et al., 2016c), tubular polyethersulphone membranes (Matella et al., 2006) and tubular composite regenerated cellulose (Ren et al., 2015) were used. Furthermore, flat sheet membrane, made by cellulose acetate (Chockchaisawasdee et al., 2005) and polyethersulfone (Das et al., 2011) and spiral-wound membrane, made by polyethersulfone (Petzelbauer et al., 2002) were used in UF-EMR for the production of GOS. Only a few experiments were carried out comparatively high scale production of GOS. In scaled-up production, hollow fiber and spiral wood membrane modules were considered taking into account some issues, such as high filtration surface area, efficiency of filtration and the cost of membrane.

The mid-pilot plant setup developed by a reactor (reactor capacity 11 L) with hollow fiber polysulfone UF membrane (membrane area of 0.5 m^2 and MWCO 10 kDa) was used for the production of GOS from lactose. In the process, the reaction temperature and pH were 45°C and 7, respectively. The process setup provided GOS yield $31\% \text{ w} \cdot \text{w}^{-1}$ from initial concentration of lactose $200 \text{ g} \cdot \text{L}^{-1}$ with $0.5\% \text{ w} \cdot \text{w}^{-1}$ Maxilact L 2000 (Foda and Lopez-Leiva, 2000). A tubular

ceramic UF membrane with a membrane area of 0.36 m² and MWCO 20 kDa was applied for pilot scale trials utilizing Maxilact LX 5000 within the initial concentration of lactose 200 g·L⁻¹. In the process, the reaction temperature and pH were 40°C and 7.5, respectively. The process provided GOS yield of 20% w·w⁻¹ (~2.9 kg) (Czermak et al., 2004).

3.8.4. *Effects of operation parameters*

Operational parameters of UF-EMR have some influence on the final yield of GOS to a certain extent. More specifically, the trans-membrane pressure (TMP) and residence time (τ) influence the membrane permeability and the yield of GOS yield; however, reaction temperature and pH also have influence on yield of GOS. The effects of mentioned operational parameters on permeate flux and yield of GOS are elucidated in subsequent sections.

3.8.4.1. Transmembrane pressure (TMP) and Permeate flux

Control of operational parameters of UF-EMR, such as TMP and flow rate is accomplished using pumps and restriction valves. Pumps capable of continuously supplying a controlled and constant flow rate of feed, permeate and recirculation. In the current experiments of GOS synthesis by UF-EMR, most of the pumps for controlling the feed and permeate flows are peristaltic pumps (Das et al., 2011, Ebrahimi et al., 2008, Matella et al., 2006), electronic diaphragm pump (Ren et al., 2015) and positive displacement pump (Córdova et al., 2016c). For the continuous production of GOS by the UF-EMR, a stable catalytic performance of the EMR, i.e., a stable lactose conversion and the yield of GOS can be ensured when the feed flow and permeate flow are consistent. Restriction valves are another important control factor during UF-EMR operation and can be used to control the pressure of the retentate-side and permeate-side. Thus, TMP during the reaction, i.e., the pressure difference between the permeate end and the retention end can be controlled. The relationship between TMP and permeate flux can be categorized to pressure-dependent and pressure-independent states. Permeate flux increases with the increase of TMP up to a certain range and subsequently, permeate flux tends to stabilize (the increase of pressure will not increase

permeate flux). Permeate flux in the stable state is usually called the limiting flux (He et al., 2017).

The UF process is a size-exclusion based pressure-driven separation process (Khan et al., 2022). Generally, UF membrane filtration process is performed a range of pressure, i.e., 1 to 7 bars. There is a general consensus that the TMP is proportional to the permeate flux ($\text{kg}\cdot(\text{m}^2\cdot\text{h})^{-1}$), which is the amount of permeate produced per unit time through a unit area of membrane (Córdova et al., 2016c). The permeate flux is an important parameter in the UF-EMR process, which can reflect the permeability of the membrane. A decrease in permeate flux was commonly observed under fixed TMP. The permeate flux decreased from approximately $10 \text{ L}\cdot(\text{m}^2\cdot\text{h})^{-1}$ at the beginning of the experiment to $7.4 \text{ L}\cdot(\text{m}^2\cdot\text{h})^{-1}$ after four hours of reaction when the TMP was fixed at 2.25 bar. This result implies a 26% decrease in membrane permeability after four hours of reaction (Ren et al., 2015). Similar observation was reported by other investigators. The average permeate flux in UF-EMR with Maxilact L 2000 was reduced by about 35% (from $55.8 \text{ L}\cdot(\text{m}^2\cdot\text{h})^{-1}$ at 1st hour to $36.5 \text{ L}\cdot(\text{m}^2\cdot\text{h})^{-1}$ at 4th hour) after 4 hours of fixed TMP 2.75 bar (Chockchaisawasdee et al., 2005). This might be caused by concentration polarization on membrane surface during filtration process. During the process of retention, the retained material (enzyme) forms a layer on the membrane surface, which prevents permeation through membrane pores to some extent. In this regard, the amount of GOS collected in the permeate is relatively low.

An effective strategy to prevent the declination of permeate flux in a pressure-dependent range is to adjust the return-side pressure by adjusting the pressure valve. This directly regulates the TMP, which influences permeate flux by changing the permeate flow rate. The permeate flux was increased significantly from $5.45 \text{ L}\cdot(\text{m}^2\cdot\text{h})^{-1}$ to $10.13 \text{ L}\cdot(\text{m}^2\cdot\text{h})^{-1}$ due to increase of TMP from 0.75 bar to 2.75 bar when biocatalytic reaction was performed with $300 \text{ g}\cdot\text{L}^{-1}$ lactose and $1 \text{ U}\cdot\text{mL}^{-1}$ Lactozym Pure 6500L, pH 6.5 and temperature 25°C in UF-EMR (Ren et al., 2015). A similar type of research outcome is published by other investigators. The average permeate flux increased by about 40% when the TMP was raised from 0.75 bar to 2.75 bar when a trans-glycosylation reaction (concentration of lactose $250 \text{ g}\cdot\text{L}^{-1}$ and $8 \text{ U}\cdot\text{mL}^{-1}$ Maxilact L2000) was performed within UF-EMR (Chockchaisawasdee et al., 2005). Physical or chemical cleaning of membrane was considered

after each experiment with aqueous solution of NaOH or HCl for regeneration of membrane and to restore permeability completely or to a certain extent (Das et al., 2011).

3.8.4.2. Residence time

In UF-EMR, the residence time, which defined as the ratio of reactant volume to permeate flow rate is a key control factor. There have been numerous reports demonstrating that residence time plays a significant role for the synthesis of GOS by UF-EMR. In general, yield of GOS and residence time are correlated positively. Nevertheless, if the residence time exceeds a certain value (usually one hour), the concentration of GOS is decreased. In an investigation, Maxilact L 2000 and β -galactosidase from *Aspergillus oryzae* were used in the initial concentration of lactose $230 \text{ g}\cdot\text{L}^{-1}$, and effect of residence time was studied. The yield of GOS was decreased from $34\% \text{ w}\cdot\text{w}^{-1}$ to $26\% \text{ w}\cdot\text{w}^{-1}$ for Maxilact L 2000 and $18\% \text{ w}\cdot\text{w}^{-1}$ to $14\% \text{ w}\cdot\text{w}^{-1}$ for β -galactosidase from *Aspergillus oryzae* when residence time increased from 0.5 h to 2h, respectively (Czermak et al., 2004). Meanwhile, the authors observed the increasing tendency of monosaccharides and disaccharides in solution with increasing residence time. Therefore, the decrease in GOS production under long residence time can be attributed to the enzymatically catalyzed hydrolysis of the product GOS to mono- and disaccharides. In addition, authors claimed that higher concentration of monosaccharides might hinder the trans-glycosylation reaction (Czermak et al., 2004). Similar types of results were observed by other investigators. In an investigation, the yield of GOS was increased to $28\% \text{ w}\cdot\text{w}^{-1}$ at a residence time of 0.5 h using Lactase F from *Aspergillus oryzae* under reaction conditions of pH 4.8, temperature 50°C , and initial lactose concentration of $200 \text{ g}\cdot\text{L}^{-1}$ (Gonzalez et al., 2009). On the contrary, when τ exceeded 0.5 h, the concentration of GOS showed a decreasing trend. The volumetric productivity of GOS, i.e., the concentration of synthesized GOS per unit time, increased over a residence time range of 0-0.1 h, reaching a maximum value of $260 \text{ g}\cdot(\text{L}\cdot\text{h})^{-1}$ at 0.1 h of residence time. Afterwards, it showed a decreasing trend with increasing residence time, and the volumetric production rate of GOS decreased to only $10 \text{ g}\cdot(\text{L}\cdot\text{h})^{-1}$ at a residence time of 3 h (Gonzalez et al., 2009). In other investigation, β -

galactosidase from the same enzyme source (*Aspergillus oryzae*) as in Gonzalez et al.,(2009) was used in the initial lactose concentration $400 \text{ g}\cdot\text{L}^{-1}$, pH 4.5 and reaction temperature 53°C . The productivity of GOS was increased from $0.074 \text{ g GOS}\cdot\text{mg enzyme}^{-1}\cdot\text{h}^{-1}$ to $0.151 \text{ g GOS}\cdot\text{mg enzyme}^{-1}\cdot\text{h}^{-1}$ when the residence time was curtailed from 8.3 h to 6.2 h (Córdova et al.,(2016c)). In general, short ($<1 \text{ h}$) residence times are considered favorable for GOS synthesis (Czermak et al., 2004, Gonzalez et al., 2009, Pocedičová et al., 2010). There are also some other experiments were performed with UF-EMR under long residence time for the synthesis of GOS. For example, the maximum yield of GOS was about $30\% \text{ w}\cdot\text{w}^{-1}$ at a residence time of 4 h using $0.5\% \text{ w}\cdot\text{w}^{-1}$ Maxilact 2000 L and the initial concentration of lactose $200 \text{ g}\cdot\text{L}^{-1}$. The pH and temperature of reaction were maintained 7 and of 45°C , respectively (Foda and Lopez-Leiva, 2000). Long residence time during continuous production of GOS by UF-EMR increases the risk of membrane fouling. In an experiment, a significant decrease in permeate flux was caused by membrane fouling when applying a residence time of 6.3 h utilizing $50 \text{ U}\cdot\text{g}^{-1}$ *Aspergillus oryzae*-driven Lactase in a $400 \text{ g}\cdot\text{L}^{-1}$ lactose solution. In that biocatalytic reaction, temperature and pH were maintained 53°C and 4.5, respectively (Córdova et al., 2016c).

3.9. Mathematical models of trans-glycosylation reaction

In this section, I provide an overview of the currently available kinetic models and enzyme stability studies focusing on the synthesis of GOS from lactose. On the basis of these investigations, I will then attempt to develop a mathematical framework and to simulate the enzymatic biosynthesis of GOS from lactose in EMR using Biolacta N5, a β -galactosidase from *Bacillus circulans*.

3.9.1. Kinetic models

Within the last decades, numerous kinetic modeling studies have been published on the synthesis of GOS. Under specific conditions and assumptions, these models are able to predict the conversion of lactose into GOS.

A four-step, nine-parameter kinetic model was proposed by Kim et al. (2004b). The model was

used to describe the changes in the saccharide fractions in solution catalyzed by recombinant *Kluyveromyces lactis* β -galactosidase. In the proposed model, hydrolysis and trans-glycosylation occur simultaneously. It should be noted, however, that the model considers only the formation of disaccharides and trisaccharides from glucose and lactose as acceptors. The possible formation of oligosaccharides of higher DP is not considered. In addition, the competitive inhibition of GOS synthesis by galactose is not to be taken into account (Mateo et al., 2004).

Vera et al. (2011) proposed a model consisting of seven steps and eight parameters. The model is independent of the enzyme content and has a clear biochemical significance. The authors investigated the reaction mechanism using β -galactosidase extracted from *Aspergillus oryzae* and assumed a pseudo-equilibrium reaction. The predominance of transgalactosylation was ensured by employing a high concentration of lactose ($400 \text{ g} \cdot \text{L}^{-1}$) in the reaction. The model takes into account the strong inhibition of galactose, while the inhibition of glucose is negligible (Jenab et al., 2018, Neri et al., 2009). DP5 is considered to be the most synthesized oligosaccharide and the hydrolysis reaction of this reaction is considered irreversible. The authors concluded that galactobiose, a non-lactose glycosylated disaccharide, was produced during the reaction. However, the authors considered that both non-lactose disaccharides and lactose were indistinguishable and were uniformly referred to as disaccharides. These assumptions all contribute to overestimating the concentration of glucose and underestimating the consumption of disaccharides as well as the production of DP5.

Schultz et al. (2021) proposed an eight-step dynamic model with nine parameters based on the models proposed by Boon et al. (1999) and Vera et al. (2011). Authors used this kinetic model to describe the synthesis of GOS from Lactozym 3000 L HP G extracted from *Kluyveromyces lactis* under high lactose concentration conditions ($400 \text{ g} \cdot \text{L}^{-1}$). This model presents predictions about galactobiose production. Galactobiose is a disaccharide produced by the combination of two galactose in the reaction, which also has a prebiotic effect (Schultz et al., 2021). All disaccharides (including unreacted lactose) are referred to as DP2 in the model. The inhibition of the reaction by monosaccharides, such as glucose, is ignored. Model predictions underestimate the observed

concentrations of glucose, galactose and lactose.

Rico-Rodríguez et al. developed a nine steps in the proposed reaction model, with 11 ordinary equations and 18 parameters for the synthesis of GOS using different substrates (pure lactose, lactose permeates, and cheese whey) and enzyme sources (*Aspergillus oryzae*, *Kluyveromyces lactis*) (Rico-Rodríguez et al., 2021). The model did not consider the inhibitory effects of galactose and glucose as well as the production of non-lactose disaccharides. They found that the kinetic model predicts the reactions involving pure lactose as a substrate well, but a moderate agreement was found between estimated and experimental data for reactions involving cheese whey. It is also important to note that the reactions are measured for only a short reaction time (typically 5 h).

Neri et al. (2009) conducted a study on the kinetic modeling of GOS production utilizing *Aspergillus oryzae* β -galactosidase under free and immobilized conditions, based on the research of Boon et al. (1999). A model based on four ordinary differential equations with five grouped parameters is presented. This model is reported to be applicable to the prediction of both the free and immobilized enzyme applications. The model accurately reflects the conversion of lactose and the change of glucose with time. In contrast, the yield of galactose was overestimated, while the yield of DP3 was underestimated. This may result from the fact that higher degrees of oligosaccharides, such as DP4, were not taken into account in the reaction, and galactose was not considered a possible source of GOS formation.

Based on the research of Boon et al. (1999), Jenab et al. (2018) presented a model for the process of synthesizing GOS in a foam bed reactor by using the enzyme β -galactosidase extracted from *Aspergillus oryzae*. The model includes five reaction steps with five ordinary differential equations. Due to the fact that DP3 is the major component in the product accounting for around 78% of the total GOS, only the production of DP3 is considered in the prediction model instead of the total yield of GOS. A possible drawback of this approach is that the model may underestimate the final GOS yield. The reaction treated non-lactose disaccharides and lactose as disaccharides.

3.9.1.1. Kinetic model proposed by Boon et al. (1999)

Among these kinetic models regarding GOS synthesis the kinetic model of Boon et al. (1999) is the most relevant to my study. Boon et al. (1999) proposed a model to describe the kinetic reactions leading to GOS synthesis from a biological perspective using β -galactosidase from *Bacillus circulans*. Since previous studies have demonstrated that in the hydrolysis of lactose using β -galactosidase from *Bacillus circulans*, the by-products glucose (Deschavanne et al., 1978) and galactose (specially in low substrate concentration) (Bakken et al., 1992, Mozaffar et al., 1984) inhibit the reaction to some extent. Consequently, galactose and glucose were considered as inhibitors in their study. In this model, both lactose hydrolysis and trans-glycosylation reactions are taken into account, and galactose is considered to have a negligible inhibitory effect on the reaction as the initial concentration was relatively high (20% w·w⁻¹). The glucose is considered to be a competitive inhibitor in the reaction and will compete with lactose for the same active site of the enzyme, resulting in an inactive compound. Taking a fixed value of 1 for the rate of hydrolysis reaction with water as the acceptor for accuracy of prediction, the model tends to overestimate galactose and DP3 concentrations at relatively low initial lactose concentrations. Furthermore, the reaction was assumed to take place in the absence of any higher degrees of oligosaccharides except for DP3.

The model proposed by Boon et al. (1999) assumes five stepwise kinetic reactions consider glucose and galactose inhibition as showed in the following reactions:





where E, L, DP3, Glu and Gal represents the enzyme, lactose, saccharides with a DP of 3 (GOS), glucose, and galactose, respectively. E-Gal, E-I are the enzyme-galactose complex and inactive enzyme-glucose/galactose inhibitor complex. The k values represent the reaction rate constants.

The set of ordinary differential equations (ODEs) describing the rate expressions for models is given by:

$$\frac{d[L]}{dt} = (-k_{1b}k_{2b} \frac{1}{k_{4b}} [L][H_2O] - 2k_{1b} \frac{k_{3b}}{k_{4b}} [L]^2 + k_{2b}[DP3][H_2O])Y_b \quad \text{Eq. 3.9.1.1-6}$$

$$\frac{d[Glu]}{dt} = (k_{1b}k_{2b} \frac{1}{k_{4b}} [L][H_2O] + k_{1b} \frac{k_{3b}}{k_{4b}} [L]^2)Y_b \quad \text{Eq. 3.9.1.1-7}$$

$$\frac{d[Gal]}{dt} = (k_{1b}k_{2b} \frac{1}{k_{4b}} [L][H_2O] + k_{2b}[DP3][H_2O])Y_b \quad \text{Eq. 3.9.1.1-8}$$

$$\frac{d[DP3]}{dt} = (k_{1b} \frac{k_{3b}}{k_{4b}} [L]^2 - k_{2b}[DP3][H_2O])Y_b \quad \text{Eq. 3.9.1.1-9}$$

$$\begin{aligned} \frac{1}{Y_b} = & k_{2b} \frac{1}{k_{4b}} [H_2O] + \frac{k_{3b}}{k_{4b}} [L] + k_{1b} \frac{1}{k_{4b}} [L] + [DP3] + k_{2b} \frac{1}{k_{4b}} \frac{k_{5b}}{k_{6b}} [Glu][H_2O] + \\ & \frac{k_{3b}}{k_{4b}} \frac{k_{5b}}{k_{6b}} [L][Glu] + k_{2b} \frac{1}{k_{4b}} \frac{k_{7b}}{k_{8b}} [Gal][H_2O] + \frac{k_{3b}}{k_{4b}} \frac{k_{7b}}{k_{8b}} [L][Gal] \end{aligned} \quad \text{Eq. 3.9.1.1-10}$$

where [L], [Glu], [Gal] and [DP3] represent the concentration of lactose, glucose, galactose, and GOS (trisaccharide) in mol·kg⁻¹, respectively.

Table 1. Estimation of model parameters from (Boon et al., 1999).

Rate constant	Unit	Average value
k _{1b}	M ⁻¹ ·min ⁻¹	0.019 ± 0.004
k _{3b} /k _{4b}	-	4600
log(k _{3b} /k _{4b})	-	3.7 ± 0.1
1/k _{4b}	-	11 ± 5
k _{5b} /k _{6b}	-	21
log(k _{5b} /k _{6b})	-	1.3 ± 0.2

Based on the mathematical model proposed by Boon et al. (1999), I simulated data related to the synthesis of GOS in a STR using relevant data from the literature employing Eq. 3.9.1.1-6 - Eq. 3.9.1.1-10. The *k* values represent the reaction rate constants (see values in Table 1).

Figure 3 provides an example of the predicted time course of the saccharide profiles under selected reaction conditions. The maximum GOS yield of 30% w·w⁻¹ is achieved around 120 min. A continuous increase in monosaccharides (glucose and galactose) over time is observed, indicating hydrolysis activity that ultimately dominates over the trans-glycosylation reaction.

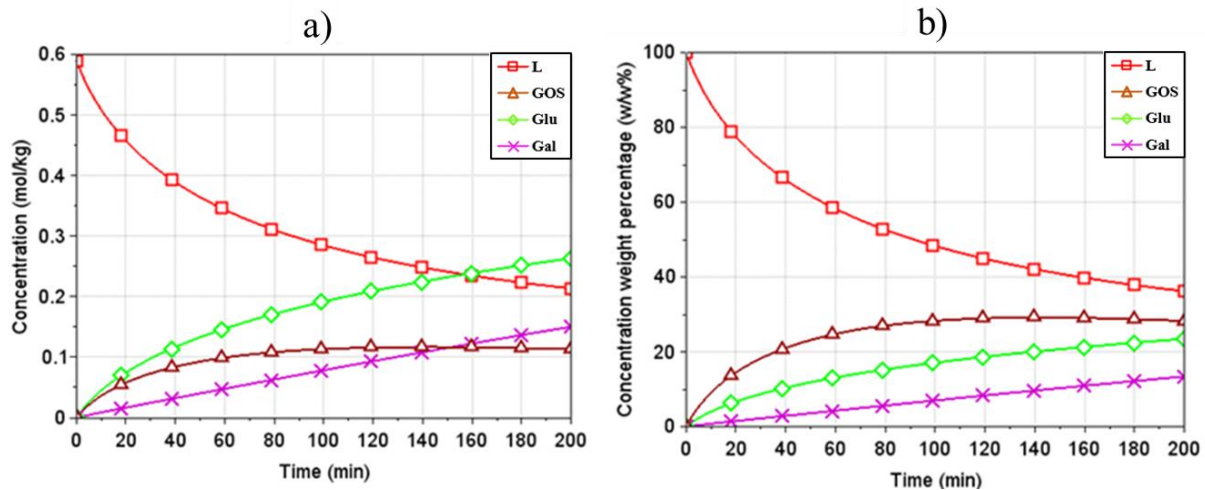


Figure 3. Simulation data reported by Boon et al. (Boon et al., 1999) presenting concentration profiles of saccharides in STR with an initial lactose concentrations of 0.59 mol·kg⁻¹, enzyme load of 1.21 g·L⁻¹, 40 °C, pH 5.0. a) in mol·kg⁻¹ b) in % w·w⁻¹.

Note that the authors operated the experiments for only a short period of time, no longer than four hours. Furthermore, the reaction did not account for the possibility of synthesizing other oligosaccharides of higher polymerization (>DP3). It is also not taken into account that non-lactose disaccharides, such as galactose and allolactose, may also be formed during this reaction.

3.9.1.2. Kinetic model proposed by Palai et al. (2012)

The kinetic modeling study by Palai et al. (2012) is also intimately related to our experiments. A kinetic model based on a four-step reaction pathway with six parameters derived from the Michaelis-Menten equation was proposed to by (Palai et al., 2012). The model was used to describe the synthesis of GOS by Biolacta FN5, an enzyme derived from *Bacillus circulans*. The model considers the synthesis of GOS at a high lactose concentration (525 g·L⁻¹). The process occurs simultaneously with hydrolysis and trans-glycosylation reactions and produces

oligosaccharides with a maximum DP of 5, DP5. A noteworthy aspect of the model is the use of monosaccharides instead of glucose and galactose uniformly. The observed results of glucose inhibition are consistent with the study of (Boon et al., 1999). The inhibition of galactose is negligible. Due to the absence of consideration for the synthesis of non-lactose disaccharides, the prediction model underestimates lactose to a certain degree. Moreover, the kinetic model does not account for the separate synthesis pathway of DP3-5 that has been uniformly replaced by a one-step GOS.

Palai et al. (Palai et al., 2012) proposed the following reaction scheme:



where E, M, L and G denote enzyme, monosaccharides (glucose and galactose), lactose and GOS (DP>3) respectively and k values are the rate constants for step reactions.

The four-step reactions can be represented by the following set of ordinary differential equations:

$$\frac{d[E]}{dt} = -k_1[E][L] + k_{-1}[EL] + k_3[EM][L] - k_{-3}[E][G] + k_4[EM][G] \quad \text{Eq. 3.9.1.2-15}$$

$$\frac{d[EL]}{dt} = k_1[E][L] - k_{-1}[EL] - k_2[EL] \quad \text{Eq. 3.9.1.2-16}$$

$$\frac{d[EM]}{dt} = k_2[E][L] - k_3[EM][L] + k_{-3}[E][G] - k_4[EM][G] \quad \text{Eq. 3.9.1.2-17}$$

$$\frac{d[L]}{dt} = -k_1[E][L] + k_{-1}[EL] - k_3[EM][L] + k_{-3}[E][G] \quad \text{Eq. 3.9.1.2-18}$$

$$\frac{d[M]}{dt} = k_2[EL] \quad \text{Eq. 3.9.1.2-19}$$

$$\frac{d[G]}{dt} = k_3[EM][L] - k_{-3}[E][G] \quad \text{Eq. 3.9.1.2-20}$$

Estimated values of model parameters reported by Palai et al. (2012) are shown in Table 2.

Table 2. Estimated values of the rate constants by (Palai et al., 2012).

Rate constant	Unit	Average value
k_1	$\text{mM}^{-1} \cdot \text{h}^{-1}$	1023.631
k_{-1}	h^{-1}	0.435
k_2	h^{-1}	1.191×10^{11}
k_3	$\text{mM}^{-1} \cdot \text{h}^{-1}$	5703.084
k_{-3}	$\text{mM}^{-1} \cdot \text{h}^{-1}$	1.404×10^6
k_4	$\text{mM}^{-1} \cdot \text{h}^{-1}$	17.758

I implemented the model with the reported kinetic parameters in a numerical software package (see Sect. 4.3) to replicate the behavior of STR as reported by the authors. The results obtained are in agreement with those presented in the authors' article. Figure 4 gives an example of predicted saccharides concentration over time under the reaction conditions of $417 \text{ g} \cdot \text{L}^{-1}$ initial lactose concentrations, $1.459 \text{ g} \cdot \text{L}^{-1}$ enzyme load, 40°C , pH 6.0. Results indicate that, under the given reaction conditions, a GOS yield of $34\% \text{ w} \cdot \text{w}^{-1}$ can be achieved by terminating the reaction at 5 h.

A limitation of the proposed model is that it does not take into account the non-lactose disaccharides produced during the reaction. In addition, the inhibitory effect of glucose is not considered in the model, although they acknowledge that glucose exerts some inhibition during the reaction. Also, the model does not distinguish between glucose and galactose, only accounts for monosaccharides as the sum of both glucose and galactose. Another simplification of the proposed reaction scheme is that oligosaccharides of different polymerization degrees (DP3-6) produced during the reaction are modeled together as a single state variable.

The units used in the model for enzymes and products are also ambiguous. For example, both $\text{g} \cdot \text{L}^{-1}$ and $\text{mol} \cdot \text{L}^{-1}$ are used to express concentrations. Since authors failed to report the molar masses of enzyme and GOS they used for their modeling study, replication of their results is troublesome. As another noteworthy point, authors claim that they used a high concentration of lactose as substrate for the reaction at temperature 40°C . According to available evidence, solubility of lactose is about $25\% \text{ w} \cdot \text{w}^{-1}$ at the reported temperature. According to the authors, the samples were centrifuged and microfiltered prior to HPLC analysis. Thus, the possible removal of lactose precipitates during sample preparation when solubility limits are exceeded raises some concerns.

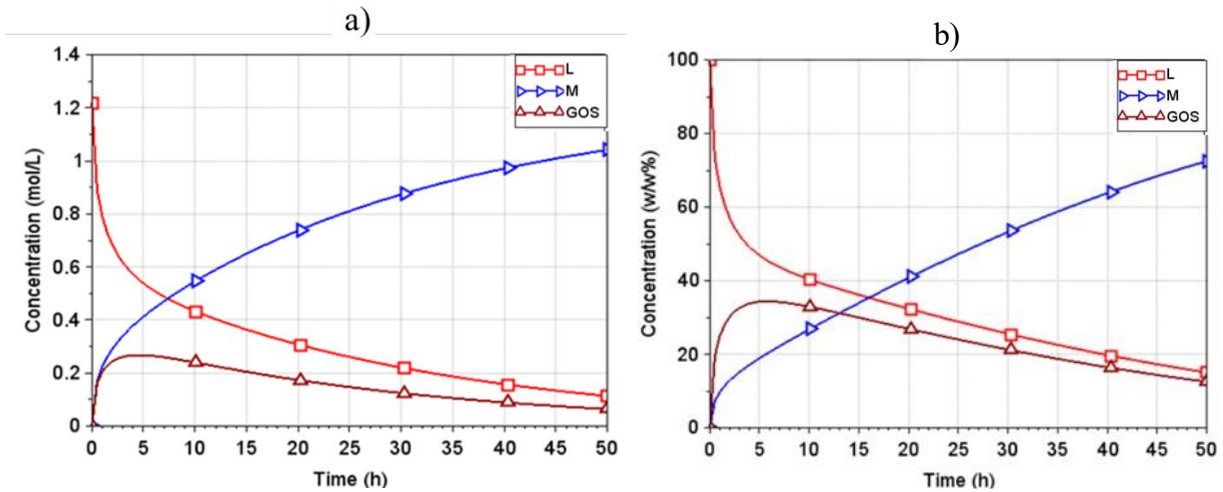


Figure 4. Simulation data reported by Palai et al. (2012) concentration profiles of saccharides in STR with an initial lactose concentrations of $417 \text{ g} \cdot \text{L}^{-1}$, enzyme load of $1.459 \text{ g} \cdot \text{L}^{-1}$, 40°C , pH 6.0. a) in $\text{mol} \cdot \text{L}^{-1}$ b) in $\% \text{w} \cdot \text{w}^{-1}$.

3.9.2. Enzyme inactivation models

The mechanisms of enzyme inactivation are generally classified into two categories: series-type mechanisms and single-step mechanisms. As a general rule, the series-type mechanism assumes that there is an intermediate transition stage during the enzyme inactivation process, i.e., an enzyme that is non-stable and has lost some of its enzymatic activity, followed by further inactivation to achieve a state of complete inactivation or residual activity. On the contrary, the single-step mechanism assumes that the inactivation of the enzyme is a one-step process without intermediate transitions. It can further be subdivided into reaction mechanisms, depending on whether the final enzyme has been completely deactivated. The reaction mechanisms assume a complete deactivation of the enzyme in its final state as well as the residual activity being retained by the final enzyme, respectively.

I should point out that literature models describing the stability of GOS-catalyzing β -galactosidases can be considered as specific cases of the general series-type model proposed by Henley and Sadana et al. (1985, 1987).

The two-stage series mechanism of inactivation is represented by the scheme:

$$E_0 \xrightarrow{k_1} E_1^{\alpha_1} \xrightarrow{k_2} E_2^{\alpha_2}, \quad \text{Eq. 3.9.2-21}$$

where E_0 , E_1 , and E_2 represent the enzyme activity at initial, intermediate, and final state, respectively, k_1 and k_2 are the deactivation velocity coefficients, and α_1 and α_2 are the ratio of specific activities of E_1/E_0 and E_2/E_0 , respectively.

The relative enzyme activity y at specific time t can be calculated as:

$$y = \left[1 + \frac{\alpha_1 k_1 - \alpha_2 k_2}{k_2 - k_1} \right] \exp(-k_1 t) - \left[\frac{\alpha_1 k_1 - \alpha_2 k_2}{k_2 - k_1} \right] \exp(-k_2 t) + \alpha_2, \quad \text{Eq. 3.9.2-2}$$

If the enzyme is assumed to be completely inactivated at its final state, i.e., $\alpha_2=0$, then Eq. 3.9.2-2 is reduced to

$$y = \left[1 + \frac{\alpha_1 k_1}{k_2 - k_1} \right] \exp(-k_1 t) - \left[\frac{\alpha_1 k_1}{k_2 - k_1} \right] \exp(-k_2 t) \quad \text{Eq. 3.9.2-3}$$

A specific case of the above model is the single-step model with non-zero activity at the final enzyme state, such that $k_2=0$. In this case, the reaction scheme is reduced to:



and Eq.3.9.2-2 can be simplified to:

$$y = (1 - \alpha_1) \exp(-k_1 t) + \alpha_1, \quad \text{Eq. 3.9.2-5}$$

If the native (active) enzyme is assumed to be converted in a one-step reaction into an inactive structure, i.e., $\alpha_1 = 0$, then the model can be further reduced to:

$$y = \exp(-k_1 t), \quad \text{Eq. 3.9.2-6}$$

This latter, simplified model is known as the single-step first-order model, and it has been validated for β -galactosidases of various origins by several studies.

Only a few studies have investigated the stability of beta-galactosidases during GOS production. A summary of the models proposed in the literature is provided in Table 11 (in A2 Additional information).

As indicated in Table 11, the half-life of β -galactosidase in the generation of GOS ranges from 10⁻

² to 10⁵ h, depending on the source of enzyme, type of application (free or immobilized), and various reaction conditions, such as pH, temperature, and substrate concentration.

The most widely used model is the first-order inactivation model. Albayrak and Yang (2002) applied this model to investigate the stability of free and immobilized β -galactosidase from *Asperillus oryzae*. It was concluded that the immobilized enzyme was more thermally stable than the free enzyme, with half-lives of 399 h and 10040 h at 40°C and pH 4.5, respectively. It is worth noting that the presence of high amounts of lactose reported to enhance enzyme stability (Warmerdam et al., 2013). However, Albayrak et al. conducted the stability tests in a 0.2 M acetate buffer deficient in lactose.

Huang et al. (2020) described the effect of different temperatures on the stability of *Klebsiella oxytoca* ZJUH1705-derived β -galactosidase at high lactose concentrations (40% w·w⁻¹) using a first-order inactivation model. The stability of the enzyme was inversely proportional to temperature in the range of 30°C-60°C in their experiments. Under optimal conditions (*Kluyveromyces marxianus* CCT 7082, 37°C, pH 7.0 and *Kluyveromyces marxianus* ATCC, 30°C, pH 7.0), the half-life of both purified enzymes was 115.5 hours. In addition, the purified enzymes had greater thermal stability and higher GOS yields (more than 30% w·w⁻¹) compared to the crude enzyme.

Torres and Batista-Viera (2012) used a series-type model to explain the stability of β -galactosidase (Biolacta N5) from *Bacillus circulans* in GOS production. The thermal stability of the enzyme was determined in a buffer without lactose for 24 hours. The immobilized enzyme had better thermal stability compared to the free enzyme under the same conditions, which supports the study of Albayrak and Yang (2002). The half-lives of immobilized and free enzymes were determined to be ca. 21 and 12 hours at 50°C and pH 8.0, respectively.

Urrutia et al. (2013a) described the changes in enzyme activity during GOS synthesis using β -galactosidase from *Bacillus circulans* (Biolactasa-NTL CONC X2) using a two-stage series mechanism. At 60 °C and pH 6, citrate-phosphate buffer 0.1 M, the results show that the model

can accurately predict the remaining activity of the free and immobilized enzymes in the reaction with half-lives of approximately 0.05 h and 0.25-3 h, respectively.

Huerta et al. (2011) utilized a more complex two-stage series mechanism to describe changes in β -galactosidase activity from *Aspergillus oryzae* during GOS synthesis. Measurements of enzyme stability were performed in a buffer without the presence of substrate. The half-lives of the free and immobilized enzymes decreased sharply with increasing temperature in the range of 50°C to 60°C. At 50 °C and pH 4.5, the half-life of immobilized enzymes was approximately four times that of soluble enzymes.

As shown in Table 11, enzyme stability is usually assessed by the oNPG method. Although it is a convenient and fast method, it provides an indirect way to measure the true GOS production activity. This method can underestimate and/or overestimate true enzyme activity and requires a complex computational procedure to correct oNPG conversion activity for the presence of lactose, glucose, galactose and oligosaccharides in the activity assay (Warmerdam et al., 2013).

3.9.2.1. Enzyme inactivation model proposed by Warmerdam et al. (2013)

Among the available studies on enzyme stability, the study of Warmerdam et al. (2013) is the most relevant for my modeling study (as presented later in Sect. 5.2). Warmerdam and her coworkers (2013) have experimentally investigated the stability of Biolacta N5 obtained from *Bacillus circulans* at different lactose concentrations and temperatures in STR. The results indicate that the enzyme has higher thermal stability at high initial lactose concentrations. A half-life of 0.82 h and 16 h was measured at initial lactose concentrations of 5% w·w⁻¹ and 30% w·w⁻¹, respectively. Furthermore, this study found that the enzyme maintained greater activity in lactose-containing solutions than buffer with absence of substrate. For example, in buffer at 60 °C, the enzyme had a half-life of 0.048 hours, while in a 30% w·w⁻¹ lactose solution, it had a half-life of 16 hours. Molecular crowding, or complexation with the substrate or with the galactose moiety, may be responsible for the higher stability of the enzyme.

Enzyme inactivation in STR was modeled with a first order inactivation model, such as:



where E and I are the concentrations of active and inactive enzyme, respectively. k_d is the enzyme inactivation constant in h^{-1} . The enzyme activity (experimentally measured with oNPG activity assay) is then given as

$$v = -k_d[E] \quad \text{Eq. 3.9.2.1-2}$$

Using an initial lactose concentration of 30% w·w⁻¹, half-life time of Biolacta N5 is reported to be 29 h, 29 h, and 16 h, for 25 °C, 40 °C, and 60°C, respectively.

4. MATERIALS AND METHODS

4.1. Materials

All experiments utilized Biolacta N5 (Amano Enzyme Inc., Nagoya, Japan), a β -galactosidase derived from *Bacillus circulans*, as a catalyst to convert lactose into GOS. The activity of the crude enzyme preparation used in this study was 9230 ± 558 U per gram of crude enzyme, as determined by the activity assay detailed in Sect. 4.2. Except for the long-term experiments, Lactochem Fine Powder, a pharmaceutical-grade α -lactose monohydrate provided by FrieslandCampina Domo B. V. (Amersfoort, The Netherlands), was utilized as the substrate in all tests. Lactopure Regular Power 150 M (FrieslandCampina Domo B.V., Amersfoort, The Netherlands), a food-grade lactose preparation derived from whey with a typical lactose content of 99.7%, was used for the long-term campaigns (see Sect. 4.5.4).

4.2. Enzyme activity assay

A direct measurement method was used to measure the activity of Biolacta N5 using $300 \text{ g} \cdot \text{kg}^{-1}$ lactose as substrate. Deionized water was served as a reaction buffer, and NaOH was added in order to adjust the pH to 6.0. Biolacta N5 at a concentration of $0.91 \text{ g} \cdot \text{kg}^{-1}$ was added to the reaction solution to commence the reaction. Three replications were performed for the reaction. Upon completion of a 20-minute incubation at 50°C , the reaction was further heated for 30 minutes at 90°C to terminate the reaction. The concentration of DP2 was determined by High Performance Liquid Chromatography (HPLC) as described in Sect. 4.8. Under the specified reaction conditions, one unit of enzyme activity (U) was defined as the amount of enzyme needed to transform (or converted) $1 \mu\text{mol}$ of DP2 per minute.

4.3. Modelling transgalactosylation reactions

In-silico studies were carried out to predict the performance of STRs and continuous-EMRs in producing GOS. First, selected kinetic models (see Eq. 3.9.1.2-5 – Eq. 3.9.1.2-10 in Sect. 3.8.1.2)

and enzyme stability models (see Eq. 3.8.2.1-1 - Eq. 3.8.2.1-2 in Sect. 3.8.2.1) reported in literature were adopted for simulation purposes of STR performance. Then, a mathematical framework was developed for describing GOS conversion in continuous-EMRs. Simulation studies were performed by using Scilab (version 6.1.1, 2021), a numerical software package by Scilab Enterprises (France). Model simulations were carried out by the numerical integration of sets of ordinary differential equations (ODEs) using the function *ode*, the built-in ODE solver of Scilab.

4.4. STR

4.4.1. *Enzymatic conversion in batch fashion*

Using the batch STR shown in Figure 5, small-scale batch experiments were conducted with enzyme activities ranging from 923 to 92301 U·kg⁻¹ to determine whether enzyme load has a significant effect on reaction rate. In each test, a reaction solution consisting of 300 g·kg⁻¹ lactose was prepared in a beaker and placed on hotplate magnetic stirrer for 24 to 48 h. A temperature control unit was included in the C-MAG HS7 hot plate magnetic stirrer (IKA-Werke GmbH & Co. KG, Staufen, Germany) to maintain the solution temperature at 50 °C. The pH of the reaction solution was adjusted to 6.0 by adding NaOH liquid, and the magnetic stirrer was continuously agitated at a rate of 60 rpm throughout the operation. Prior to HPLC analysis, samples were collected at periodic intervals (5min, 30min, and/or 1h) and inactivated at 90 °C for 30 minutes.

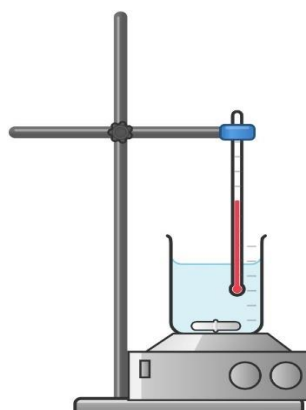


Figure 5. Schematic diagram of a STR.

4.4.2. Evaluation of process curves

According to the model adopted from Pázmándi et al., (2018), the progression curves of individual saccharides fractions in STR were evaluated at different enzyme loads (from 0.1 g·kg⁻¹ to 10 g·kg⁻¹). The saturation model describes the concentration of the generated saccharides fractions (e.g., glucose, galactose, and GOS fractions) in relation to incubation time:

$$F(t) = C_0 + p_1(1 - e^{-p_2 t}) \quad \text{Eq. 4.4.2-1}$$

where t was the reaction time, C_0 was the initial concentration of saccharides, and $p_1 \times p_2$ was the initial reaction velocity (i.e., slope of the curve at time point $t = 0$). While $p_2 > 0$, in case of DP2 (expressed in g·kg⁻¹), $p_1 < 0$ (F was decreasing), in all other cases $p_1 > 0$ (F was increasing).

As a next step, a linear function with no intercept was fitted to the enzyme activity of various saccharide fractions (presented by saccharide concentrations) in relation to their initial reaction velocities ($p_1 \times p_2$). The normality of the model residuals was checked by their skewness and kurtosis (the absolute values were all below 1). An ANOVA F-test was conducted to determine the accuracy of the model. Additionally, t-tests were performed on the parameter estimations. Finally, the explained variance rates (R^2) were computed, and their significance was evaluated. The statistical assessment was performed with the statistical software IBM SPSS v27 (Armonk, NY) (IBM Corp. Released 2017. IBM SPSS Statistics for Windows).

4.5. Continuous-EMR

4.5.1. Construction of continuous-EMR

An overview of the flowsheet for the (semi-) pilot scale EMR used in the continuous production of GOS can be seen in Figure 6. It consists of two components: a stirred-tank reactor (TK-1) and an external UF module (M-1). Through this set-up, it was possible to control the recirculation flow rate, the retentate pressure, the temperature, the permeate flow, and the liquid level in TK-1 during operation.

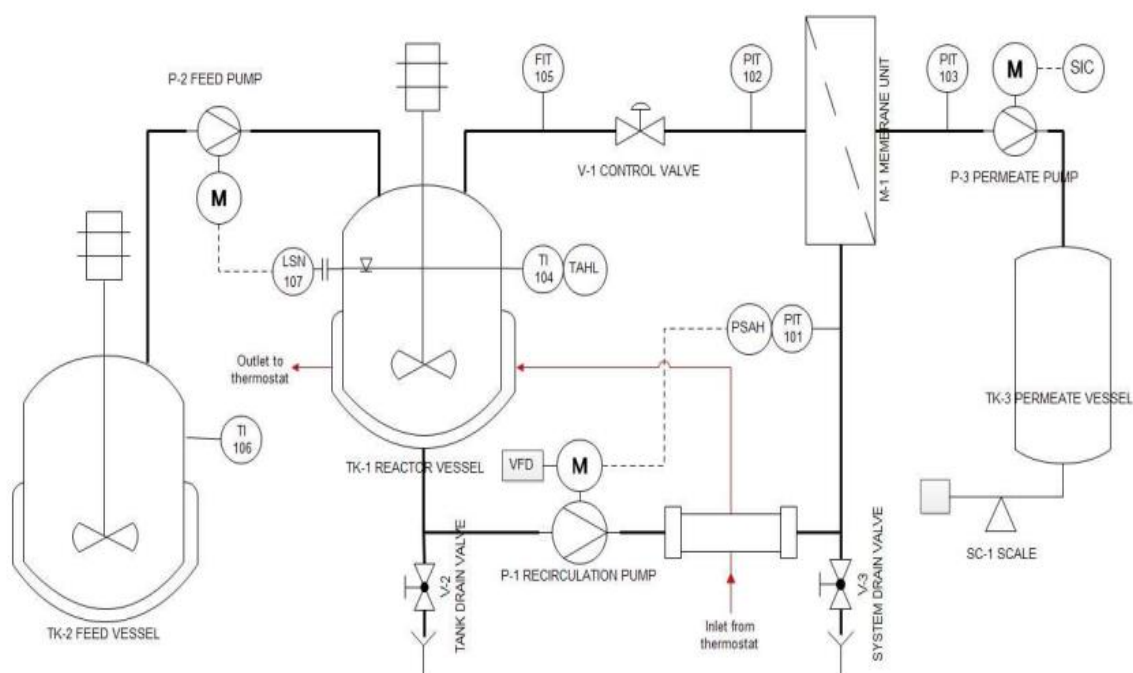


Figure 6. Piping and instrumentation diagram of continuous UF-assisted enzymatic reactor (EMR).

In the 4 L reaction vessel (TK-1), soluble enzymes were used to catalyze the enzymatic reaction. The recirculation pump (P-1) that circulates the reaction liquor through the UF module was a Hydra-Cell D-10 diaphragm pump (Wanner Engineering, Inc., US). A magnetic-inductive flow meter SM6000 (FIT) manufactured by IFM electronic GmbH (Essen, Germany) measures the recirculation flowrate set by the frequency drive (VFD). The control valve V-1 was used to manually adjust the retentate-side pressure to a desired value. The pressures on the retentate-side and permeate-side were measured by the pressure gauges PIT-102 and PIT-103 (SUKU 6850, SUKU GmbH, Germany), respectively. A scale SC-1 (FKB 30K1A, KERN&SOHN GmbH, Germany) monitors the weight of the permeate collected in the permeate vessel TK-3. The desired value for permeate flow was achieved by adjusting the speed of the peristaltic pump P-3 (323SD, Watson Marlow Inc, US). As a result of the weight and time measurements of the collected samples of permeate, permeate flux can be determined. The substrate solution consisting of $300 \text{ g} \cdot \text{kg}^{-1}$ lactose was stored in the 50 L jacketed stainless-steel feed vessel (TK-2). In the 50 L stainless steel jacketed feed vessel (TK-2), the fresh $300 \text{ g} \cdot \text{kg}^{-1}$ lactose substrate solution was stored. The peristaltic pump P-2 (OEM M1500, Verder Hungary Kft, Budapest, Hungary) was regulated by a

Nivocont KKH-212-5 compact conductive level switch installed in TK-1 to ensure a constant volume in the reactor TK-1. By circulating warm water generated by a Julabo VC (Julabo GmbH, Germany) laboratory thermostat through a double pipe heat exchanger and the jacket of TK-1, the substrate solution in TK-2 was maintained at 50 °C. A digital temperature sensor TI-101 was used to measure the actual temperature in the reactor. This sensor was purchased from Dostmann GmbH, Germany. In the stainless-steel housing of M-1, a 2" spiral-wound element was installed. A ST-2B-1812PHT-F element in sanitary full-fit design was purchased from Synder Filtration Inc, USA. The 10 kDa UF membrane with a filtration area of approx. 0.37 m² was made of a polyethersulfone active layer cast on polypropylene backing material.

4.5.2. Preliminary filtration tests

In order to narrow the operating conditions of the filtration process, two preliminary tests were performed, as described in Sect 4.5.2.1 and 4.5.2.2. The tests were performed in a total-recycle mode, in which both retentate and permeate streams were recycled back into the reactor. The recirculation flowrate of the retentate was set to 0.18 m³·h⁻¹. The experiments were performed with 2 kg of process liquid consisting of 30% w·w⁻¹ lactose under the condition of pH 6.0 and temperature at 50 °C. The permeate flux was monitored during the test runs to investigate the filtration performance of the UF membrane. Chemical analysis of the samples was not conducted.

4.5.2.1. Pressure-scan

The reaction was initiated with the addition of 10 g·kg⁻¹ of Biolacta N5 into the reaction vessel, with the TMP gradually raised from 1 to 4 bar during the reaction process. The permeate flux was monitored.

4.5.2.2. Determination of limiting flux

Initialization of the reaction was achieved by dosing 1g·kg⁻¹ Biolacta N5 into the process liquid. A TMP of 4.0 bar was set. During the experiment, the permeate flux was monitored for an increasing enzyme load between 1 and 120 g·kg⁻¹ until it reached a (quasi) steady state (ca. 1 hour

later). A variation of enzyme concentrations (from 1 and 120 g·kg⁻¹) was used in the same procedure.

4.5.3. Short-term enzymatic conversion

An EMR was operated continuously for eight short-term tests (typically for 6 to 9 hours) using a 30 w·w⁻¹% lactose solution at pH 6.0 and 50°C. The experiments were performed by varying the enzyme load (between 923 to 92301 U·kg⁻¹) and the permeate flow (between 0.8 and 1.8 kg·h⁻¹) under otherwise identical conditions. There was a two-kilogram solution of lactose added to the reactor, and the remaining solution was stored in a thermostatic substrate tank. Once a certain amount of Biolacta N5 dosage (from 23 to 92301 U·kg⁻¹) has been administered, the circulation pump has been operated at a crossflow rate of 0.17 ± 0.01 m³·h⁻¹. A pressure-adjusting valve was used to set a retentate pressure of 0.5 bar. A constant permeate flow rate was achieved by adjusting the rotational speed of the permeate pump. This resulted in a constant residence time for the permeate. A constant volume in the reactor was maintained by continuously adding 300 g·kg⁻¹ fresh substrate solution and removing the enzyme-free product at the same rate during the entire process. Throughout the process, temperature, pressures on the retentate and permeate sides, flow rates of the permeate, and the total mass of the collected permeate were monitored. In order to analyze the carbohydrate content of the permeate stream (i.e., from the enzyme-free product stream), samples were taken periodically. The membrane was cleaned in accordance with the procedure described in Sect.4.7.

4.5.4. Long-term enzymatic conversion

Two long-term experiments, designated L1 and L2, were conducted under identical operating conditions for an extended period of time (over 100 hours). In both runs, the operation was conducted by dosing 46151 U·kg⁻¹ (10 g of crude enzyme) of Biolacta N5 in 2 kg of reaction liquid with 30 w·w⁻¹% lactose concentration at 50 °C and pH 6.0. The retentate pressure was adjusted to 1.0 bar in both runs. The permeate pump was set to generate a constant flowrate of 1.1 kg·h⁻¹, resulting in a residence time of 1.8 h. The recirculation flowrate was set to 0.17 m³·h⁻¹.

HPLC analysis was conducted on three samples taken from the permeate stream during each periodic sampling. Analyses of samples taken from L1 were conducted by HPLC without pretreatment. The deactivation of three samples in L2 was accomplished by heat deactivation (90 °C, 30 min), acid deactivation (HCl), and analysis without deactivation pretreatment. Membrane cleaning was performed as described in Sect. 4.7.

4.5.5. Performance assessment

Nonlinear regression was employed to evaluate the relationship between the steady-state carbohydrate composition and the operational factor ($\tau \times c_E$). An arbitrary selected empirical model was fitted to the experimental measurements of the reaction products, including DP3-6, glucose, and galactose, as a function of operational parameters to derive the following quantitative relationship:

$$w_i = \frac{b_1 c_E \tau}{b_2 c_E \tau + 1} + \varepsilon \quad \text{Eq. 4.5.5-1}$$

where w_i represents the relative mass percentage of the individual saccharide fraction at steady state, b_1 and b_2 stand for the model coefficients, τ was the residence time, c_E indicates the enzyme concentration, and ε was the error term. This regression model was used for the DP2 fraction as follows:

$$w_{DP2} = 100 - \frac{b_1 c_E \tau}{b_2 c_E \tau + 1} + \varepsilon \quad \text{Eq. 4.5.5-2}$$

The statistical assessment was carried out using the statistics and curve fitting toolboxes implemented in (MATLAB, R2015a) (The Mathwork Inc., Natick, MA, USA).

4.6. Cyclic-EMR

4.6.1. Construction of cyclic-EMR

With the lab-scale equipment shown in Figure 7, the production of GOS was carried out batchwise, over a number of cycles. A STR and an exterior UF membrane unit were the main components of

the cyclic-EMR.

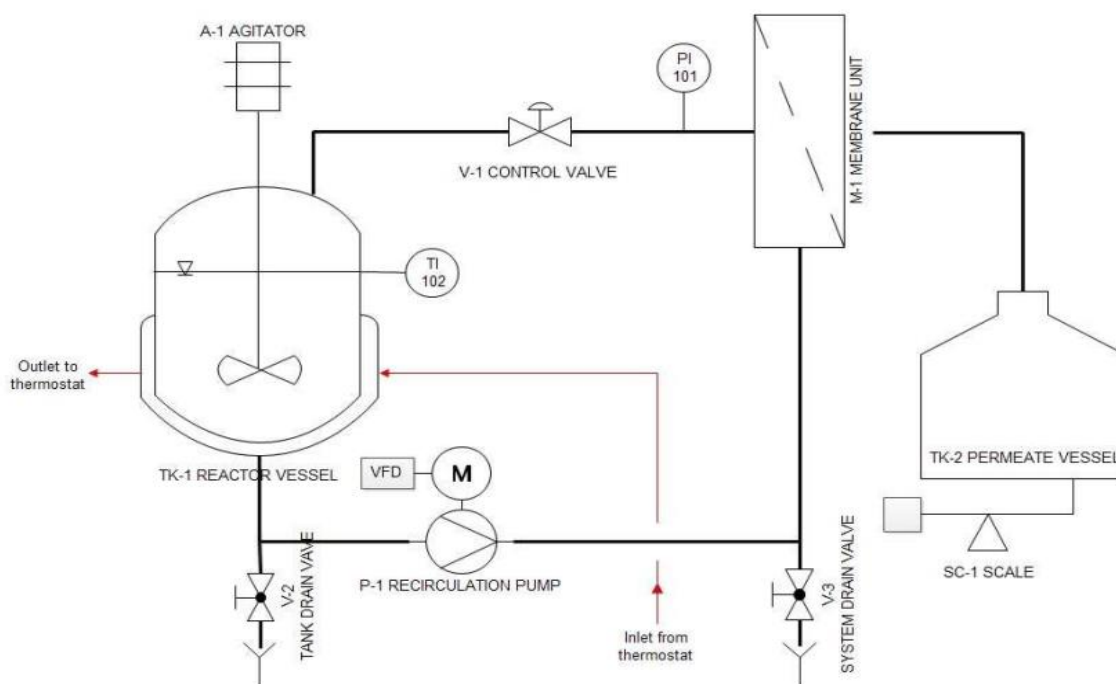


Figure 7. Piping and instrumentation diagram of cyclic enzymatic membrane reactor (cyclic-EMR).

Enzymatic conversion of lactose into GOS was performed in a stainless-steel double-jacketed vessel (TK-1) equipped with an overhead stirrer (A-1). The reaction temperature was maintained at 50 °C using a Julabo 5B water bath thermostat (Julabo GmbH, Germany). The temperature was monitored using a digital TI-102 thermometer (Dostmann GmbH, Germany).

The reaction liquid was concentrated by UF after the reaction step was completed in the STR. Recirculation of retentate from the ultrafilter was accomplished by using a Hydra-Cell D-10 diaphragm pump (Wanner Engineering, Inc., Minneapolis, MN, USA). The recirculation flowrate was set to 180 L·h⁻¹ by using a variable frequency drive (VFD). The pressure was adjusted by the retentate control valve (V-1) and monitored by the pressure gauge (PI-101). A polyethersulfone hollow-fiber module (type: FB02-CC-FUS-0382) of 0.26 m² and 30 kDa was included in the membrane unit (M1). This module was purchased from Microdyn Nadir GmbH (Wiesbaden, Germany). A scale (SC-1) was used to monitor the weight of the permeate collected during UF in a permeate vessel (TK-2).

4.6.2. *Enzymatic conversion in cyclic-EMR*

A protocol consisting of three operational steps in five successive cycles was used to carry out the enzymatic conversion:

1. In the first step, a traditional STR, TK-1, was employed to carry out a batchwise reaction. The reaction was initiated by dosing an initial enzyme activity of $8307 \text{ U} \cdot \text{kg}^{-1}$ ($0.9 \text{ g} \cdot \text{kg}^{-1}$) to 9.5 kg reaction solution with an initial lactose concentration of $300 \text{ g} \cdot \text{kg}^{-1}$ at 50°C and $\text{pH } 6.0$. Periodic samples were taken from the reactor and heat-treated at 90°C for 30 minutes prior to the measurement of saccharides by HPLC.
2. Following the first step, the membrane unit M-1 was attached to the reactor, and the reaction liquid was filtered through UF at 0.5 bar TMP until 8.4 kg of permeate was collected.
3. A third step involved the de-attachment of the membrane module M-1 from the plant. 8.4 kg of fresh substrate solution consisting of $300 \text{ g} \cdot \text{kg}^{-1}$ of lactose was added to the concentrated enzyme solution in the reactor to maintain a constant volume in TK-1. Afterward, step 1 of the next cycle was initiated. After the membrane was de-attached, it was cleaned in accordance with Sect.4.7.

4.6.3. *Performance assessment*

The saturation model described in Sect. 4.4.2 was used to verify the concentration of the generated saccharide fractions (e.g., glucose, galactose and GOS fractions) in relation to the reaction time.

The two-stage series mechanism (Torres and Batista-Viera, 2012, Urrutia et al., 2013a, Vera et al., 2011) and its simplified forms (Albayrak and Yang, 2002, Huang et al., 2020, Warmerdam et al., 2013) (mentioned in Sect. 3.9.2) were used to quantify the stability of lactose-converting β -galactosidase over time.

4.7. **Membrane regeneration**

Deionized water was tested for permeability prior to each test with the process liquor. Upon

completion of each filtration step, the membrane was cleaned in four steps as follows:

The membrane module was draining and flashing repeatedly with deionized water.

1. A NaOH solution (pH = 10-11) was circulated for 1-2 hours at 40-50 °C under 0.5-1 bar pressure for the purpose of cleaning the membrane.
2. For the removal of the cleaning agent, the plant was drained and flushed with water several times.
3. The permeability of the cleaned membrane was determined using DI water. Occasionally, when the original membrane permeability was recovered less than 75% by alkaline cleaning, subsequent cleaning with citric acid and/or Ultrasil 10 (sodium based alkaline EDTA) membrane cleanser (Ecolab, Paul, MN, USA) has been performed (1 w·w⁻¹%, 40-50 °C, 0.5⁻¹ bar, 0.5⁻¹ h).
4. During overnight storage, the module was immersed in a saturated salt solution to prevent microbial growth and membrane drying out.

4.8. HPLC

In accordance with the methodology described in (Pázmándi et al., 2018), carbohydrate compositions of samples (glucose, galactose, and DP2-6 fractions) were determined by high performance liquid chromatography (HPLC). There were three main components to the HPLC system, including (1) Thermo Separation, which includes an Intersciences SCM1000 degasser, a gradient pump P200, a built-in column oven, and an Autosampler AS100; (2) a Shodex R-101 refractive index detector from Showa Denko Europe GmbH, Munich, Germany; and (3) an N2000 Chromatography Data System from Science Technology (Hangzhou) Inc. (Hangzhou, China). Chromatography Data System N2000 performs peak detection and integration. The RNM carbohydrate 8 % Na⁺ 300 × 7.8 (Phenomenex, Torrance, CA, USA) analytical column and a guard column were used under the condition of 50 °C at 0.2 mL·min⁻¹ with a mobile phase of pre-filtered (2 µm) DI water. If not otherwise stated, samples collected from the permeate stream of the EMR were not subjected to heat deactivation prior to HPLC analysis. Prior to HPLC analysis,

samples collected during batch experiments and cyclic EMR were heat treated (90°C, 30 minutes).

4.9. Terminology

In this investigation, the following measures were employed:

Relative mass percentage fraction (w_i) was calculated as the ratio of the mass of a saccharide fraction i (m_i) to the total mass of saccharides present in the solution:

$$w_i = \frac{m_i}{\sum m_i} \times 100\% \quad \text{Eq. 4.9-1}$$

Residence time (τ) was determined by the weight of the reaction liquor in the reactor (V) dividing the mass flow rate of the permeate (q):

$$\tau = \frac{V}{q} \quad \text{Eq. 4.9-2}$$

Yield (Y) in percentage was defined as the concentration of the synthesized GOS (DP3-6) fractions (c_{DP3-6}) divided by the concentration of lactose in the feed (c_L):

$$Y = \frac{c_{DP3-6}}{c_L} \times 100\% \quad \text{Eq. 4.9-3}$$

Biocatalyst productivity (P) was defined as the total quantity of DP3-6 formed by one unit of crude enzyme preparation per hour:

$$P = \frac{c_{DP3-6}}{c_E \tau} \quad \text{Eq. 4.9-4}$$

5. RESULTS AND DISCUSSION

In this chapter, I first present the prediction results of a revised extended model based on the previously reported kinetic model by Palai et al. (2012) (in Sect. 5.1). The model was adapted to the mode of operation of our experiments, i.e., continuous GOS production utilizing free enzymes (β -galactosidases extracted from *Bacillus circulans*) in an ultrafiltration membrane-assisted enzymatic reactor (UF-EMR). The model predicts continuous-EMR reaction performance with respect to the relevant parameters (residence time and enzyme activity) (in Sect. 5.1.1), while enzyme inactivation during the process was also considered (in Sect. 5.1.2).

Furthermore, I present the results of a series of GOS generation catalyzed by Biolacta N5 in STR under different enzymatic activities (in Sect. 5.2.1). The study was conducted on the effect of various glucose concentrations on the inhibition of trans-glycosylation in STR (in Sect. 5.2.2).

Additionally, in Sect. 5.3, I provide laboratory results for a continuous enzymatic membrane reactor. I conducted a series of short-term experiments (~ 6 h) (in Sect. 5.3.2) as well as long-term runs (over 100h) (in Sect. 5.3.3). EMR performance was measured in terms of GOS productivity as a direct measure of the effectiveness of the biocatalyst. The effect of reaction parameters (residence time and enzyme activity) on the synthesis of each oligosaccharide in the reaction was also reported.

In Sect. 5.4, I describe laboratory results on the performance of an UF-EMR operated in a batch cycle (i.e., continuous cycles of reaction, filtration, and addition of fresh substrate) (in Sect. 5.4.2). I quantify the cycle-by-cycle loss of enzyme in the EMR (in Sect. 5.4.3) on the basis of a series of calibration curves obtained from small-scale STR experiments (in Sect. 5.4.1).

5.1. Modelling transgalactosylation reactions

The main objective of the modeling study reported in this Sect. was to simulate the performance of continuous-EMRs utilizing free enzymes and to predict the system behavior as a function of main operational parameters such as enzyme load and residence time.

As discussed in Sect. 3.9.1 in detail, there was a limited number of studies available in the literature on the mathematical modeling of the reactions catalyzed by β -galactosidases derived from *Bacillus circulans*. For my in-silico analysis, as a first step, I adopted the kinetic model proposed by Palai et al. (2012) and successfully recovered their simulation results for an STR set-up (see Sect. 5.1.1). Then, I have developed a mathematical framework for continuous-EMR configuration including a set of ordinary differential equations. I have performed dynamic simulations under various settings and also evaluated the steady-state performance of continuous-EMR as functions of residence time and enzyme load. Results of these investigations are summarized in Sect. 5.1.2.

As a next step, I have extended my model for accounting also for enzyme inactivation. I adopted the enzyme stability model proposed by Warmerdam et al. (2013) and integrated it into my mathematical framework. Predicted performance of continuous-EMR under enzyme activity losses were reported in Sect. 5.1.3.

5.1.1. Kinetic model development

Among the literature studies dealing with the mathematical description of enzyme kinetics on GOS synthesis, only two works focus on β -galactosidases of *Bacillus circulans* origin. These were the study of Boon et al. (1999) on Biolacta N5 and the study of Palai et al. (2012) on Biolacta FN5 (a further purified form of Biolacta N5).

Boon and his coworkers (1999) propose a rather complex model with 8 kinetic parameters, however, the documentation of their study was incomplete. They fail to report optimized values for the glucose inhibition rate constant parameters (k_5 , k_6) that were required to replicate their results. Thus, the Palai-model (Palai et al., 2012) was used for further mathematical analysis.

The kinetic model proposed by Palai and his coworkers (2012) was discussed in Sect. 3.9.1.2. I implemented the original model (Eq.3.9.1.2-5 – Eq.3.9.1.2-10), in a numerical software package as described in Sect. 4.3 and performed simulations to have a deeper insight into the system behavior. Figure 8 shows the evaluation of concentration of saccharides over operation time in a conventional STR for various enzyme loads under otherwise identical conditions (initial lactose

concentration $320 \text{ g}\cdot\text{L}^{-1}$, pH 6.0, 40°C).

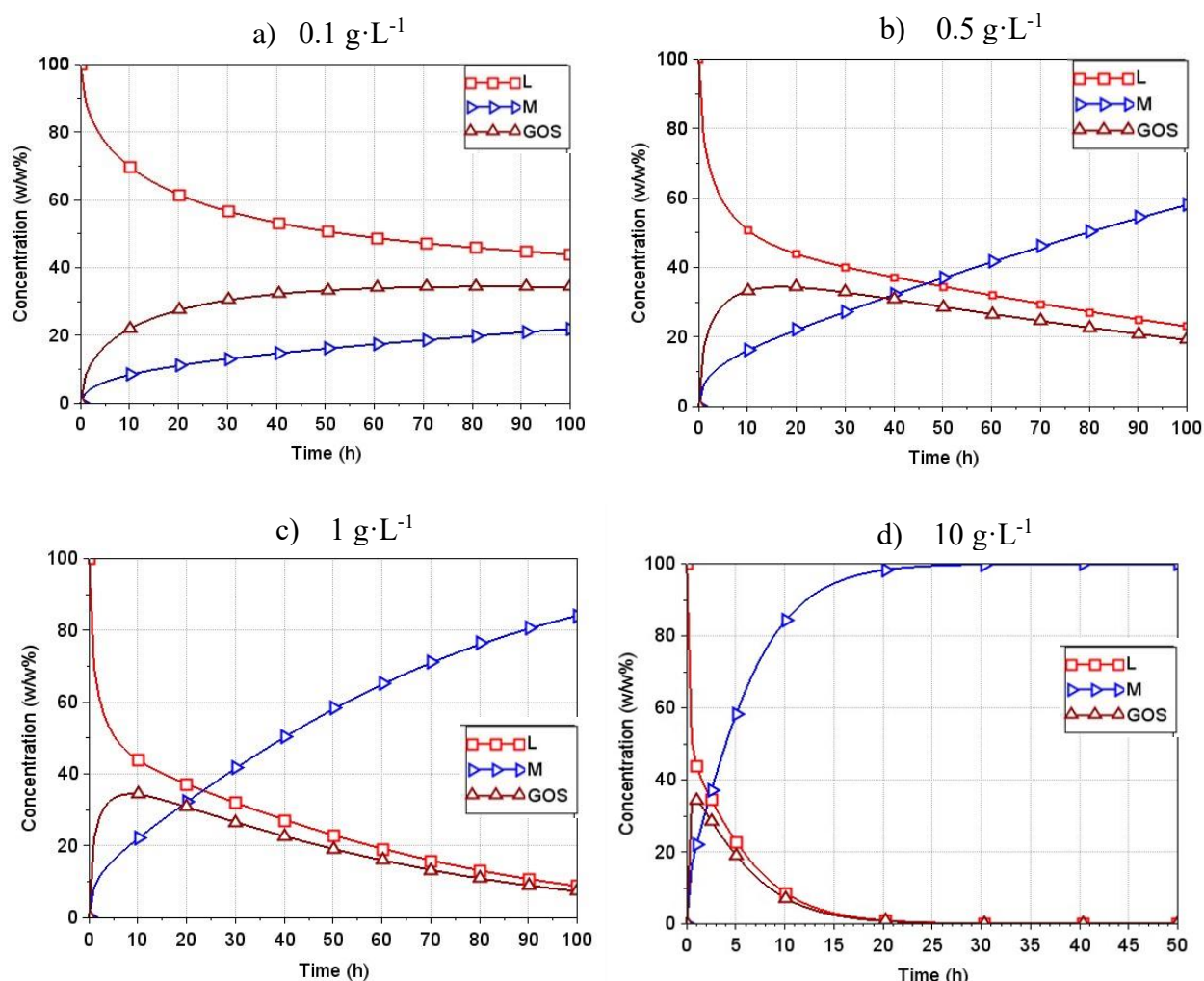


Figure 8. Simulation results of saccharide composition versus time in STR using kinetic model proposed by (Palai et al.(2012) a) $0.1 \text{ g}\cdot\text{L}^{-1}$ Biolacta N5, b) $0.5 \text{ g}\cdot\text{L}^{-1}$ Biolacta N5, c) $1 \text{ g}\cdot\text{L}^{-1}$ Biolacta N5, d) $10 \text{ g}\cdot\text{L}^{-1}$ Biolacta N5. Reaction conditions: initial lactose concentration $320 \text{ g}\cdot\text{L}^{-1}$, pH 6.0, 40°C . \square : DP2, Δ : GOS, \triangleright : Monosaccharides (glucose and galactose).

The simulation results suggest that a gradual decrease in lactose concentration occurs in the solution over time. Lactose undergoes both hydrolysis and trans-glycosylation reactions. The former produces monosaccharides (glucose and galactose), and the latter results in oligosaccharides of varying degrees of polymerization and glucose as by-product. It was to note that the concentration of GOS increases continuously after the start of the reaction until reaching a maximum of approx. 35% w·w⁻¹. After that, the concentration of GOS tends to decrease. The time of reaching GOS peak was greatly influenced by the actual enzyme load. The concentration

of monosaccharides in the solution consistently increases over time. A drawback of the proposed model was that it only accounts for the total monosaccharide content, irrespectively of the ratio of glucose to galactose. It was, however, obvious from the simulation results that a careful selection of enzyme load and incubation time was required in order to terminate the reaction at maximum GOS yield. Figure 8 suggests that the trans-glycosylation reaction dominates at the beginning of the reaction, and after reaching the peak of GOS yield, the hydrolysis reaction gradually overtakes the trans-glycosylation reaction and predominates.

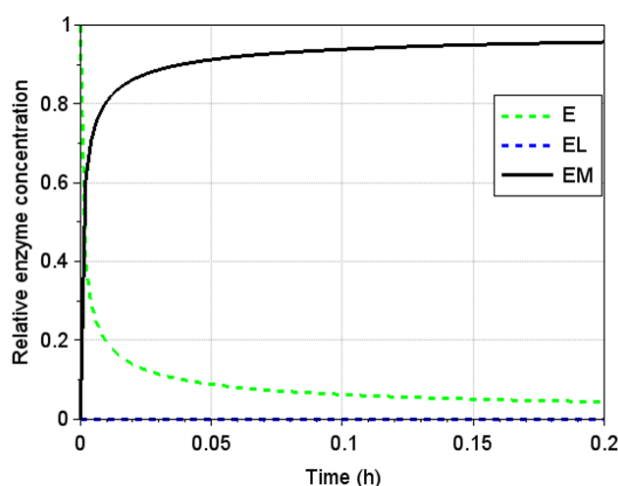


Figure 9. Relative enzyme concentration changes over time in (Palai et al., 2012) enzyme kinetic model. Green dash presents the initial concentration of Biolacta N5, blue dot line was the concentration of enzyme-lactose complex, and the black solid line shows the concentration of enzyme-monosaccharides complex. Reaction conditions: initial lactose concentration $320 \text{ g}\cdot\text{L}^{-1}$, $1 \text{ g}\cdot\text{L}^{-1}$ Biolacta N5, pH 6.0, 40°C .

Another interesting aspect of reaction kinetics was the formation of the enzyme complexes during the reaction. Figure 9 represents the change in concentrations over time for the enzyme E and its complexes.

According to the model, the β -galactosidase was present in three forms, including the non-reacted enzyme, the enzyme-lactose complex, and the enzyme-monosaccharide complex. It can be clearly observed in Figure 9 that within a short time after the reaction begins, the enzyme forms enzyme-sugar complexes with e.g., lactose and monosaccharides. There was a predominance of enzyme-monosaccharide complexes in the mixture (approx. 99%), while uncatalyzed enzymes and

enzyme-lactose complexes constitute a small percentage of the total enzymes and can be neglected.

5.1.2. Performance simulation of continuous-EMRs

It is important to note that previous modeling studies considered batch synthesis of GOS in STRs. The scope of my experimental investigations was, however, continuous GOS synthesis in EMRs. In this section, I report the mathematical problem formulation for EMR set-ups and perform simulations under ideal conditions, i.e., assuming no activity losses during EMR runs.

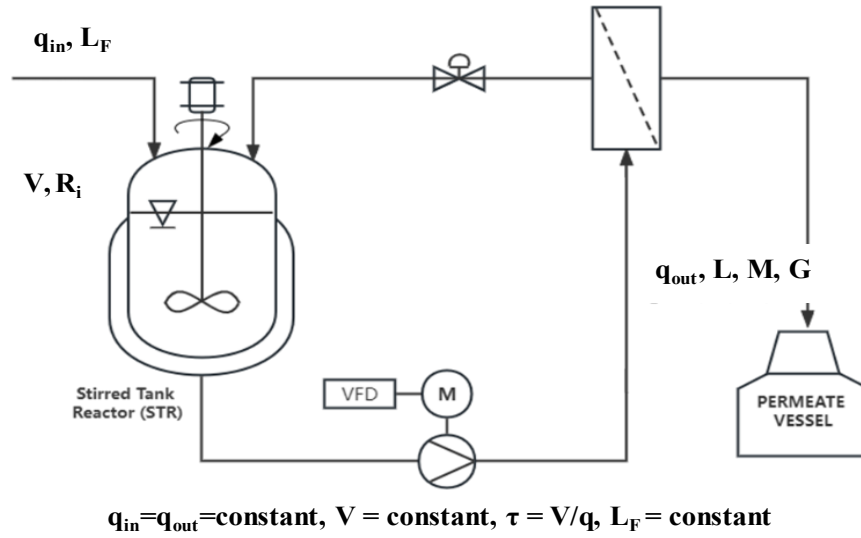


Figure 10. Schematic diagram of the UF-assisted enzymatic reactor.

For the performance assessment, I consider continuous GOS synthesis carried out by an EMR utilizing soluble Biolacta N5. The flowsheet of the continuous-EMR was schematically shown in Figure 10.

In continuous-EMR, the fresh substrate with a lactose concentration of L_f was continuously supplied into the reactor, and the enzyme-free product stream was continuously removed. The volumetric flow rate of the feed (q_{in}) was equal to that of the permeate (q_{out}), thus the volume of the reaction liquid (V) in the EMR was kept constant. The residence time was then given as $\tau = V/q$.

Assuming a well-mixed state in the reactor, and there is no concentration polarization caused by

the saccharide's mixture or the enzyme, the general mass balancing equation for component i can be written as:

$$\frac{d[m_i]}{dt} = q_{in}[C_{i,in}] - q_{out}[C_{i,out}] + V[R_i] = \frac{V}{\tau} [[C_{i,in}] - [C_{i,out}]] + V[R_i] \quad Eq.5.1.2-1$$

where m_i , C_i , and R_i were the mass, the concentration, and the production rate of component i in the reaction vessel, respectively.

Given that $q_{in}=q_{out}=q$ and $q = V/\tau$, the following differential equations can be derived for the individual saccharide fractions.

Component balance describing the change in lactose concentration in the EMR:

$$\frac{d[L]}{dt} = \frac{V}{\tau} ([L_F] - [L]) + V[R_L] \quad Eq.5.1.2-2$$

where L and L_f were the concentration of lactose in the permeate stream and feed respectively.

Component balance for monosaccharides, given that the monosaccharides concentration in the feed was zero:

$$\frac{d[M]}{dt} = -\frac{V}{\tau} [M] + V[R_i] \quad Eq.5.1.2-3$$

Component balance for GOS, the feed GOS concentration equals to zero, then:

$$\frac{d[G]}{dt} = -\frac{V}{\tau} [G] + V[R_i] \quad Eq.5.1.2-4$$

Integrating the enzyme kinetics model proposed by Palai et al. (2012) into our mathematical framework, the following initial value problem can be defined:

$$\frac{d[E]}{dt} = -k_1[E][L] + k_{-1}[EL] + k_3[EM][L] - k_{-3}[E][G] + k_4[EM][G] \quad Eq.5.1.2-5$$

$$\frac{d[EL]}{dt} = k_1[E][L] - k_{-1}[EL] \quad Eq.5.1.2-6$$

$$\frac{d[EM]}{dt} = k_2[EL] - k_3[EM][L] + k_{-3}[E][G] - k_4[EM][G] \quad Eq.5.1.2-7$$

$$\frac{d[L]}{dt} = -k_1[E][L] + k_{-1}[EL] - k_3[EM][L] + k_{-3}[E][G] + \frac{V}{\tau} ([L_F] - [L]) \quad Eq.5.1.2-8$$

$$\frac{d[M]}{dt} = k_2[EL] - \frac{V}{\tau} [M] \quad Eq.5.1.2-9$$

$$\frac{d[G]}{dt} = k_3[EM][L] - k_{-3}[E][G] - \frac{V}{\tau}[G] \quad \text{Eq.5.1.2-10}$$

where $[E]$, $[E_1]$, $[M]$, $[L]$ and $[G]$ denote the concentration of enzyme, inactive enzyme in the retention side, and monosaccharides (glucose and galactose), lactose and GOS (DP3 \geq) in the permeate given in $M \cdot L^{-1}$, respectively. The k values represent the reaction rate constants showed in Table 3.

Table 3. Estimated values of the rate constants by (Palai et al., 2012) and (Warmerdam et al., 2013).

Rate constant	Unit	Average value
k_1	$mM^{-1} \cdot h^{-1}$	1023.631
k_{-1}	h^{-1}	0.435
k_2	h^{-1}	1.191×10^{11}
k_3	$mM^{-1} \cdot h^{-1}$	5703.084
k_{-3}	$mM^{-1} \cdot h^{-1}$	1.404×10^6
k_4	$mM^{-1} \cdot h^{-1}$	17.758
k_d	h^{-1}	0.024 ± 0.015

The above reported set of ordinary differential equations (ODEs) were then employed to describe the formation and transformation of individual carbohydrate compounds in the EMR.

The initial value problem represented in (Eq.5.1.2-5-Eq.5.1.2-10) with the model parameter values listed in Table 3 was implemented in Scilab, and the dynamic behavior of the EMR system was simulated. More specifically, I investigated the time-course of the concentration of the individual saccharide compounds for varying the residence time (up to 10h) and the enzyme activity (up to 92301 $U \cdot kg^{-1}$, i.e. up to an enzyme load of 10 $g \cdot L^{-1}$). The scenario analysis was performed at fixed reaction conditions of 320 $g \cdot L^{-1}$ initial lactose concentration, pH 6.0, and 40°C.

An example of some typical EMR runs was given in Figure 11 a)-d), showing the profiles of carbohydrate fractions at a fixed residence time ($\tau = 2.2h$) for varying the enzyme load between 0.1 $g \cdot L^{-1}$ and 10 $g \cdot L^{-1}$.

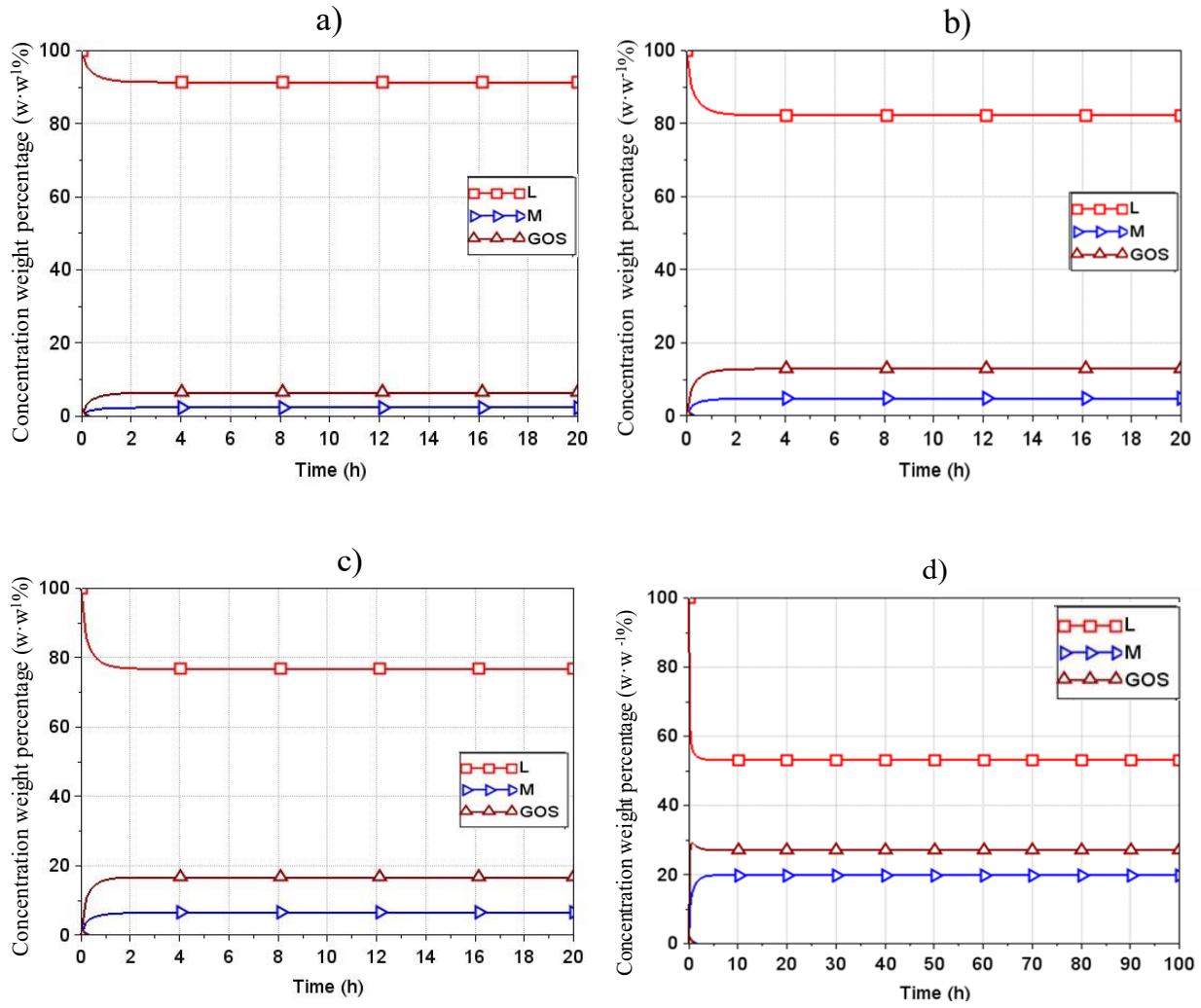


Figure 11. Simulation results of saccharide composition in continuous-EMR versus time employing Eq.5.1.2-5 to Eq.5.1.2-10 for various enzyme loads of 0.1 g·L⁻¹ (a), 0.5 g·L⁻¹ (b), 1 g·L⁻¹ (c), and 10 g·L⁻¹ (d). Reaction conditions: initial lactose concentration 320 g·L⁻¹, residence time 2.2h, pH 6.0, 40 °C. □: DP2, Δ: GOS, ∴: monosaccharides (glucose and galactose).

The steady state was typically reached after about one hour of process run. Under the given operational settings, as indicated in Figure 11, by increasing enzyme activity from 923 U·kg⁻¹ to 92301 U·kg⁻¹, lactose conversion increases from 18% w·w⁻¹ to approximately 48% w·w⁻¹, whereas GOS yield increases by approximately 5% w·w⁻¹ (from 13% w·w⁻¹ to 28% w·w⁻¹).

The interrelated effect of residence time and enzyme activity on GOS synthesis can be expressed by using a combined operational parameter, $\tau \times c_E$, which was the product of residence time (τ) and enzyme load (c_E). Figure 12 depicts the variation of GOS, monosaccharides, and DP2

concentrations as a function of $\tau \times c_E$.

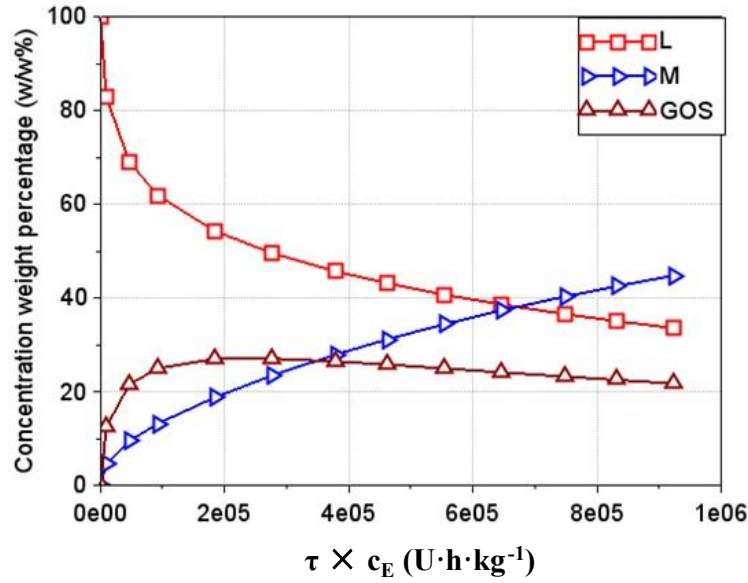


Figure 12. Steady-state composition saccharides as function of $\tau \times c_E$ (U·h·kg⁻¹). □: DP2, Δ: GOS, ▷: Monosaccharides (glucose and galactose).

It is important to highlight that GOS yield peaks at a certain value of $\tau \times c_E$. According to my simulation results, in the continuous-EMR, the maximal GOS production (28% w·w⁻¹) was obtained by adjusting the product of residence time and enzyme activity to a value of approx. 180,000 U·kg⁻¹. As depicted in Figure 12, a distinct characteristic of the examined reactor configuration is that beyond a certain threshold value of $\tau \times c_E$, the GOS yield ceases to increase.

As opposed to the simplified analysis achieved with the combined operational factor of $\tau \times c_E$, Figure 13 (a-c) present 3D plots showing the separate effects of residence time and enzyme activity on the production of individual carbohydrate fractions (GOS, monosaccharides, and DP2).

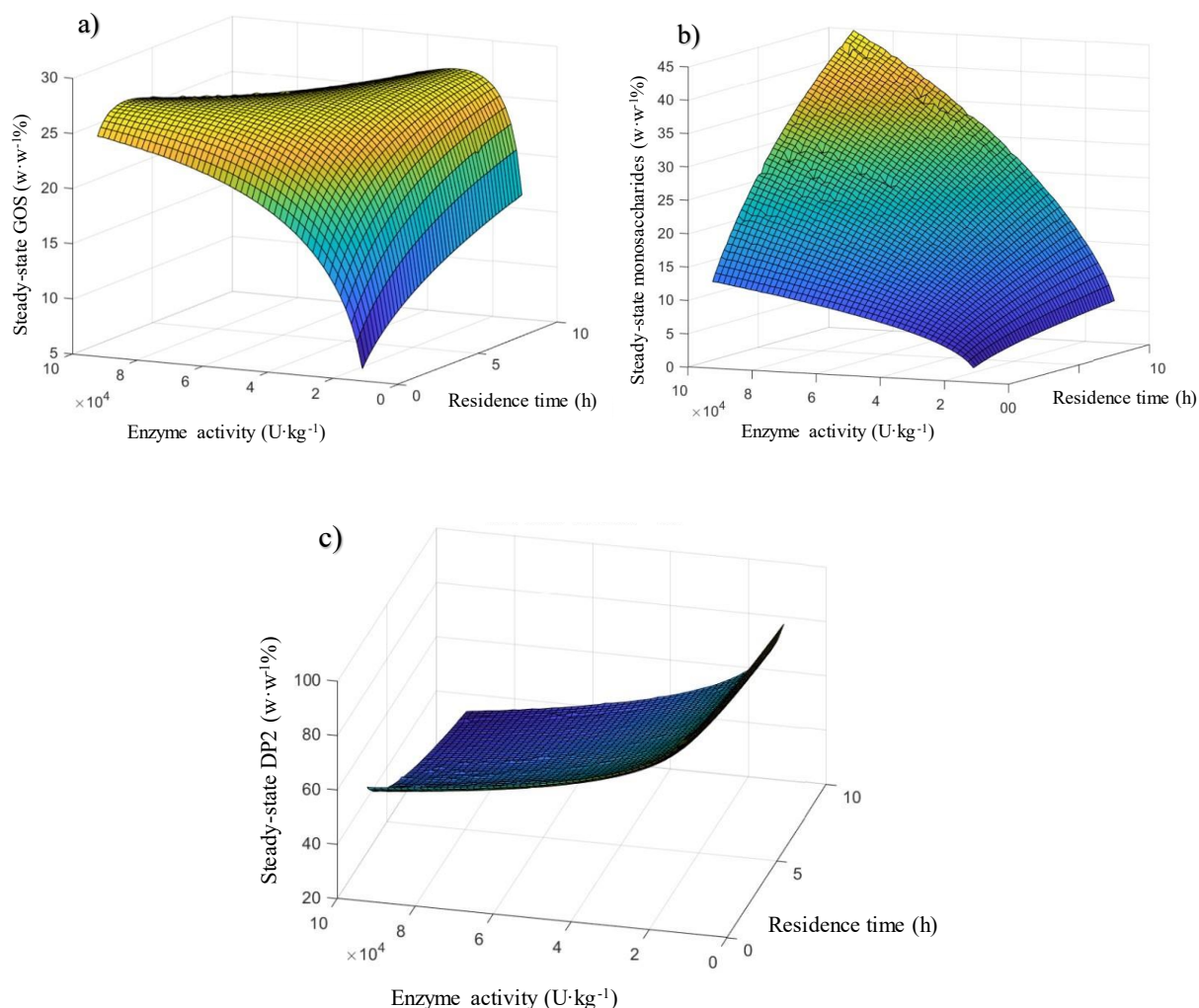


Figure 13. Steady-state composition of saccharides at various residence time τ (0-10 h), and enzyme activity c_i (0-92301 U·kg⁻¹) for GOS (a), monosaccharides (b), and DP2 (c).

Figure 13 shows the steady-state saccharide composition in the product stream of continuous-EMR for various residence time (0-10 h) and enzyme activity (0-92301 U·kg⁻¹) values. My results indicate that concentrations of GOS were in the range of 0-28% w·w⁻¹ depending on the settings of operational parameters. It is noteworthy that this yield was less than the maximum GOS yield (35% w·w⁻¹) obtained in biocatalytic reactions in STR under the same reaction conditions. There was an overall trend for an increase in GOS concentration with an increase in residence time and enzyme activity. It should be noted, however, that as a result of the cross-influence of the two variables, GOS concentration shows a slight decline trend after reaching its maximum level (25% w·w⁻¹). Accordingly, I was to determine the optimal range of operating parameters for achieving

maximum GOS yield in continuous-EMR. As shown in Figure 13 b), the monosaccharide concentration increased with increasing residence time and enzyme activity, reaching 7% w·w⁻¹ and 12% w·w⁻¹ at $\tau=10$ and $c_E=93201 \text{ U}\cdot\text{kg}^{-1}$, respectively. However, under their combined influence, 45% of monosaccharides can be observed. On the other hand, Figure 13 c) shows that DP2 concentration was inversely related to τ and c_E , i.e., the larger τ and c_E values, the lower DP2 concentration.

5.1.3. Accounting for enzyme activity losses

It is important to note that all mathematical models reported in the open literature, that deal with the kinetics of GOS synthesis, ignore enzyme inactivation. However, previous experimental research by Warmerdam et al. (Warmerdam et al., 2013) has demonstrated that, in the batch STR enzyme catalysis process, a considerable enzyme inactivation occurs. According to their research, a first-order enzyme inactivation model provides an adequate explanation for the degradation of Biolacta N5 over time. Biolacta N5 has been determined to have half-lives of 29, 29 and 16 hours at 25°C, 40°C, and 60°C, respectively, at a 30% w·w⁻¹ initial lactose concentration. Warmerdam and her coworkers considered 4 forms of the enzyme during the reaction, which include unreacted enzyme, enzyme-lactose complex, enzyme-monosaccharide complex, and inactivated enzyme. To be more precise, the first three forms of enzyme undergo varying degrees of inactivation over time. According to (Palai et al., 2012), the predominant enzyme-monosaccharide compound will also play a significant role in enzyme inactivation.

The inactivation model proposed by Warmerdam et al. (2013) can be integrated into our mathematical framework presented in Eq.5.1.2-5 to Eq.5.1.2-10. Thus, if assuming that there is no concentration polarization caused by the saccharide's mixture or the enzyme, the extended reaction scheme, that accounts also for activity losses during the continuous-EMR process, reads as:





Then, a set of ordinary differential equations (ODEs) that describe the performance of the EMR were given as:

$$\frac{d[E]}{dt} = -k_1[E][L] + k_{-1}[EL] + k_3[EM][L] - k_{-3}[E][G] + k_4[EM][G] - k_d[E] \quad \text{Eq. 5.1.3-8}$$

$$\frac{d[E_1]}{dt} = k_d[E] + k_d[EL] + k_d[EM] \quad \text{Eq. 5.1.3-9}$$

$$\frac{d[EL]}{dt} = k_1[E][L] - k_{-1}[EL] - k_d[EL] \quad \text{Eq. 5.1.3-10}$$

$$\frac{d[EM]}{dt} = k_2[EL] - k_3[EM][L] + k_{-3}[E][G] - k_4[EM][G] - k_d[EM] \quad \text{Eq. 5.1.3-11}$$

$$\frac{d[L]}{dt} = -k_1[E][L] + k_{-1}[EL] - k_3[EM][L] + k_{-3}[E][G] + \frac{V}{\tau}([L_F] - [L]) + k_d[EL] \quad \text{Eq. 5.1.3-12}$$

$$\frac{d[M]}{dt} = k_2[EL] - \frac{V}{\tau}[M] + k_d[EM] \quad \text{Eq. 5.1.3-13}$$

$$\frac{d[G]}{dt} = k_3[EM][L] - k_{-3}[E][G] - \frac{V}{\tau}[G] \quad \text{Eq. 5.1.3-14}$$

where [E], [E₁], [M], [L] and [G] denote the concentration of enzyme, inactive enzyme in the retention side, and monosaccharides (glucose and galactose), lactose and GOS (DP₃≥) in the permeate given in M·L⁻¹, respectively. The *k* values represent the reaction rate constants, and *k_d* was the enzyme inactivation constant in h⁻¹. The estimated values of parameters were adopted from literature, as presented in Table 3.

I conducted a series of simulation trials under various enzyme activities (up to 10⁵ U·h·kg⁻¹, i.e. 10 g·L⁻¹) and residence times (ranging from 0 to 10 h). Eq.5.1.3-8-Eq.5.1.3-14 were employed to determine the concentration of different carbohydrates as a function of time in the biocatalytic

reaction process.

Figure 14 (a) shows a typical short-term (4-hour) EMR run under fix operational settings of 320 g·L⁻¹ initial lactose concentration, 10 g·L⁻¹ enzyme load, 2.2 h residence time, pH 6.0, and 40 °C. During this exemplary process run, lactose was converted into monosaccharides and GOS, reaching a maximum lactose conversion of approximately 42% w·w⁻¹ after two hours. Meanwhile, the concentrations of monosaccharides and GOS also reached maximum of 28% w·w⁻¹. Note that the maximum GOS concentration achieved in continuous-EMR (28% w·w⁻¹) was lower than that of STR (35% w·w⁻¹) under the same reaction conditions (initial lactose concentration 320 g·L⁻¹, 10 g·L⁻¹ Biolacta N5 load, pH 6.0, 40 °C).

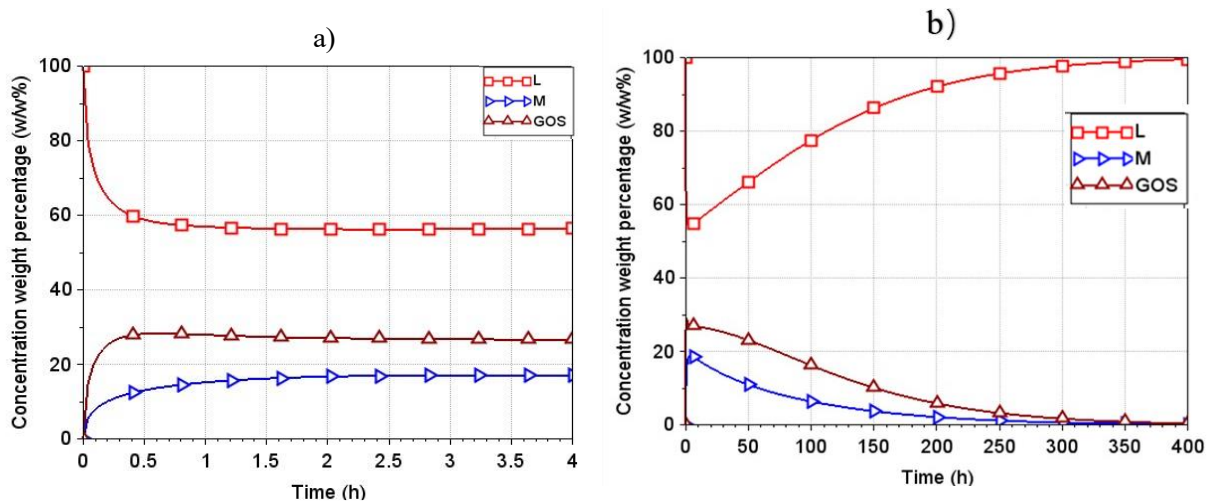


Figure 14. Simulation data of saccharide composition versus time employing new kinetic model in continuous-EMR. a) time = 4 h, b) time = 100 h, Reaction conditions: initial lactose concentration 320 g·L⁻¹, 10 g·L⁻¹ Biolacta N5, τ = 2.2h, pH 6.0, 40 °C. □: DP2, Δ: GOS, ▷: Monosaccharides (glucose and galactose).

Figure 14 (b) illustrates the system behavior predicted by the model for a long-term run (400 h). As enzyme activity declines over time, the GOS catalysis deteriorates. At the stage of complete inactivation, the lactose concentration in the permeate was the same as in the feed. Also, the concentration of GOS eventually decreases to zero.

Figure 15 shows the change within the different forms of the enzyme during the process run.

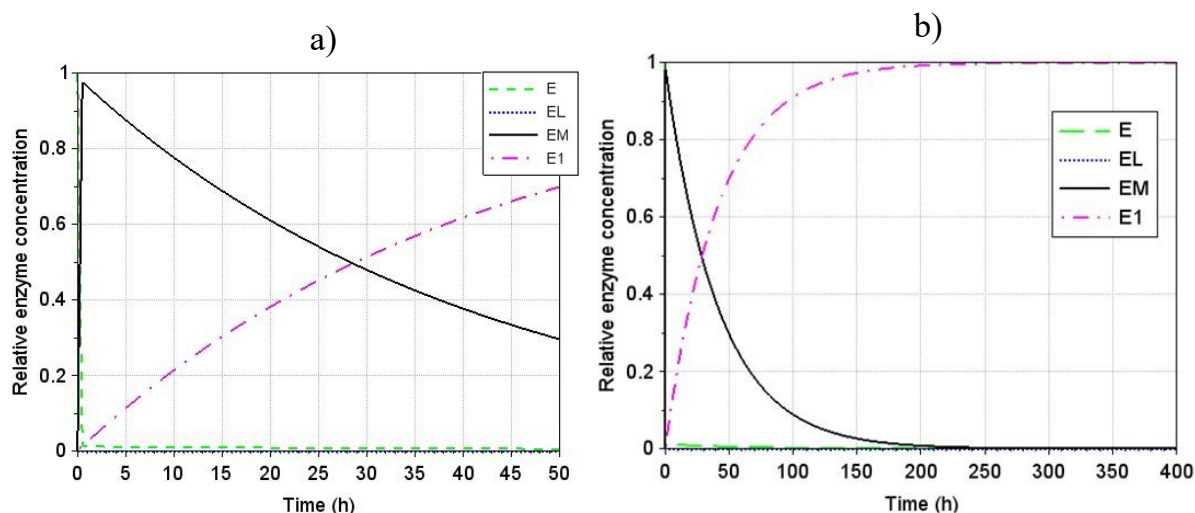


Figure 15. Relative enzyme concentration changes over time employing new kinetic model in continuous-EMR. Green dash presents the initial concentration of Biolacta N5, blue dot line was the concentration of enzyme-lactose complex, the black solid line shows the concentration of enzyme-monosaccharides complex, and the purple long dash dot line was the concentration of inactive enzyme. Reaction conditions: initial lactose concentration $320 \text{ g}\cdot\text{L}^{-1}$, $10 \text{ g}\cdot\text{L}^{-1}$ Biolacta N5, $\tau = 2.2\text{h}$, pH 6.0, 40°C .

According to my simulations, within a short time after starting the reaction, the active enzyme rapidly binds to the substrate and releases the monosaccharide. The enzyme binds to the monosaccharide to form an enzyme-monosaccharide complex. Within a short time, the majority of the enzyme in solution exists as an enzyme-monosaccharide complex and the concentration increases rapidly. The enzyme activity gradually decreases with time and ultimately becomes completely inactive. When the enzyme was completely inactivated, the concentration of the enzyme-monosaccharide complex in the reaction solution was zero at this time.

5.1.4. Enzyme inactivation model development

Within the scope of my modeling study, I conducted a systematic literature review (reported in Sect. 3.9) and identified a number of models applicable to describing the transgalactosylation reaction catalyzed by β -galactosidase from a *Bacillus circulans* source. These include the model describing the kinetics of transgalactosylation proposed by Palai et al. (2012) and the model of

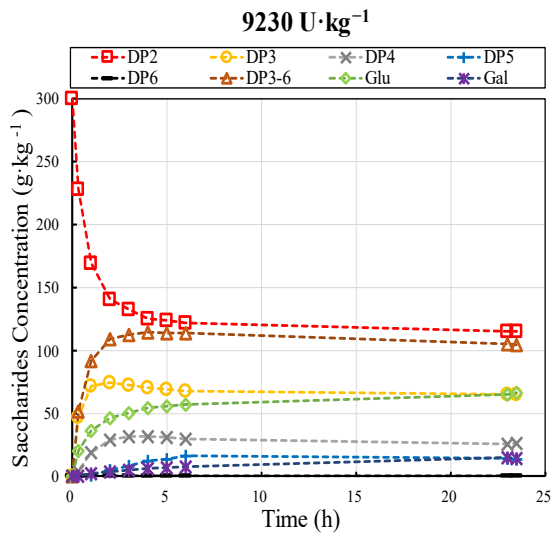
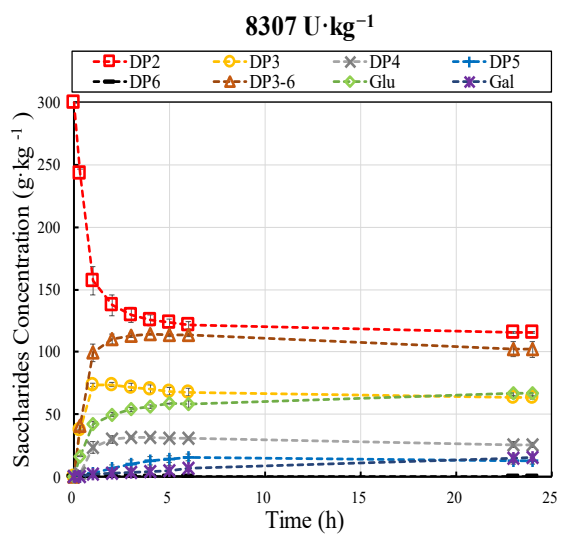
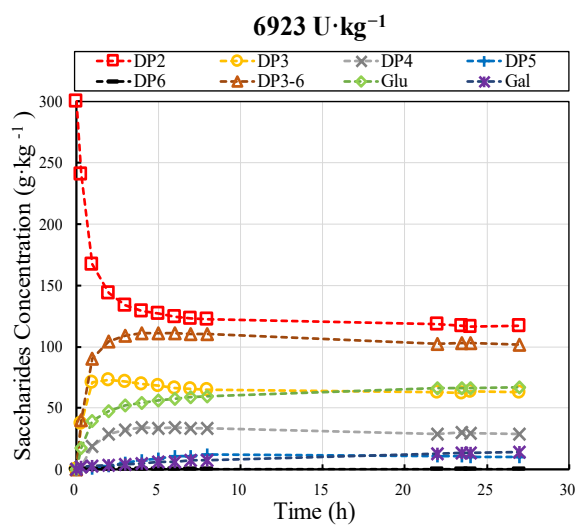
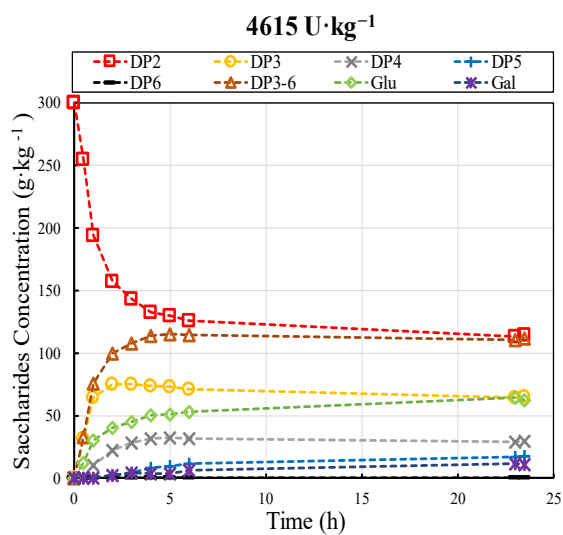
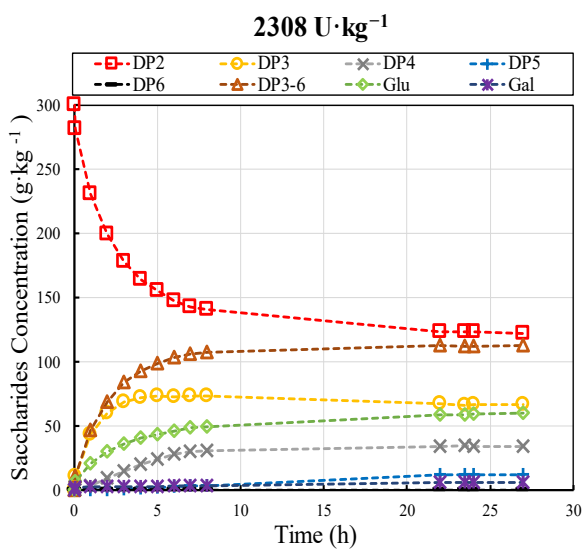
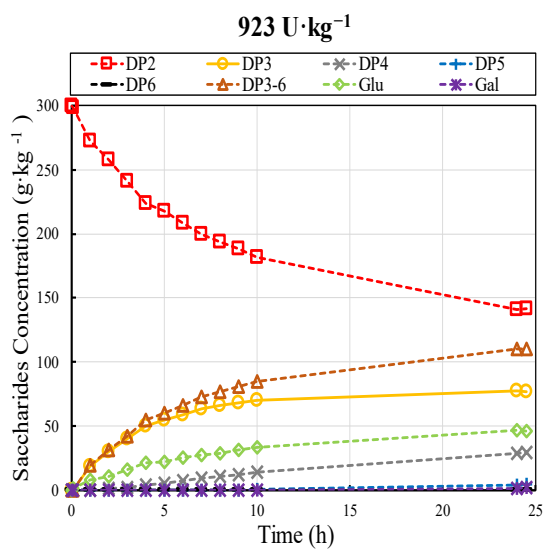
enzyme inactivation proposed by Warmerdam et al. (2013). I successfully replicated their reported results in STR and confirmed their validity. Then, I have developed a mathematical framework for describing GOS synthesis in EMR without and with enzyme inactivation.

I found that, under ideal conditions of no enzyme inactivation, the predicted steady-state GOS yield in the EMR ($\sim 30\% \text{ w}\cdot\text{w}^{-1}$) was slightly lower than the maximum yield in the STR ($\sim 34\% \text{ w}\cdot\text{w}^{-1}$) under optimal reaction conditions. When enzyme inactivation was considered, the GOS concentration in the EMR decreases over time and eventually reaches zero. My simulation results suggest that the activity of the enzyme during EMR runs must be strictly monitored. In order to maintain a stable GOS yield in the product stream, different control strategies can be applied, such as an increase in the residence time or the addition of fresh enzymes to compensate for the loss of enzyme activity.

5.2. Performance in STR

Eight lab-scale (typically 0.1-0.3 L) batch experiments were carried out using Biolacta N5 from *Bacillus circulans*. The enzyme concentration on GOS yield was investigated under the reaction conditions of an initial lactose concentration of $300 \text{ g}\cdot\text{kg}^{-1}$, temperature of 50°C , and pH 6.0. The reaction was carried out for an operation time of 24h.

Figure 16 illustrates the changes of individual component concentration over time in STR at different enzyme activity ($923 \text{ U}\cdot\text{kg}^{-1}$ to $92301 \text{ U}\cdot\text{kg}^{-1}$). Samples were taken from the reactor and thermostated at 90°C for 30 minutes prior to HPLC analysis.



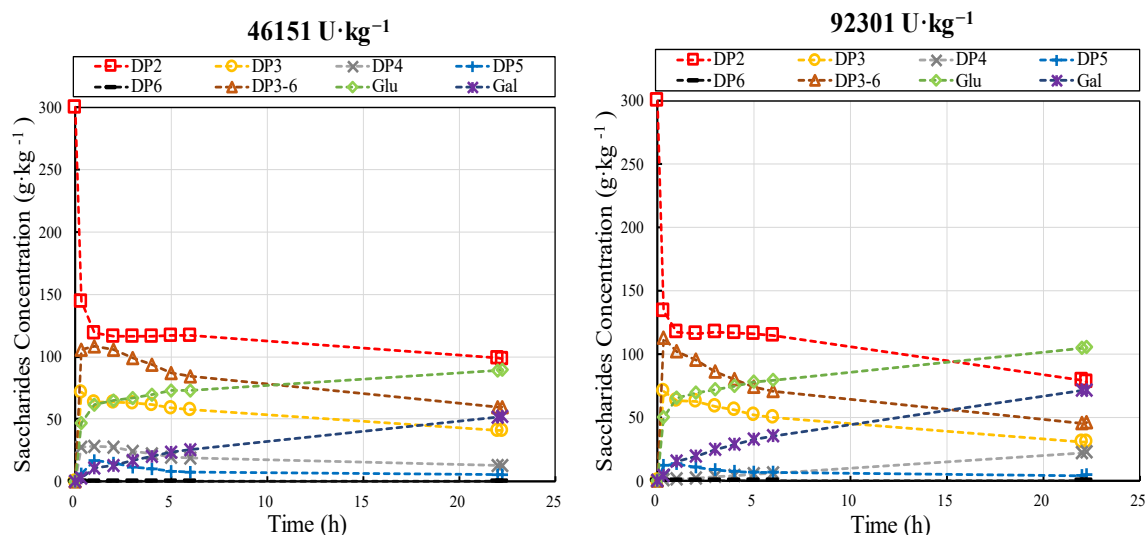


Figure 16. Progress curves of saccharides fractions for various enzyme loads ranging from 923 $\text{U}\cdot\text{kg}^{-1}$ to 92301 $\text{U}\cdot\text{kg}^{-1}$. Mean values and standard deviation of triplicate measurements were shown for 8307 $\text{U}\cdot\text{kg}^{-1}$. The solid lines present to guide the symbols represent measured values. Operational conditions: 300 $\text{g}\cdot\text{kg}^{-1}$ initial lactose concentration, pH 6.0, 50 °C, 60 rpm.

During the catalytic reaction, lactose was converted into oligosaccharides with different DP (3-6) and monosaccharides, including glucose and galactose. Figure 16 showed that, within the enzyme activity range from 923 $\text{U}\cdot\text{kg}^{-1}$ to 92301 $\text{U}\cdot\text{kg}^{-1}$, all experiments showed the same tendency, i.e., the GOS concentration increasing up to a maximum of approx. 38% on the basis of total carbohydrates then it decreases. The decrease in GOS over time may be due to the reversible hydrolysis of DP3-6, producing monosaccharides. This is supported by the continuously increasing of galactose concentration over time in solution. In the case of enzyme activities in the range 923-9230 $\text{U}\cdot\text{kg}^{-1}$, the galactose production from the hydrolysis reaction was negligible. The galactose concentration has remained typically below 1-3% $\text{w}\cdot\text{w}^{-1}$. However, a significant increase in galactose concentration was observed when the enzyme concentration exceeded 9230 $\text{U}\cdot\text{kg}^{-1}$. It can be observed from Figure 16 that, when the enzyme concentration was 46151 $\text{U}\cdot\text{kg}^{-1}$ and 9230 $\text{U}\cdot\text{kg}^{-1}$, the galactose concentration was achieved at a high level of 52 $\text{g}\cdot\text{kg}^{-1}$ and 71 $\text{g}\cdot\text{kg}^{-1}$ at 24h, respectively. The products of the reaction are mainly monosaccharides at this point, and the hydrolysis reaction is significant. Therefore, under the reaction conditions of my experiment, i.e., 30% $\text{w}\cdot\text{w}^{-1}$ lactose, pH 6.0, 50 °C, high concentration of the enzyme ($>9230 \text{ U}\cdot\text{kg}^{-1}$) will not be considered for GOS production.

These results provided a reference for the enzyme concentrations to be applied in subsequent GOS synthesis experiments using EMR. GOS yields obtained from STR will be later compared to GOS yields achieved in EMR (see Sect.5.3 and Sect. 5.4). The results of STR will also be used as a calibration curve for quantifying enzyme loss during cyclic-EMR (Sect. 5.4.1).

5.3. Enzymatic conversion in continuous-EMR

In this chapter, I describe the results of continuous GOS production using the free enzyme Biolacta N5, which catalyzes lactose in EMR. I conducted some preliminary experiments to determine the optimal operating conditions (pressure and flux) for continuous GOS production (Sect. 5.3.1). A series of short-term (Sect. 5.3.2) and long-term experiments (Sect. 5.3.3) were performed in continuous-EMR. The effect of different operational factors (e.g., residence time and enzyme activity) on the transglycosylation for GOS synthesis was also investigated (Sect. 5.3.2).

5.3.1. Preliminary filtration experiments

Preliminary filtration tests were conducted to investigate the effects of reaction fluids and operating parameters on the filtration performance of UF membranes during enzyme-catalyzed reactions. More specifically, the effects of TMP, enzyme load, and operating time were determined in terms of membrane permeability, or rather, the permeate flux. In the long-term operation of an EMR, membrane fouling, and loss of enzyme activity were inevitable. It is usually possible to compensate for the latter, in order to maintain consistent product quality, by gradually adding fresh enzymes to the reactor. There will be a decrease in flux over time as a result of both membrane fouling and increased enzyme load. The purpose of this study was to determine the set of design parameters of the EMR (such as the membrane area, the reactor volume, the residence time, and the trans-membrane pressure) that will ensure stable product flow levels over a long period of time.

5.3.1.1. Pressure-scan

In Figure 17(a), the permeate flux was plotted against operating time as the TMP was gradually increased from 1 bar to 4 bar. Permeate flux decreased by an insignificant amount over operating

time, which indicates that membrane fouling was not significant. Figure 17(b) depicts the variation in (quasi) steady state flux values as TMP increases. As a result, it is not difficult to conclude that the membrane filtration system operates in the pressure-dependent regime at TMPs below about 4 bar. More specifically, increasing the TMP increases the permeate flux.

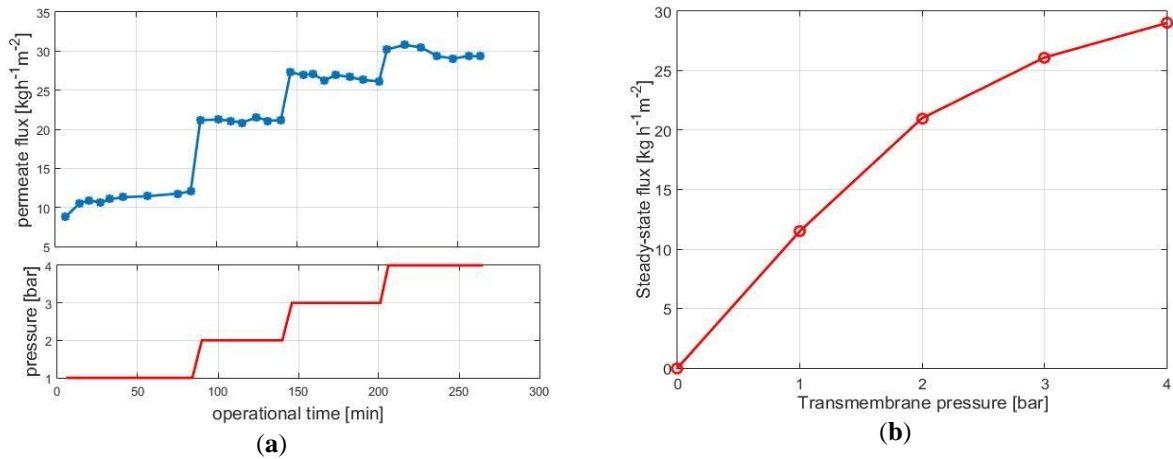


Figure 17. Permeate flux as function of operational time for various TMPs (a) and quasi steady-state flux values versus pressure (b). Operational conditions: 30 w·w⁻¹% lactose concentration, 10 g·kg⁻¹ enzyme load, pH 6.0, 50 °C, 0.18 m³·h⁻¹ crossflow rate.

Conversely, when the pressure exceeds 4 bar, an increase in pressure seldom results in an increase in flow. Pressure-independent regimes were characterized by this phenomenon. For ultrafiltration, the pressure-dependent regime was usually recommended, as the pressure-independent regime was known for significant fouling.

5.3.1.2. Limiting flux

There was a possibility of explaining experimental ultrafiltration data with the limiting flux model (Paulen et al., 2011). In the course of filtration, retained solutes tend to accumulate on the membrane surface, resulting in the formation of a concentration-polarized layer at the membrane-solution contact surface. At a steady state, the amount of solute delivered by the solvent to the membrane was equal to the amount of solute that diffuses back from the membrane. The permeate flux was essentially pressure-independent at high pressures in most ultrafiltration applications (e.g., (Élysée-Collen and Lencki, 1997, Yazdanshenas et al., 2005)). This phenomenon was explained

by a physical model known as the limiting flux model (or, more traditionally, the gel polarization model).

Under conditions of high protein retention and membrane fluxes, this model assumes that the protein concentration at the membrane surface reaches a limiting concentration. In the presence of fixed hydrodynamic conditions, the flux can be related to the limiting concentration as follows:

$$J_{lim} = k \ln \left(\frac{c_{lim}}{c_b} \right) \quad Eq. 5.3.1.2-1$$

Under the control of polarized layers, k represents the mass transfer coefficient, c_b was the concentration of enzyme in the bulk, and c_{lim} stands for the limiting concentration of enzyme. Alternatively, this term also refers to gel concentration; however, the limiting flux was generally independent of any alleged gelation effects. In fact, c_{lim} was more of a phenomenological variable than it is a true physical property of a solution (Ma et al., 2009).

As shown in Figure 18, the experimental flux data collected in the pressure-independent regime vary with the enzyme concentration. The limiting flux model (Eq. 5.3.1.2-1) fits well the observed data ($R^2=0.985$). For the polarized layer control condition, mass transfer coefficient k and limiting concentration c_{lim} were calculated to be $3.17 \text{ kg} \cdot \text{h}^{-1} \cdot \text{m}^{-2}$ and $2405 \text{ g} \cdot \text{kg}^{-1}$, respectively.

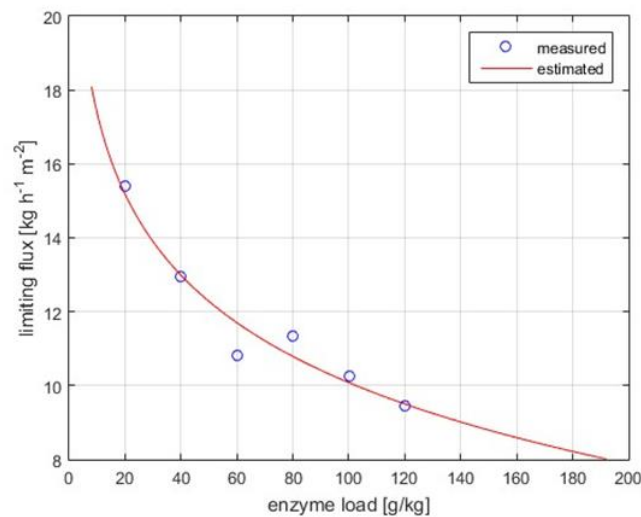


Figure 18. Limiting flux versus. bulk enzyme concentration in the pressure-independent zone. Operational conditions: 4 bar, 30% w·w⁻¹ lactose concentration, pH 6.0, 50 °C, 0.18 m³·h⁻¹ crossflow rate, 10 kDa UF membrane. Measured and estimated (using Eq. 5.3.1.2-1) data were illustrated with symbols and continuous lines, respectively.

5.3.2. Enzymatic conversion short-term

Examinations of the steady-state performance of the EMR in relation to enzyme loading and residence time was carried out in eight short-term (6-8 h) experiments. For illustration, Figure 19 (a) and (b) shows the variation in carbohydrates composition in the product solution as a function of operational time for a typical process run (No.1 and No.2) at different initial enzyme concentrations.

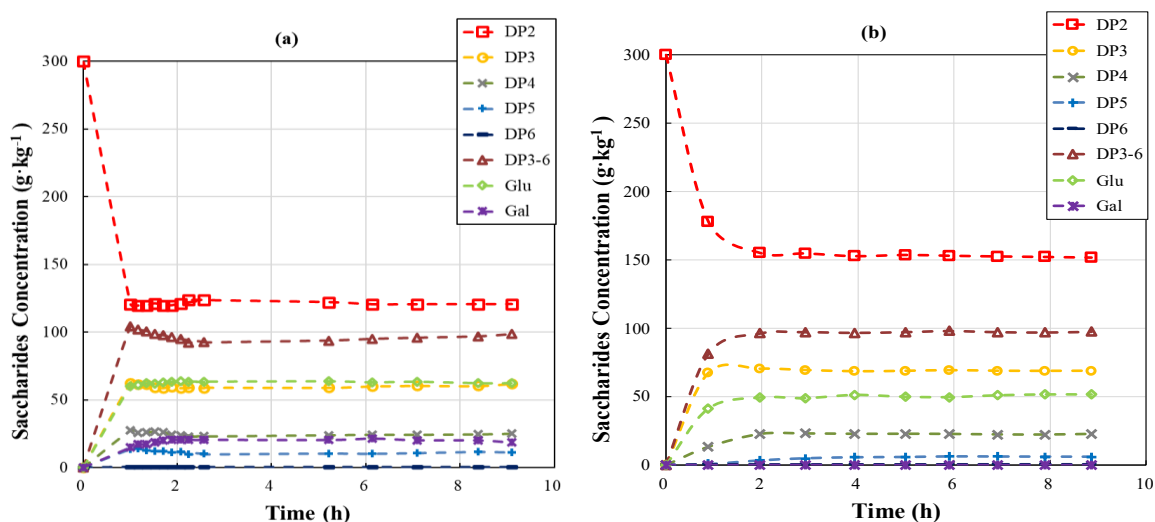


Figure 19. Saccharide composition in permeate as function of operational time during Run No1 (a) and 2 (b). Operational conditions: 30% w·w⁻¹ feed lactose concentration, 30% w·w⁻¹ initial lactose concentration, 92301 U·kg⁻¹ (a), 9230 U·kg⁻¹ (b) enzyme load, pH 6.0, 50 °C, 2.2 h residence time, 0.18 m³·h⁻¹ crossflow rate, 0.5 bar retentate-side pressure, ca. 0.40–0.45 bar permeate-side pressure, 10 kDa UF membrane.

In each of the eight short-term experiments, reactions were performed using 2 kg of reaction fluid, and the permeate flow rate was set to a constant value by adjusting the permeate pump to control the reaction fluid flow rate. To adjust the required residence time for each experiment, different permeate flow rates varied from 0.9 to 1.9 kg·h⁻¹. An HPLC system was applied to measure the composition of the periodic samples as the experiment progressed to determine the carbohydrate concentration changes in the reaction solution.

A brief summary of the composition of the steady-state carbohydrate during short-term runs can be found in Table 4.

Table 4. Steady-state saccharides' composition in w·w⁻¹% for short-term EMR runs. The composition obtained for batch process (at 6 h) was indicated for comparison purpose.

Component:	No3	No5	No2	No7	No4	No6	No1	No8	Batch
τ [h]	1.1	2.1	2.2	2.6	1.1	2.1	2.2	2.8	6.0
c_E [U·kg ⁻¹]	9230	8307	9230	9230	92301	83994	92301	92301	8307
$\tau \times c_E$ [U·h·kg ⁻¹]	10153	17279	20306	24090	104300	174708	205113	260289	49842
P [g·h ⁻¹ ·U ⁻¹] $\times 10^{-3}$	7.263	4.757	4.787	3.860	0.955	0.574	0.480	0.368	2.280
DP2	63.8	61.7	50.5	53.8	45.0	41.9	40.2	41.7	40.5
Glu	11.7	10.5	17.1	14.3	18.6	20.8	20.8	22.2	19.5
Gal	0.0	0.4	0.0	0.9	3.3	3.8	6.2	4.2	2.2
DP3	19.7	22.0	22.9	22.9	21.6	20.6	20.6	20.7	22.5
DP4	4.4	5.4	7.5	6.8	7.9	8.8	8.3	8.6	10.2
DP5	0.6	0.0	1.9	1.3	2.7	4.0	3.7	2.6	5.1
DP6	0.0	0.0	0.2	0.0	1.0	0.0	0.1	0.0	0.0
DP3-6	24.6	27.4	32.4	31.0	33.2	33.4	32.8	31.9	37.9

As indicated in Sect. 5.1.2, both enzyme dosages (c_E) and the residence time (τ) have certain effects on the synthesis of GOS. Undoubtedly, when $c_E = 0$ or $\tau = 0$, there were no enzymatic conversion occurred. In general, lowering the enzyme dosage results in a lower conversion of lactose. Expectedly, an increase in residence time enhanced the lactose conversion. In order to explain and visualize the combined impacts of both factors, I employ the product of enzyme load and residence time ($\tau \times c_E$, in U·h·kg⁻¹) as a straightforward indicator of the applied settings that determine product quality. A gradual decline in productivity from approx. 7.263×10^{-3} to 0.368×10^{-3} g of DP3-6 per hour and unit enzyme activity has been observed when the value of $\tau \times c_E$ increased from 10153 to 260289 U·h·kg⁻¹.

Figure 20 illustrates the saccharides composition as function of $\tau \times c_E$. In practice, I may set any values of τ and c_E , the factor $\tau \times c_E$ will determine the concentration of each component as dictated by the curves shown in Figure 20. Eq. 4.5.5-1 and Eq. 4.5.5-2 were fitted to the observed carbohydrate fraction concentrations. The interaction of residence time (τ) and enzyme load (c_E) were used as a predictor, and the relative mass percentage of the sugar fraction (w_i) was used as a response variable for the nonlinear regression. Results of the fittings are summarized in Table 5. A

diagram illustrating the model estimates and the simultaneous 95% confidence bounds was depicted in Figure 20.

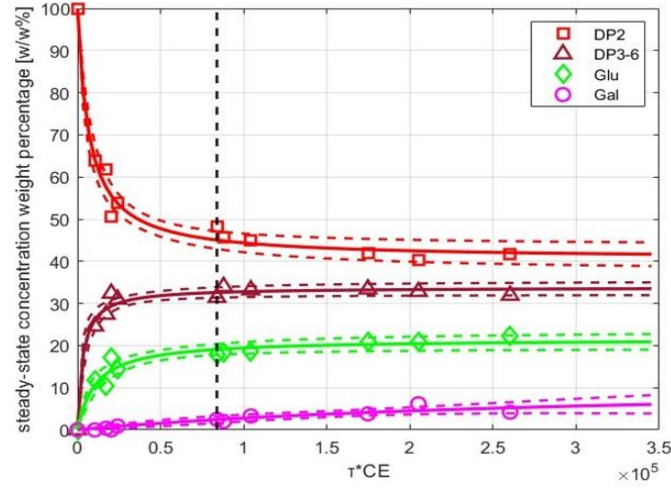


Figure 20. Steady-state composition saccharides as function of $\tau \times c_E$ for short-term runs. Experimental data fitted regression models, and simultaneous 95% confidence bounds were illustrated with symbols, solid lines, and dashed lines, respectively. Data obtained for long-term runs L1 and L2 at 8 h of operation was highlighted with a vertical line at $\tau \times c_E = 83070 \text{ U} \cdot \text{h} \cdot \text{kg}^{-1}$.

As indicated in Figure 20, the DP3-6 fraction initially showed a trend of increasing in concentration with a higher value of $\tau \times c_E$ and gradually reached stability at $Y \approx 33 \% \text{ w} \cdot \text{w}^{-1}$ after $\tau \times c_E = 100,000$. A continued increase in the content of $\tau \times c_E$ results in the formation of hydrolysis by-products. Furthermore, in comparison with the STR (38% $\text{w} \cdot \text{w}^{-1}$), the EMR DP3-6 yield (25-33% $\text{w} \cdot \text{w}^{-1}$) was lower. This result is consistent with findings of my in-silico study (see Sect. 5.1.2). More precisely, the predicted GOS yield in continuous-EMR is slightly lower than in STR (30% $\text{w} \cdot \text{w}^{-1}$ vs 34% $\text{w} \cdot \text{w}^{-1}$, respectively). In addition, the same trend was observed for the factor $\tau \times c_E$ on GOS yield. That is, GOS concentration increases with increasing $\tau \times c_E$ and reaches a maximum GOS concentration at a fixed value ($\tau \times c_E = 1.8 \times 10^5 \text{ U} \cdot \text{h} \cdot \text{kg}^{-1}$ in-silico vs $\tau \times c_E = 1.7 \times 10^5$ continuous-EMR), followed by a decline.

The results of Table 5 indicate that the nonlinear model has an excellent predictive ability for the concentrations of DP2, DP3-6 (GOS), and glucose in solution at a steady state for different the factor $\tau \times c_E$. The model achieved an R^2 value exceeding 0.95 for both DP2, DP3-6 (GOS), and glucose. Galactose, on the other hand, was not predicted by the model successfully, with an R^2

value of 0.78. There was a possibility that the cause of this phenomenon was that the concentration of galactose in the solution was much lower than that of other components, such as DP2 and GOS, leading to larger errors in calculations.

Table 5. Estimated regression coefficients and goodness of fit statistics.

Response Variable	Model Parameters		Goodness of Fit			
	b1	b2	SSE	R ²	Adjusted-R ²	RMSE
DP2	0.008607	0.000145	61.2434	0.9803	0.9781	2.3596
DP3-6	0.011093	0.000328	20.1983	0.9765	0.9739	1.3551
Glu	0.002	0.000093	24.1088	0.9528	0.9476	1.4804
Gal	0.000037	0.000037	4.9913	0.7892	0.7657	0.6736

5.3.3. Enzymatic conversion in long-term

The long-term experiments (runs L1 and L2) were conducted under the same operating conditions as the short-term experiments, i.e., 30% w·w⁻¹ feed lactose, 30% w·w⁻¹ initial lactose concentration, pH 6.0, and 50 °C. The EMR was run continuously for more than 120 hours in both runs, with an initial enzyme concentration of 46151 U·kg⁻¹. The average amount of lactose used as feed was 40 kg (30% w·w⁻¹ lactose solution), resulting in an output of 130 kg of liquid product per run. Since the feed enzyme in the EMR was approximately 10 g, for the entire campaign, an average of approx. 1.4 kg of DP3-6 was produced by one gram of crude enzyme preparation.

Figure 21 illustrates the composition of saccharides in the product stream as a function of operating time for Run L1 and Run L2.

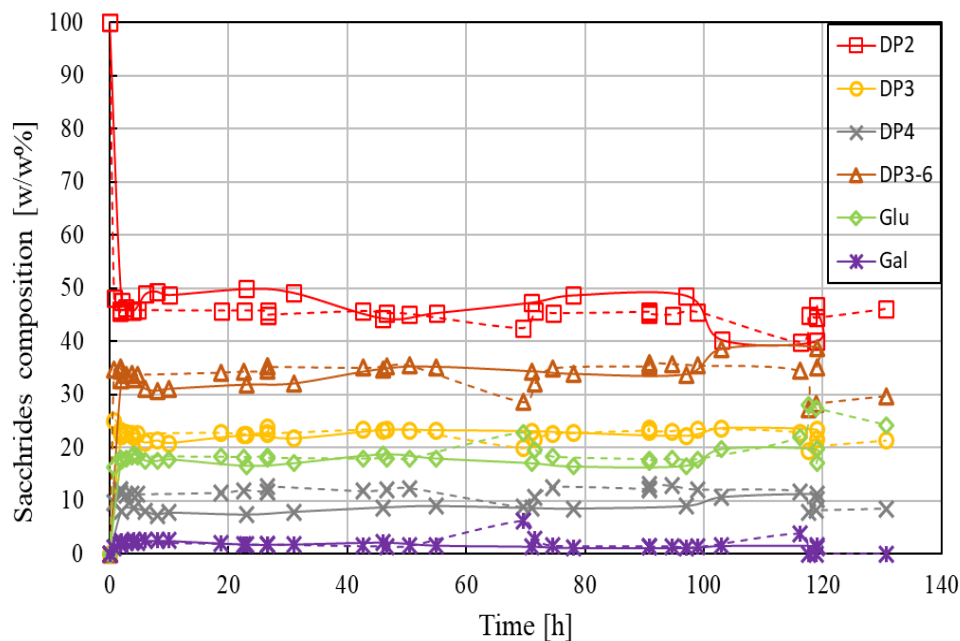


Figure 21. Saccharides composition in permeate as function of operational time in enzymatic membrane reactor for both Run L1 (solid line) and Run L2 (dashed line). Operational conditions: 30% $w \cdot w^{-1}$ feed lactose concentration, 30% $w \cdot w^{-1}$ initial lactose concentration, 46151 $U \cdot kg^{-1}$ enzyme load, pH 6.0, 50 °C, ca. 1.8 h residence time, 0.16 $m^3 \cdot h^{-1}$ crossflow rate, 1.0 bar retentate-side pressure, 0.7-0.2 bar permeate-side pressure, 10 kDa UF membrane.

These manipulations provide comparable results, more specifically, intercomparisons between long-term experiments and short-term manipulation results. From Figure 21, it was obvious that the changes of different carbohydrates during the reaction were essentially the same for two long-term EMR experiments. The steady-state compositions obtained in the long-term runs (averages calculated from samples taken over a period of approximately 5-10 hours) were consistent with those obtained in the previous short-term runs (see the horizontal line in Figure 20). In long-term runs, the steady-state concentrate of DP2 in a range of 40-50% $w \cdot w^{-1}$, and GOS yield between 30-40% $w \cdot w^{-1}$. Experimental conditions were conducted with a constant reactor volume by using an on/off-triggered feed pump with a level sensor, as described in Sect. 4.5.1. While a constant permeate flow rate was controlled by the permeate pump, with the return fluid pressure adjusted to 1 bar and the permeate flow rate set at approx. 1.1 $kg \cdot h^{-1}$. Therefore, the residence time can be controlled. According to the results over the two long-term experiments, membrane fouling occurred. It was demonstrated by a gradual decrease in the permeate pressure from approximately 0.7 bar to 0.2 bar as the experiment progressed, i.e., an increase in the transmembrane (net)

pressure from 0.3 bar to 0.8 bar as the experiment progressed. The small amount of whey residue (e.g., about 0.1% w·w⁻¹ protein) present in lactose may be responsible for this phenomenon. The whey residue may be rejected in part or in whole by the UF membrane. The accumulation of this macromolecular compound in the system may contribute to the development of fouling. However, it has no significant impact on the experiment and, specifically, does not cause a decrease in flux below the set. In both short- and long-term investigations, more than 75% of the initial membrane permeability was restored after the membrane cleaning process, indicating that the membrane was successfully regenerated after the experiment. In most instances, water permeability ($\approx 18 \pm 3.6$ kg·h⁻¹·m⁻²) was restored by applying alkaline cleaning. In some cases, it was necessary to apply additional cleaning steps to obtain the original flux as described in Sect. 4.7.

Based upon the comparison of long-term results with those of STR, the STR experiment was clearly superior to the EMR experiment, both in terms of yield (38% w·w⁻¹ vs 33% w·w⁻¹) and biocatalyst productivity (2.280×10^{-3} vs 1.180×10^{-3} g·h⁻¹·U⁻¹). However, the amount of product (DP3-6) obtained per hour for one kg of reactor content was calculated as 54.5 g·kg⁻¹·h⁻¹ for the long-term runs which was significantly higher than the amount obtained with STR (18.9 g·kg⁻¹·h⁻¹). Additionally, under the studied operational conditions, the amount of DP3-6 produced by one gram of enzyme preparation was significantly greater in EMR (ca. 1.4 g·kg⁻¹) than in STR (ca. 0.13 g·kg⁻¹).

It was primarily intended to demonstrate that the conversion data obtained from the L1 experiment were reliable. Therefore, the L2 experiment was a repeat run of the L1 experiment. Prior to analyzing the samples obtained from the L2 experiment by HPLC, different pretreatments were performed on the samples obtained from the permeate to eliminate the possibility of residual enzyme activity (e.g., resulting from accidental enzyme leakage during operation). The samples taken from the L2 experiment were subjected to no pretreatment, acid treatment, and heat treatment, respectively. The results of the HPLC analysis showed that none of the three pretreatments affected the results. This further confirms that the enzyme leakage problem during the experiments did not exist, i.e., the enzyme was completely retained by the UF membrane.

As reported in Figure 21, the stability of Biolacta N5 and the consistent degree of lactose

conversion maintained throughout such an extended operational period was unexpected. In addition to what has been said previously, no reports have been published pertaining to the operational stability of Biolacta N5 in EMR. Warmerdam et al. (2013) have provided the only data available on the half-life of Biolacta N5 in a batch setup using the oNPG assay. According to the results of their study, the enzyme has half-lives of 29 h, 29 h, and 16 h at temperatures of 25 °C, 40 °C, and 60 °C, respectively. In light of this, I anticipate a significant decrease in the conversion rate over time. Additionally, the $\tau \times c_E$ factor for the long-term run was adjusted to approximately 83070 U·h·kg⁻¹. It is obvious that this setting does not necessarily represent optimal operating conditions. Consequently, the experiments may not yield optimal results. In this setting, however, it is possible to gain a greater understanding of the mechanism of enzyme activity decline during a long-term EMR experiment. In this experiment, Biolacta N5 was expected to have a half-life of approximately 24 hours according to Warmerdam et al. (2013).

Starting a long run with an enzyme dosage of 46151 U·kg⁻¹ ($\tau \times c_E = 83070$ U·h·kg⁻¹) means that the concentration of active enzyme was expected to drop to 23075.5 U·kg⁻¹ ($\tau \times c_E = 41536$ U·h·kg⁻¹) after approximately one day of running. As shown in Figure 20, this decrease in activity would result in a much lower degree of conversion of the various carbohydrate components in the reaction solution, such as lactose consumption and DP3-6 synthesis. HPLC was capable of readily detecting this degree of conversion. By the end of the experiment, at ca. 120 hours, $\tau \times c_E$ was expected to reach the value of 2596 U·h·kg⁻¹. Figure 20 reports the proven output of EMR for any given value of $\tau \times c_E$. Therefore, by following the expected decrease in $\tau \times c_E$ from our starting situation ($\tau \times c_E = 83070$ U·h·kg⁻¹) to $\tau \times c_E = 2596$ U·h·kg⁻¹, one can read the corresponding degree of conversion from the vertical axis in Figure 20. Presuming a half-life of 24 h, the regression models (Eq. 4.5.5-1 and Eq. 4.5.5-2) estimated a dramatic drop in product quality after 5 days of operation, resulting in a saccharide composition of 84.1 ± 4.4% w·w⁻¹ DP2, 15.5 ± 5.2% w·w⁻¹ DP3-6, and 4.2 ± 2.0% w·w⁻¹ glucose. However, despite prolonged EMR operation (within 120-130 h), no significant decrease in conversion was observed for each component of the reaction solution. This result differs from the predicted results in in-silico (Sect. 5.1.3) and the results of Warmerdam et al. (2013) that the half-life of Biolacta N5 at pH 6.0, 40°C is approx. 29h. In view of the stable

performance of the EMR, HPLC data collected from L1 and L2 cannot be extrapolated to determine the true value of the half-life of the enzyme. It is therefore necessary to conduct additional experiments in order to determine the half-life of Biolacta N5. It is possible to extrapolate accurate half-life values through longer experiments at a reduced EMR scale. Alternatively, this can be done by performing under-repeat experiments at suboptimal operational settings, i.e., at lower initial values of $\tau \times c_E$, which can minimize feedstock costs.

5.4. Cyclic-EMR

This section describes the use of a stirred-tank reactor (STR) to convert lactose into GOS over five consecutive cycles by means of the soluble enzyme Biolacta N5. The enzyme was recovered from the STR by UF at the end of each cycle. The reaction was restarted by adding fresh substrate solution prior to the start of the next cycle. Throughout the cycle, the concentration of each saccharide component in the reactor was monitored. Furthermore, a series of additional tests were performed in the STR by varying the enzyme load. To quantify the loss of enzyme activity per cycle, I compared the results obtained in STR at known enzyme loadings (see Sect. 5.4.1 for details) with the progression curves obtained by cycling EMR (see Sect. 5.4.2).

5.4.1. Performance assessment in STR

The enzyme activity shown in Figure 22 varies from 923 to 8307 U·kg⁻¹ for the five batches of experiments used for calibration purposes. In the presence of elevated enzyme activity (above 8307 U·kg⁻¹), the production of DP3-6 and the consumption of lactose were at an astounding rate, and galactose was produced at significant rates. These phenomena make the results of operations performed at these enzyme concentrations unsuitable for calibration. Thus, the measured and predicted model under the enzyme activity range 923 to 8307 U·kg⁻¹ can be seen in Figure 22.

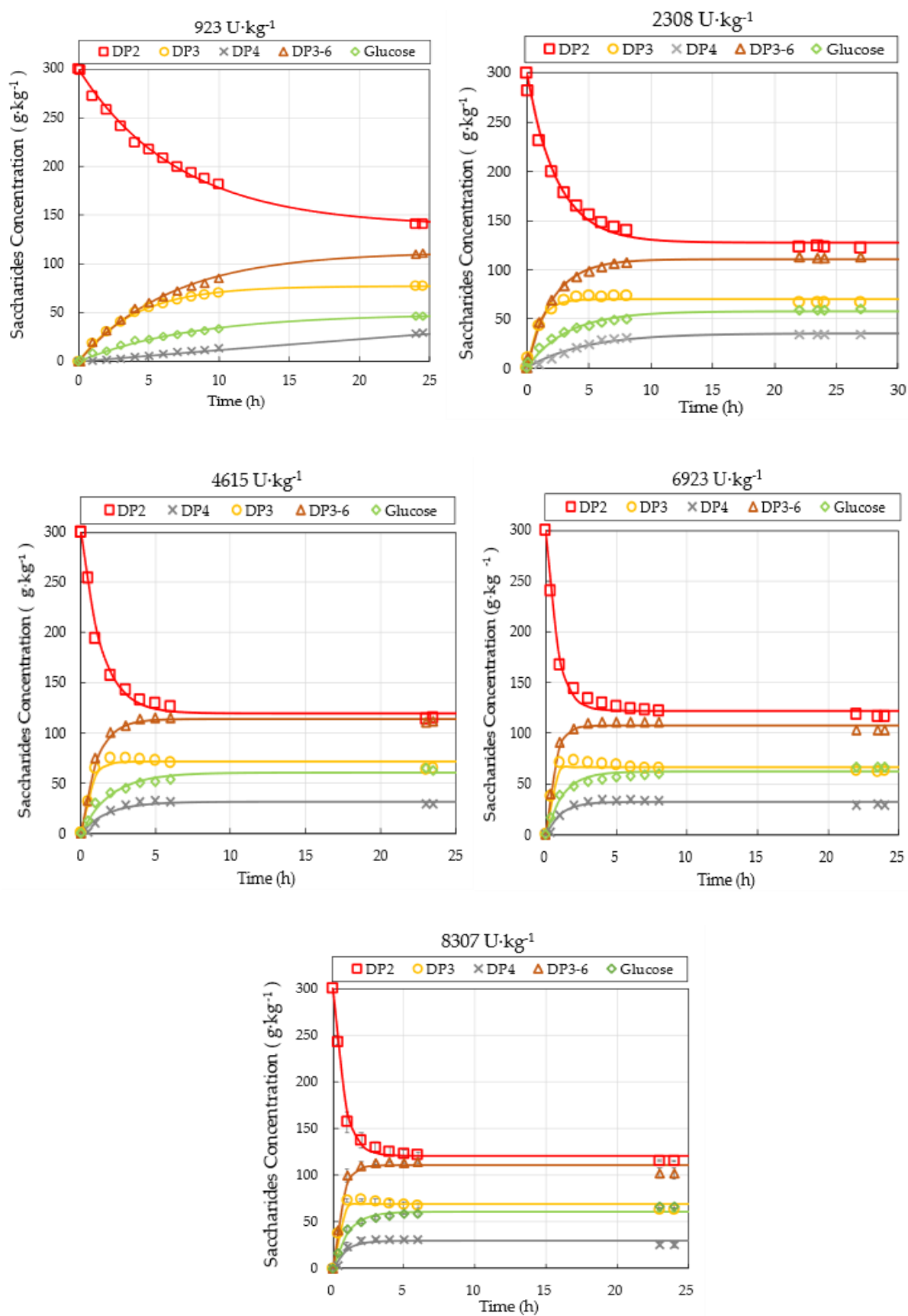


Figure 22. Progress curves of saccharides fractions for various enzyme loads ranging from 923 U·kg⁻¹ to 8307 U·kg⁻¹. Mean values and standard deviation of triplicate measurements were

shown for 8307 U·kg⁻¹. The solid lines present model predictions (Eq. 4.4.2-1), while symbols represent measured values. Operational conditions: 300 g·kg⁻¹ initial lactose concentration, pH 6.0, 50 °C, 60 rpm.

Table 6. Estimated parameters for the saturation model (Eq. 4.4.2-1) for different enzyme activities (rounded for two digits), their standard errors and 95 % confidence intervals together with the model accuracy F-tests and the explained variance rates (R^2) and the initial reaction velocity values ($p_1 \times p_2$).

Enzyme activity (U·kg ⁻¹)	Parameters	Estimate	Std. Error	95% Confidence Interval		F (2; df ₂)	R ²	p ₁ × p ₂ (g·kg ⁻¹ ·h ⁻¹)
				Interval				
				Lower Bound	Upper Bound			
923	p ₁	-162.07*	3.11	155.30	168.84	28504.6*	>0.99*	-22.69
	p ₂	0.14*	0.01	0.13	0.15	df ₂ =12		
2307	p ₁	-172.91*	2.92	166.56	179.27	5352.4*	0.99*	-70.03
	p ₂	0.41*	0.03	0.35	0.46	df ₂ =12		
4615	p ₁	-180.19*	3.35	172.60	187.76	4539.8*	0.99*	-134.24
	p ₂	0.75*	0.06	0.62	0.87	df ₂ =9		
6923	p ₁	-177.63*	1.64	174.07	181.20	6763.6*	0.99*	-220.44
	p ₂	1.24*	0.08	1.08	1.41	df ₂ =12		
8307	p ₁	-179.05*	1.72	175.53	182.56	8630.4*	0.99*	-237.95
	p ₂	1.33*	0.07	1.20	1.46	df ₂ =29		

* Significant at p<0.001

In all cases, the DP3-DP6 fraction increased gradually by the reaction time, then reached a plateau at $35.9 \pm 1.8\%$ w·w⁻¹ on total carbohydrate basis. The extent of hydrolysis activity, as measured by the amount of generated galactose, was negligible. The galactose concentration has remained typically below 1-3% w·w⁻¹. The saturation models (Eq. 4.4.2-1) were fitted to the observed concentration profiles. The results of curve fitting procedure, including the estimated parameters, their standard errors and 95 % confidence intervals together with the model accuracy F-tests, the explained variance rates (R^2) and the initial reaction velocity values ($p_1 \times p_2$) were summarized in

Table 6. In general, the observed data were consistent with the models that were assumed.

Each saccharide fraction was subjected to a determination of the initial reaction rate, or parameter $p_1 \times p_2$. This value will be subsequently used as a measure of enzyme activity. Figure 23 illustrates the basic relationship between the initial reaction rate and enzyme activity.

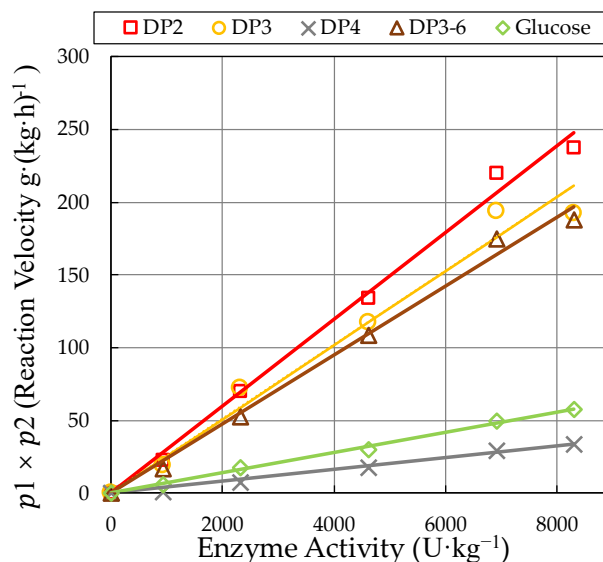


Figure 23. No-intercept linear relationship between enzyme activity and initial reaction velocity ($p_1 \times p_2$) of various saccharide fractions.

According to Table 7, linear models fit well with the observed data for all saccharide fractions within the investigated range of enzyme load (from 923 to 8307 U·kg⁻¹). All the linear models and their parameters were proven to be significant ($p < 0.001$).

Table 7. The slopes of the no-intercept linear regression functions fitted to the reaction velocity (Y) depending on enzyme activity for different saccharides fractions.

Saccharides compounds	no-intercept linear regression slopes	R ²
DP2	0.03 *	0.997 *
DP3	0.025 *	0.991 *
DP4	0.004 *	0.995 *
DP3-6	0.024 *	0.997 *
Glucose	0.007 *	0.999 *

* Significant at $p < 0.001$

By integrating the reaction rate data in the experiment with the slopes of the linear models listed

in Table 7 which can be used for calibration purposes. The amount of unknown enzyme loading can be calculated from the progress curve.

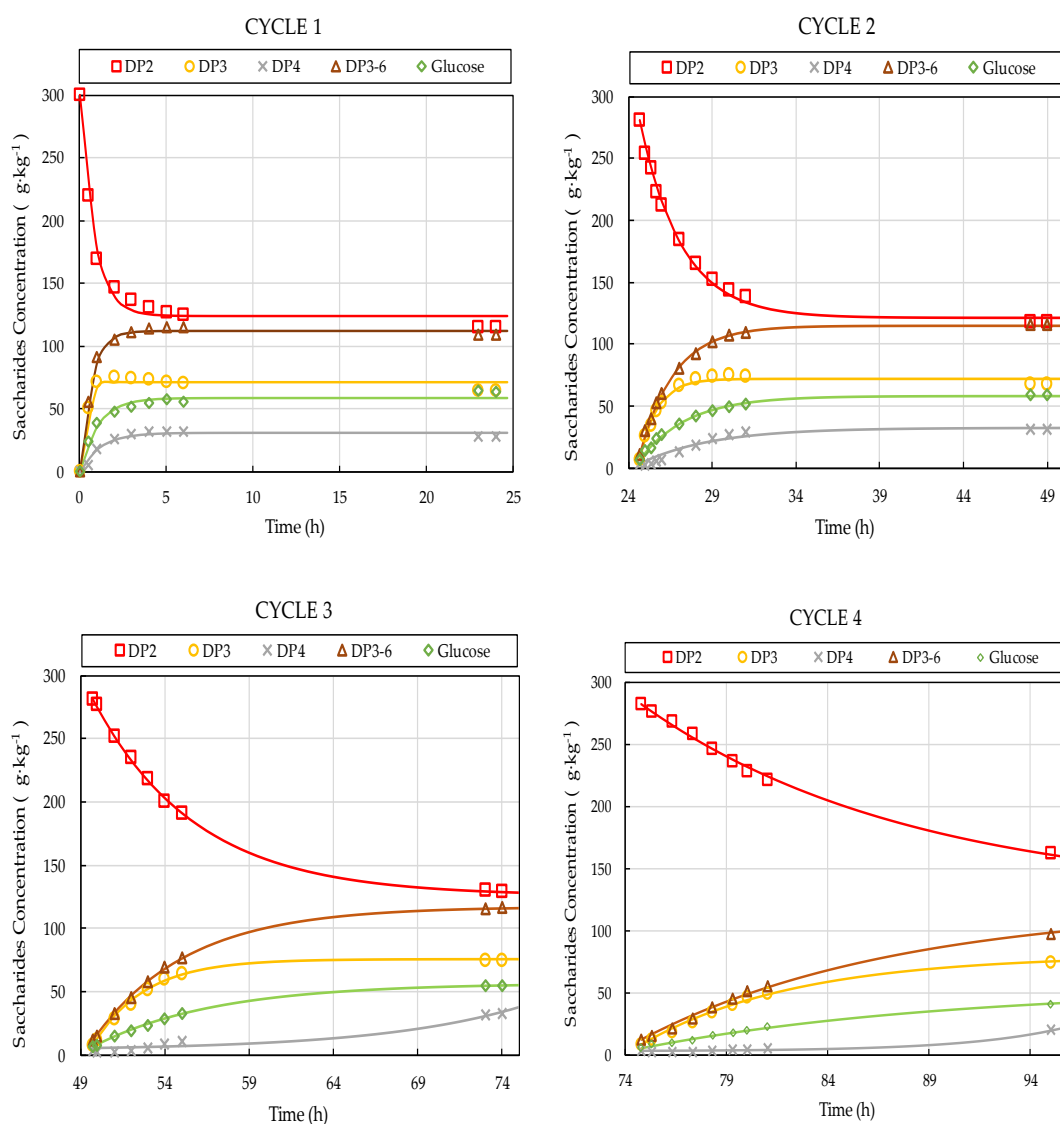
5.4.2. *Enzymatic conversion in cyclic-EMR*

The cyclic EMR system consists of a STR and an external UF module. Under the prescribed conditions, the GOS generation process was carried out in five consecutive cycles. Each cycle consists of a three-step procedure. Firstly, lactose was converted into GOS by an enzymatic reaction using soluble enzymes in a STR. Then, an UF unit was used to separate the reaction solution and obtain a carbohydrate mixture at the permeate end. This process allows large molecules of enzyme, which cannot pass through the UF membrane, to be recovered. Finally, fresh lactose was added to the enzyme concentrate to start the next cycle. The enzyme was reused to repeat GOS production in subsequent cycles.

A progression curve for each saccharide over five consecutive cycles was shown in Figure 24. Each reaction step was conducted under the same reaction conditions, pH 6.0 and 50°C, for a period of about 24 hours. The initial lactose concentration and initial enzyme activity were set at 300 g·kg⁻¹ and 8307 U·kg⁻¹, respectively. During the reaction, lactose was converted to oligosaccharides of different polymerization degrees (DP3-6), glucose, and small amounts of galactose. Modeling of experimental data was conducted using the saturation model described in Sect. 4.4.2. Specifically, initial reaction rates ($p_1 \times p_2$) for each saccharides' fraction were determined by estimating the parameters p_1 and p_2 .

Following the lactose conversion reaction in STR, the complete reaction mixture was transported to the UF procedure. The reaction solution was concentrated by a volume concentration factor of 8.6. Upon completion, the reaction solution was filtered in order to collect the GOS product from the permeate and to recover the enzyme from the concentrate, enabling the reaction step to be repeated. A membrane with a molecular weight cut-off of 30 kDa was used in the experiments. It is assumed that low molecular weight carbohydrates (< 1 kDa) can freely pass through the membrane and flow out to be collected in the permeate vessel. According to previous reports, several types of β -galactosidases were present in commercial enzyme preparations derived from

Bacillus circulans (Song et al., 2011, Vetere and Paoletti, 1998). Moreover, the enzyme responsible for lactose transgalactosylation has a molecular weight of approximately 90 to 240 kDa (Song et al., 2011, Vetere and Paoletti, 1998). Consequently, it can be assumed that the enzymes were completely retained by the UF membrane during filtration, and there was very little permeation loss through the membrane.



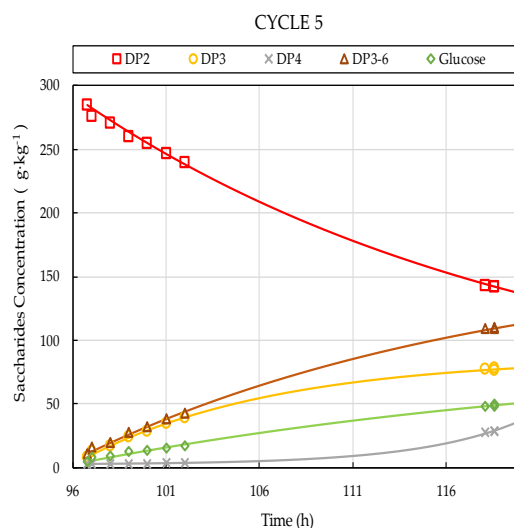


Figure 24. Saccharides composition in the reactor as function of operational time for 5 consecutive cycles. Symbols represent measured values; solid lines were model predictions evaluated by using Eq.4.4.2-1. Operational conditions: $300 \text{ g}\cdot\text{kg}^{-1}$ initial lactose concentration, $8307 \text{ U}\cdot\text{kg}^{-1}$ initial enzyme load, pH 6.0, 50°C .

By applying a high concentration factor, components that may inhibit the transgalactosylation reaction in subsequent cycles, such as glucose and galactose, should be removed from the reaction mixture. The inability to retain small molecules of sugar by the UF membrane and the membrane cleanup process was required before the start of each cycle. Therefore, glucose and galactose concentrations were kept below approx. $7 \text{ g}\cdot\text{L}^{-1}$ and $2 \text{ g}\cdot\text{L}^{-1}$ respectively at the beginning of each reaction step. It has been reported that residue inhibition at such concentration levels was negligible (Boon et al., 1999, Palai et al., 2012, Warmerdam et al., 2014).

The enzyme concentration in the reaction mixture increases over time during UF, and the permeate flux gradually decreases as filtration proceeds. As described in Sect. 4.6.2, the membrane modules were removed from the reactor system and cleaned upon completion of the concentration process. The alkaline cleaning was found to be effective in restoring the membrane to its original water permeability with no more than 25% loss of membrane permeability. In the UF step, an average permeates of $81 \pm 6 \text{ L}\cdot\text{h}^{-1}\cdot\text{m}^{-2}\cdot\text{bar}^{-1}$ was measured for the reaction mixture, and a water permeability of $207 \pm 16 \text{ L}\cdot\text{h}^{-1}\cdot\text{m}^{-2}\cdot\text{bar}^{-1}$ was observed in the repeated cleaning cycles.

5.4.3. Quantification of enzyme losses

It is clear from Figure 24 that there has been a progressive decline in the rate at which GOS was synthesized, and lactose was converted from cycle 1 to cycle 5. A loss of enzyme activity was believed to be responsible for the observed decreases. To quantify these losses, I first determined the initial reaction rates of the individual saccharides by fitting the obtained experimental data to the progression curves shown in Figure 24 through a saturation model. Following previous STR experiments using known enzyme concentrations (Table 7), linear models were used to calculate the respective enzyme activity values for each cycle. These models were used as calibration curves to determine the unknown (residual) enzyme activity values for successive cycles.

In Table 8, residual enzyme activity values were presented for DP2, DP3, DP3-6, and glucose in the reaction solution for five consecutive cycles. Since galactose and oligosaccharides with higher polymerization (DP4-6) were present in low concentrations in the reaction solution, the model fitted with these data has limited predictive power. Consequently, these low-concentration fractions were not included in the estimation process. According to the results, the activity values obtained were independent of the type of saccharides used in the estimation process. In other words, all listed components return with close approximations of the remaining activity. Table 8 indicates that enzyme activity decreases with each cycle.

Table 8. Enzyme activity values [$\text{U} \cdot \text{kg}^{-1}$] for the 5 consecutive cycles as determined by analyzing the reaction rates of different saccharides fractions.

Fractions	Cycles				
	No.1	No.2	No.3	No.4	No.5
DP2	7077	2124	846	388	329
DP3	7925	2480	890	379	306
DP3-6	6999	2081	785	355	295
Glucose	7903	2588	992	448	400
Mean	7476	2318	878	392	333
STDEV	507	254	87	40	47

In Figure 25, the relative enzyme activity was plotted against the operational time for the 5 cycles.

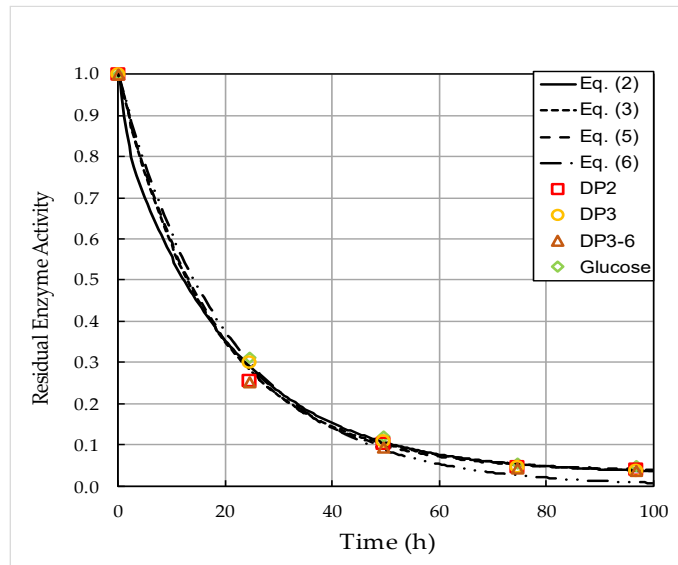


Figure 25. Decline of relative enzyme activity over operation time during the 5 consecutive cycles. Symbols represent data obtained by using different saccharides fractions in the estimation procedure. Predictions obtained by inactivation models were illustrated with lines.

The various enzyme deactivation models (Eq. 3.9.2-2 - Eq. 3.9.2-6) mentioned previously in Sect. 3.9.2 with respect to enzymes were fitted globally to all available data points by introducing non-negative constraints on the model parameters.

Table 9 summarizes the results of parameter estimation. In general, favorable overall fittings were achieved for all implemented models. It should be noted that the first-order deactivation model (Eq. 3.9.2-6) tends to underestimate activity in the last phases of the investigation period, i.e., for lower activity values. The goodness of fit was not significantly different between the single-stage model with a non-zero final stage (Eq. 3.9.2-5), and the more complex two-stage models (Eq. 3.9.2-2 and Eq. 3.9.2-3) with 3 and 4 fitting parameters, respectively.

Table 9. Estimated parameters of the inactivation models (Eq. 3.9.2-2 - Eq. 3.9.2-6).

Model	k_1	k_2	α_1	α_2	R^2	SSR
Eq. 3.9.2-2	9.692×10^{-1}	4.839×10^{-2}	8.125×10^{-1}	2.977×10^{-2}	0.9974	7.338×10^{-3}
Eq. 3.9.2-3	5.947×10^{-2}	9.980×10^{-3}	7.493×10^{-2}	0	0.9987	3.535×10^{-3}
Eq. 3.9.2-5	5.537×10^{-2}	0	3.651×10^{-2}	0	0.9986	3.674×10^{-3}
Eq. 3.9.2-6	4.891×10^{-2}	0	0	0	0.9957	1.194×10^{-2}

It is noted that the half-life of 15.3 h achieved in this study was in reasonable agreement with the

results reported by Warmerdam et al.(2013) using similar operational settings. In their prior investigation, the half-life of Biolacta N5 at an initial lactose content of $300 \text{ g}\cdot\text{L}^{-1}$ was determined to be 29 hours, 29 hours, and 16 hours, respectively, at temperatures of 20, 40, and 60 °C.

It is worth noting that modeling the observed enzyme activity data using Eq. 3.9.2-2 - Eq. 3.9.2-6 was performed under the assumption that the reactions were performed under stable operating conditions. Under the assumed conditions, the activity of the enzyme decreases continuously and gradually during the reaction. However, in my study, a series of repeated reactions and filtration steps were performed. In the filtration step, the enzymes were recirculated by the retention of the membrane assembly and concentrated in the retentate. Therefore, there were some limitations associated with the model developed. Retained enzymes accumulate on the membrane surface during crossflow filtration, forming a concentration polarization layer that may enhance fouling and partially inactivate biocatalysts (Botelho et al., 2022, Córdova et al., 2016a, Córdova et al., 2016b, Su et al., 2020). The methods used for this study do not allow to quantify the extent of the activity decline caused by the filtration procedure and its relation to the stability in STR during the reaction steps. Nevertheless, the estimated half-life was consistent with the estimate obtained by Warmerdam et al.(2013) for STR under similar conditions. Despite the fact that this fact suggests that the filtration steps do not affect enzyme stability to a pronounced extent, further investigation was required to determine the separate effects of the reaction and the filtration procedure on enzyme stability.

6. CONCLUSIONS AND RECOMMENDATIONS

Galacto-oligosaccharides (GOS) are prebiotic compounds widely used for their health-promoting effects. Current industrial production of GOS using free enzymes (non-immobilized enzyme) in conventional STRs is associated with complex downstream operations and high operating costs. One of the major expenditures in enzymatic biocatalytic process is the high cost of enzyme. The implementation of an external filtration module on the conventional STR has been reported as a possible solution to this problem. Several studies have been conducted on the utilization of ultrafiltration-assisted enzyme membrane reactors (UF-EMR) for the production of GOS using free enzymes. However, to the best of my knowledge, the application of β -galactosidase from *Bacillus circulans* in EMRs is scanty. The aim of my study was to investigate the synthesis of GOS from lactose by a commercially available *B. circulans* β -galactosidase (Biolacta N5) in an EMR setups.

In the first step of my experiment, several batch experiments were performed by STR with initial lactose concentration of $300 \text{ g}\cdot\text{L}^{-1}$, pH 6.0 and temperature 50°C . Effect of different concentrations of Biolacta N5, ranging from $0.1\text{--}10 \text{ g}\cdot\text{kg}^{-1}$ on the yield of GOS was studied. In later exercise, series of experiments were performed to produce the GOS by continuous-EMR and cyclic-EMR considering initial concentration of lactose $300 \text{ g}\cdot\text{L}^{-1}$, soluble Biolacta N5, pH 6.0 and temperature of 50°C . A series of short-term (typically 6–9 h total time) as well as two long-term (more than 120 h total time) were conducted in continuous-EMR experiments. In the short-term experiments, the effects of residence time (τ , in the range of 1.1 to 2.8 h) and enzyme activity (c_E : 8307-92301 $\text{U}\cdot\text{kg}^{-1}$) on catalytic performance were investigated at fixed recirculation flow rate $0.18 \text{ m}^3\cdot\text{h}^{-1}$. In cyclic-EMR experiment, five consecutive cycles were considered. Each cycle comprised a three-step procedure, mentioned herein. At first step, biocatalytic reaction was performed with mentioned initial concentration of lactose, pH and temperature in STR. In cyclic-EMR, concentration of Biolacta N5 was selected $8307 \text{ U}\cdot\text{kg}^{-1}$ from batch mode of experiment in STR. The mentioned enzyme activity provided highest GOS productivity in STR. In the second step, the enzyme was separated from saccharides mixture by UF membrane with MWCO 30 kDa. In the third step, recovered enzyme was reused for GOS production in the next cycle. Saccharides were

removed from the reaction liquor with a high-volume concentration factor of 8.6.

Kinetic equations for bioacatalytic reactions (Palai et al., 2012) and the enzyme deactivation (Warmerdam et al., 2013) were considered for the production of GOS in STR using free β -galactosidase from *Bacillus circulans*. Based on that, an extended mathematical framework dedicated to the performance of continuous-EMR for the production of GOS was developed. I considered the influence of different residence times (τ) and enzyme activity (c_E) on the production of GOS in continuous-EMR using a numerical software package.

According to the results of experiments in STR, the relative amount of DP3-6 fraction increases to a highest yield (38% w·w⁻¹), then decreases with time progress. Shorter reaction time is required to reach the highest concentration of GOS with increase of the concentration of β -galactosidase; however, with high concentration of β -galactosidase (>1 g·kg⁻¹), the hydrolysis reaction was significant, i.e., the increasing concentration of galactose. Therefore, concentration of β -galactosidase less than 1 g·kg⁻¹ (9230 U·kg⁻¹) was considered in subsequent continuous-EMR and cyclic-EMR experiments.

In continuous-EMR experiments, no irreversible membrane fouling was detected, and it was noted that regeneration of the membranes was possible through a membrane cleaning process. The maximum yields of GOS in continuous EMR was 33% w·w⁻¹ when the initial concentration of lactose, pH, reaction temperature and recirculation rate were 300 g·kg⁻¹, 6.0, 50°C and 0.18 m³·h⁻¹, respectively. The yield value was slightly lower than the results, obtained from STR (yield was 38% w·w⁻¹ from STR). In continuous-EMR, the yield of GOS was increased from 25% w·w⁻¹ to 33% w·w⁻¹ as the operating coefficient, $\tau \times c_E$, increased from 10153 to 260289 U·h·kg⁻¹, while the productivity decreased from approximately 7.263×10^{-3} to 0.368×10^{-3} g of DP3-6 per hour and unit enzyme activity was observed under the studied operational settings (g·h⁻¹·U⁻¹). Long-term experiments were conducted in duplicate to determine the operational stability of continuous-EMR. It was noted that no significant decline in GOS yield over a period of more than 120 hours, which indicates negligible enzyme losses. In long-term continuous-EMR, one gram of crude enzyme preparation produced on average about 1.4 kg of DP3-6. Experimental results highly satisfied the simulated results from developed mathematical model of continuous-EMR. According to the

simulation results, the activity of enzyme must be strictly monitored during continuous-EMR runs.

Experimental results of cyclic-EMR revealed that a gradual decrease in GOS production rate and lactose conversion from the first to the fifth cycle. A linear relationship was found between initial reaction rate and enzyme activity by analyzing the time course of the concentration of individual saccharides fractions from the previous STR experiments within an enzymatic activity range of $923 \text{ U}\cdot\text{kg}^{-1}$ to $92301 \text{ U}\cdot\text{kg}^{-1}$. Thus, in cyclic-EMR, the loss of enzyme activity in successive cycles can be estimated by determining the initial velocity of individual saccharide fractions from a progress curve. Furthermore, it was noted that the enzyme had an estimated half-life of 15 h in cyclic-EMR.

According to the investigation, enzyme-free GOS product and enzyme recovery were achieved by both continuous-EMR and cyclic-EMR processes. In long-term continuous-EMR experiments, it was observed a stable operational performance in terms of GOS yield and lactose conversion; however, the enzyme loss was negligible. Cyclic-EMR may provide ranges of advantages, such as enzyme recovery and improve the yield of GOS. In cyclic-EMR, the obtained experimental data on progress curves and activity declines might be useful for design considerations of such multi-step processes and may serve as a basis for further studies optimizing process parameters, such as the duration of reaction steps and scheduling enzyme dosage. These results suggest that EMR may serve as a promising alternative to conventional batch production schemes, especially considering the high price of biocatalysts. Furthermore, more in-depth studies related to optimization of process parameters, characteristics of membrane fouling and economic analysis of GOS production by UF-EMR might be interesting future research scope. It may expect that my investigation will be useful for scaling up the process and reduce the limitation of GOS production in industrial scale.

7. NEW SCIENTIFIC RESULTS

Within the frame of this work, I investigated the technical feasibility of galacto-oligosaccharides (GOS) production by ultrafiltration (UF)-assisted enzyme membrane reactors (EMR) operating in both continuous and cyclic fashion using free enzymes Biolacta N5 originating from *Bacillus circulans*. My new scientific achievements can be summarized as:

- 1) I have developed an extended mathematical framework to predict production of GOS in continuous-EMRs by free β -galactosidases. By simulating the dynamics of formulation of saccharides in continuous-EMR for various residence times (0-10 h) and enzyme load of Biolacta N5 (0-10 g \cdot kg⁻¹), my in-silico study suggests that continuous-EMR underperforms STR in the term of steady-state GOS yield (30% w \cdot w⁻¹ vs. 34% w \cdot w⁻¹ for continuous-EMR and STR, respectively) under the same operational conditions (320 g \cdot kg⁻¹ lactose solution, pH 6.0, and 40°C).
- 2) By using soluble Biolacta N5, a *Bacillus circulans*-derived commercial enzyme preparation, I have experimentally investigated the steady-state performance of the continuous-EMR as function of residence time (1.1-2.8 h) and enzyme load (8307-92301 U \cdot kg⁻¹) under fixed operational settings (50°C, pH 6.0, lactose feed concentration of 300 g \cdot kg⁻¹, and recirculation flowrate of 0.18 m³ \cdot h⁻¹). My results indicate that the yield increased from 24% w \cdot w⁻¹ to 33% w \cdot w⁻¹, whereas the productivity decreased from ca. 7 \times 10⁻³ to 0.4 \times 10⁻³ g \cdot h⁻¹ \cdot U⁻¹, when adjusting $\tau \times c_E$, from 10153 to 260289 U \cdot h \cdot kg⁻¹. I also found that the yield of oligosaccharides with higher DP (3-6) in STR (approx. 38% on total carbohydrate basis) slightly exceeds that measured in continuous-EMR (ranging from 24% w \cdot w⁻¹ to 33% w \cdot w⁻¹). This finding is in good agreement with my preliminary simulation results, as in reported above in 1).
- 3) A stable catalytic performance without a significant deterioration in product quality was observed when operating the continuous-EMR for an extended period of time (>120 h). Under the investigated operational settings (46151 U \cdot kg⁻¹ Biolacta N5, 30% w \cdot w⁻¹ lactose solution, pH 6.0, 50°C, 0.16 m³ \cdot h⁻¹ recirculation flowrate, and residence time of 1.8h), approx. 1.4 kg of DP3-6 was produced per one gram of crude enzyme preparation over the long-term

campaigns. I proved that the operational stability of the enzyme in continuous-EMR is considerably higher than previously reported for STR in the literature (Warmerdam et al., 2013).

- 4) I proposed a process scheme for enzyme recovery by operating the EMR in cyclic fashion. Repeated reaction steps ($8307 \text{ U} \cdot \text{kg}^{-1}$ initial Biolacta N5, 30% w·w⁻¹ lactose solution, pH 6.0, 50°C) were performed and followed by UF steps employing a volume concentration factor of 8.6 to separate the carbohydrate products from enzymes. I quantified the enzyme losses with a direct method by analyzing the underlying relationship between reaction rates and enzyme dosage obtained from additional experiments conducted with known enzyme loads. I found that the enzyme activity in the cyclic-EMR declined gradually from $8307 \text{ U} \cdot \text{kg}^{-1}$ to $923 \text{ U} \cdot \text{kg}^{-1}$ within five cycles, resulting in a half-life of approx. 15.3 h. The result of half-life of Biolacta N5 is comparable to those previously reported by Warmerdam et al. (2013) in STR.

8. SUMMARY

Galacto-oligosaccharides (GOS) are indigestible oligosaccharides with prebiotic effects and are widely used as an additive in infant formulas, dairy products, and beverages. Commercially, GOS were produced primarily through catalytic reactions in STRs using soluble β -galactosidase. However, one significant limitation of this conventional method were the high operational costs, which related to the non-reusability of the enzyme. Ultrafiltration membrane-assisted enzyme membrane reactors have been reported to have the ability to achieve enzyme reuse. However, the performance of Biolacta N5, a commercial enzyme preparation derived from *Bacillus circulans* in generating GOS in EMR has not been studied.

In my Ph.D. research, I evaluated the potential of using soluble Biolacta N5 for GOS production in continuous-EMR and cyclic-EMR, respectively. An extended mathematical model was successfully applied to simulate the performance of continuous-EMR for the synthesis of GOS. In other words, the changes in the individual saccharide fractions over time. Different residence times and enzyme activities were found to have effects on GOS yield, and it was found that the maximum GOS yield at steady-state (approx. 30% w·w⁻¹) was obtained at $\tau \times c_E$ of $2 \times 10^5 \text{ U} \cdot \text{h} \cdot \text{kg}^{-1}$ within the studied range. Simulation experiments considering enzyme inactivation in continuous-EMR obtained an enzyme half-life of ca. 29h. The simulation results demonstrated that in the actual continuous-EMR process, timely replenishment of fresh enzymes is necessary to ensure consistent quality.

I performed a series of short and long experiments to investigate the operational stability of Biolacta N5 in continuous-EMR. The results observed for the effect of different residence times and enzyme concentrations on GOS production showed a similar tendency as in the previous simulations. When controlling the operating factor ($\tau \times c_E$) from $10^4 \text{ U} \cdot \text{h} \cdot \text{kg}^{-1}$ to $2.6 \times 10^5 \text{ U} \cdot \text{h} \cdot \text{kg}^{-1}$, the GOS yield increased from 24% w·w⁻¹ to 33% w·w⁻¹. However, GOS productivity decreased from approximately 7×10^{-3} to $0.4 \times 10^{-3} \text{ g} \cdot \text{h}^{-1} \cdot \text{U}^{-1}$. The maximum GOS yield of 33% w·w⁻¹ obtained at steady-state in the continuous-EMR experiments was slightly lower than that in the STR under the same conditions (~38% w·w⁻¹). This phenomenon in agreement with the results of the previous

simulation experiments, i.e., lower yield in continuous-EMR. A stable catalytic performance without a significant deterioration in product quality was observed when operating the EMR for an extended period of time (>120 h). Approx. 1.4 kg of DP3-6 was produced per one gram of crude enzyme preparation over the long-term campaigns.

In cyclic-EMR, GOS synthesis was performed in a batchwise manner in five consecutive cycles. A volume concentration factor of 8.6 was achieved to successfully separate the carbohydrates from the enzyme using an UF module. The collected enzymes were used in the next cycle to catalyze the conversion of fresh lactose. Enzyme losses during consecutive cycles was successfully quantified with a direct approach by analyzing the underlying relationship between reaction rate and enzyme dosage obtained from additional experiments with known enzyme loads. Within five cycles, the enzyme activity declined gradually from 7476 to 333 U·kg⁻¹, and the half-life was estimated as ca. 15.3 h.

All these results suggest that EMR might serve as a promising alternative to conventional batch production scheme, especially considering the high price of the biocatalysts. In addition, the outcomes of my research may serve as a basis for further optimization GOS production in EMR.

9. PUBLICATIONS

1. Articles in a magazine/journal:

Cao, T., Pázmándi, M., Galambos, I. and Kovács, Z., 2020. Continuous production of galacto-oligosaccharides by an enzyme membrane reactor utilizing free enzymes. *Membranes*, 10(9), p.203. <https://doi.org/10.3390/membranes10090203> (***Membranes*, Impact Factor: 4.13 (2020), JCR – Q2 (Chemical Engineering)**).

Cao, T., Kovács, Z. and Ladányi, M., 2023. Cyclic Production of Galacto-Oligosaccharides through Ultrafiltration-Assisted Enzyme Recovery. *Processes*, 11(1), p.225. <https://doi.org/10.3390/pr11010225> (***Processes*, Impact Factor: 3.352, JCR - Q2 (Engineering, Chemical))**).

2. Abstracts in conferences

Teng, C. et al., 2021. Ultrafiltration-based enzyme recovery in the batch production of galacto-oligosaccharides. *In 4th International Conference on Biosystems and Food Engineering. Budapest, Hungary, 4th June, 2021.* <http://www.biosysfoodeng.hu/2021/USB/#proceedings>

Teng, C. et al., 2021. The continuous production and real-time monitoring of galacto-oligosaccharides. *In 9th European Young Engineers Conference. Warsaw, Poland, 19–21 April 2021.* pp. 150. https://www.eyec.ichip.pw.edu.pl/wp-content/uploads/Monografia_EYEC_9th.pdf

Teng, C. et al., 2019. Method for Real-time Monitoring of Galactooligosaccharides Production by Means of Fourier Transform Near-Infrared Spectroscopy. *In Second Aquaphotomics European Conference. Budapest, Hungary, 2-3 December 2019.* pp. 28–28.

10. APPENDICES

A1. References

2016. Generally Recognized As Safe Determination for the Use of VITAGOS in Infant Formula and Selected Conventional Foods. *GRAS Notice (GRN) No. 671*. United States Food and Drug Administration.
- AKCAN, N. 2011. High level production of extracellular β -galactosidase from *Bacillus licheniformis* ATCC 12759 in submerged fermentation. *African Journal of Microbiology Research*, 5, 4615-4621.
- ALBAYRAK, N. & YANG, S. T. 2002. Production of galacto-oligosaccharides from lactose by *Aspergillus oryzae* β -galactosidase immobilized on cotton cloth. *Biotechnology and Bioengineering*, 77, 8-19.
- BAKKEN, A. P., HILL JR, C. G. & AMUNDSON, C. H. 1992. Hydrolysis of lactose in skim milk by immobilized β -galactosidase (*Bacillus circulans*). *Biotechnology and Bioengineering*, 39, 408-417.
- BAMIGBADE, G. B., SUBHASH, A. J., KAMAL-ELDIN, A., NYSTRÖM, L. & AYYASH, M. 2022. An updated review on prebiotics: insights on potentials of food seeds waste as source of potential prebiotics. *Molecules*, 27, 5947.
- BOON, M., JANSSEN, A. & VAN DER PADT, A. 1999. Modelling and parameter estimation of the enzymatic synthesis of oligosaccharides by β -galactosidase from *Bacillus circulans*. *Biotechnology and Bioengineering*, 64, 558-567.
- BOON, M., JANSSEN, A. & VAN'T RIET, K. 2000. Effect of temperature and enzyme origin on the enzymatic synthesis of oligosaccharides. *Enzyme and Microbial Technology*, 26, 271-281.
- BOSSO, A., MORIOKA, L. R. I., SANTOS, L. F. D. & SUGUIMOTO, H. H. 2016. Lactose hydrolysis potential and thermal stability of commercial β -galactosidase in UHT and skimmed milk. *Food Science and Technology*, 36, 159-165.
- BOTELHO, V. A., MATEUS, M., PETRUS, J. C. & DE PINHO, M. N. 2022. Membrane Bioreactor for Simultaneous Synthesis and Fractionation of Oligosaccharides. *Membranes*, 12, 171.
- CAO, T., PÁZMÁNDI, M., GALAMBOS, I. & KOVÁCS, Z. 2020. Continuous production of galacto-oligosaccharides by an enzyme membrane reactor utilizing free enzymes. *Membranes*, 10, 203.
- CHEN, W., CHEN, H., XIA, Y., ZHAO, J., TIAN, F. & ZHANG, H. 2008. Production, purification, and characterization of a potential thermostable galactosidase for milk lactose hydrolysis from *Bacillus stearothermophilus*. *Journal of Dairy Science*, 91, 1751-1758.
- CHEN, X. Y. & GÄNZLE, M. G. 2017. Lactose and lactose-derived oligosaccharides: More than prebiotics? *International Dairy Journal*, 67, 61-72.
- CHOCKCHASAWASDEE, S., ATHANASOPOULOS, V. I., NIRANJAN, K. & RASTALL, R. A. 2005. Synthesis of galacto-oligosaccharide from lactose using β -galactosidase from *Kluyveromyces lactis*: studies on batch and continuous UF membrane-fitted bioreactors. *Biotechnology and*

- CÓRDOVA, A., ASTUDILLO, C., GIORNO, L., GUERRERO, C., CONIDI, C., ILLANES, A. & CASSANO, A. 2016a. Nanofiltration potential for the purification of highly concentrated enzymatically produced oligosaccharides. *Food and Bioproducts Processing*, 98, 50-61.
- CÓRDOVA, A., ASTUDILLO, C., GUERRERO, C., VERA, C. & ILLANES, A. 2016b. Assessment of the fouling mechanisms of an ultrafiltration membrane bioreactor during synthesis of galacto-oligosaccharides: Effect of the operational variables. *Desalination*, 393, 79-89.
- CÓRDOVA, A., ASTUDILLO, C., VERA, C., GUERRERO, C. & ILLANES, A. 2016c. Performance of an ultrafiltration membrane bioreactor (UF-MBR) as a processing strategy for the synthesis of galacto-oligosaccharides at high substrate concentrations. *Journal of Biotechnology*, 223, 26-35.
- CUI, Z., JIANG, Y. & FIELD, R. 2010. Fundamentals of pressure-driven membrane separation processes. *Membrane technology*. Elsevier.
- CZERMAK, P., EBRAHIMI, M., GRAU, K., NETZ, S., SAWATZKI, G. & PFROMM, P. H. 2004. Membrane-assisted enzymatic production of galactosyl-oligosaccharides from lactose in a continuous process. *Journal of Membrane Science*, 232, 85-91.
- DAI, Z., LYU, W., XIANG, X., TANG, Y., HU, B., OU, S. & ZENG, X. 2018. Immunomodulatory effects of enzymatic-synthesized α -galactooligosaccharides and evaluation of the structure–activity relationship. *Journal of Agricultural and Food Chemistry*, 66, 9070-9079.
- DAS, R., SEN, D., SARKAR, A., BHATTACHARYYA, S. & BHATTACHARJEE, C. 2011. A comparative study on the production of galacto-oligosaccharide from whey permeate in recycle membrane reactor and in enzymatic batch reactor. *Industrial & engineering chemistry research*, 50, 806-816.
- DE ALBUQUERQUE, T. L., DE SOUSA, M., E SILVA, N. C. G., NETO, C. A. C. G., GONÇALVES, L. R. B., FERNANDEZ-LAFUENTE, R. & ROCHA, M. V. P. 2021. β -Galactosidase from *Kluyveromyces lactis*: Characterization, production, immobilization and applications-A review. *International Journal of Biological Macromolecules*, 191, 881-898.
- DECASTRO, M.-E., ESCUDER-RODRIGUEZ, J.-J., CERDAN, M.-E., BECERRA, M., RODRIGUEZ-BELMONTE, E. & GONZALEZ-SISO, M.-I. 2018. Heat-loving β -galactosidases from cultured and uncultured microorganisms. *Current Protein and Peptide Science*, 19, 1224-1234.
- DESCHAVANNE, P. J., VIRATELLE, O. M. & YON, J. M. 1978. Conformational adaptability of the active site of beta-galactosidase. Interaction of the enzyme with some substrate analogous effectors. *Journal of Biological Chemistry*, 253, 833-837.
- EBRAHIMI, M., PLACIDO, L., ENGEL, L., ASHAGHI, K. S. & CZERMAK, P. 2010. A novel ceramic membrane reactor system for the continuous enzymatic synthesis of oligosaccharides. *Desalination*, 250, 1105-1108.
- EBRAHIMI, M., PLACIDO, L., ENGEL, L., SHAMS-ASHAGHI, K. & CZERMAK, P. Two-Stage Integrated Ceramic Membrane Reactor System For The Continuous Enzymatic Synthesis Of Oligosaccharides. WFC10: Discover the Future of Filtration & Separation, 2008. Filtech

Exhibitions Germany, II-492-II-496.

- ÉLYSÉE-COLLEN, B. & LENCKI, R. W. 1997. Protein ultrafiltration concentration polarization layer flux resistance I. Importance of protein layer morphology on flux decline with gelatin. *Journal of Membrane Science*, 129, 101-113.
- FIJAN, S. 2014. Microorganisms with claimed probiotic properties: an overview of recent literature. *International Journal of Environmental Research and Public Health*, 11, 4745-4767.
- FISCHER, C. & KLEINSCHMIDT, T. 2015. Synthesis of galactooligosaccharides using sweet and acid whey as a substrate. *International Dairy Journal*, 48, 15-22.
- FISCHER, C. & KLEINSCHMIDT, T. 2018. Synthesis of galactooligosaccharides in milk and whey: a review. *Comprehensive Reviews in Food Science and Food Safety*, 17, 678-697.
- FLORES, M., ERTOLA, R. & VOGET, C. 1996. Effect of Monovalent Cations on the Stability and Activity of *Kluyveromyces lactis* β -Galactosidase. *LWT-Food Science and Technology*, 29, 503-506.
- FODA, M. I. & LOPEZ-LEIVA, M. 2000. Continuous production of oligosaccharides from whey using a membrane reactor. *Process Biochemistry*, 35, 581-587.
- FÜREDER, V., RODRIGUEZ-COLINAS, B., CERVANTES, F. V., FERNANDEZ-ARROJO, L., POVEDA, A., JIMENEZ-BARBERO, J., BALLESTEROS, A. O. & PLOU, F. 2020. Selective synthesis of galactooligosaccharides containing β (1 \rightarrow 3) linkages with β -galactosidase from *Bifidobacterium bifidum* (Saphera). *Journal of Agricultural and Food Chemistry*, 68, 4930-4938.
- GÄNZLE, M. G. 2012. Enzymatic synthesis of galacto-oligosaccharides and other lactose derivatives (hetero-oligosaccharides) from lactose. *International Dairy Journal*, 22, 116-122.
- GAYNOR, P. 2015. GRAS Exemption Claim for Galacto-oligosaccharides. In: NUTRITION, N. (ed.). FDA, GRAS Notice (GRN) No.620.
- GENNARI, A., MOBAYED, F. H., VOLPATO, G. & DE SOUZA, C. F. V. 2018. Chelation by collagen in the immobilization of *Aspergillus oryzae* β -galactosidase: A potential biocatalyst to hydrolyze lactose by batch processes. *International Journal of Biological Macromolecules*, 109, 303-310.
- GIBSON, G. R., HUTKINS, R., SANDERS, M. E., PRESCOTT, S. L., REIMER, R. A., SALMINEN, S. J., SCOTT, K., STANTON, C., SWANSON, K. S. & CANI, P. D. 2017. Expert consensus document: The International Scientific Association for Probiotics and Prebiotics (ISAPP) consensus statement on the definition and scope of prebiotics. *Nature Reviews Gastroenterology & Hepatology*, 14, 491-502.
- GIBSON, G. R., PROBERT, H. M., VAN LOO, J., RASTALL, R. A. & ROBERFROID, M. B. 2004. Dietary modulation of the human colonic microbiota: updating the concept of prebiotics. *Nutrition Research Reviews*, 17, 259-275.
- GIBSON, G. R. & ROBERFROID, M. B. 1995. Dietary modulation of the human colonic microbiota: introducing the concept of prebiotics. *The Journal of nutrition*, 125, 1401-1412.
- GIBSON, G. R., SCOTT, K. P., RASTALL, R. A., TUOHY, K. M., HOTCHKISS, A., DUBERT-

- FERRANDON, A., GAREAU, M., MURPHY, E. F., SAULNIER, D. & LOH, G. 2010. Dietary prebiotics: current status and new definition. *Food Science and Technology Bulletin: Functional Foods*, 7, 1-19.
- GONZÁLEZ-DELGADO, I., LÓPEZ-MUÑOZ, M.-J., MORALES, G. & SEGURA, Y. 2016. Optimisation of the synthesis of high galacto-oligosaccharides (GOS) from lactose with β -galactosidase from *Kluyveromyces lactis*. *International Dairy Journal*, 61, 211-219.
- GONZALEZ, R., EBRAHIMI, M. & CZERMAK, P. 2009. Experimental and modeling study of Galactosyl-Oligosaccharides formation in continuous recycle membrane reactors (CRMR). *The Open Food Science Journal*, 3, 1-9.
- GOSLING, A., ALFTRÉN, J., STEVENS, G. W., BARBER, A. R., KENTISH, S. E. & GRAS, S. L. 2009. Facile pretreatment of *Bacillus circulans* β -galactosidase increases the yield of galactosyl oligosaccharides in milk and lactose reaction systems. *Journal of Agricultural and Food Chemistry*, 57, 11570-11574.
- GOSLING, A., STEVENS, G. W., BARBER, A. R., KENTISH, S. E. & GRAS, S. L. 2010. Recent advances refining galactooligosaccharide production from lactose. *Food Chemistry*, 121, 307-318.
- HACKENHAAR, C. R., SPOLIDORO, L. S., FLORES, E. E. E., KLEIN, M. P. & HERTZ, P. F. 2021. Batch synthesis of galactooligosaccharides from co-products of milk processing using immobilized β -galactosidase from *Bacillus circulans*. *Biocatalysis and Agricultural Biotechnology*, 36, 102136.
- HAIDER, T. & HUSAIN, Q. 2007. Preparation of lactose free milk by using ammonium sulphate fractionated proteins from almonds. *Jouranl of the Science of Food and Agriculture*, 87, 1278-1283.
- HASLER, C. M. & BROWN, A. C. 2009. Position of the American Dietetic Association: functional foods. *Journal of the American Dietetic Association*, 109, 735-746.
- HE, Z., MILLER, D. J., KASEMSET, S., PAUL, D. R. & FREEMAN, B. D. 2017. The effect of permeate flux on membrane fouling during microfiltration of oily water. *Journal of Membrane Science*, 525, 25-34.
- HENLEY, J. P. & SADANA, A. 1985. Categorization of enzyme deactivations using a series-type mechanism. *Enzyme Microbial Technology*, 7, 50-60.
- HUANG, J., ZHU, S., ZHAO, L., CHEN, L., DU, M., ZHANG, C. & YANG, S.-T. 2020. A novel β -galactosidase from *Klebsiella oxytoca* ZJU1705 for efficient production of galacto-oligosaccharides from lactose. *Applied Microbiology and Biotechnology*, 104, 6161-6172.
- HUERTA, L. M., VERA, C., GUERRERO, C., WILSON, L. & ILLANES, A. 2011. Synthesis of galacto-oligosaccharides at very high lactose concentrations with immobilized β -galactosidases from *Aspergillus oryzae*. *Process Biochemistry*, 46, 245-252.
- HUNZIKER, O. & NISSEN, B. 1926. Lactose solubility and lactose crystal formation: I. Lactose solubility. *Journal of Dairy Science*, 9, 517-537.
- IBM CORP. RELEASED 2017. IBM SPSS STATISTICS FOR WINDOWS, V. A., NY: IBM CORP.

- ILLANES, A., VERA, C. & WILSON, L. 2016. Enzymatic production of galacto-oligosaccharides. *Lactose-derived prebiotics: A process perspective*. Elsevier Inc.
- JAIN, M., NARAYANAN, S., TIWARI, D. P., RANJAN, B., JADHAV, A., VENKATARAMULU, D., CHANDRAYAN, G., JAYARAO, C., BHOITE, P. & KRISHNAPPA, M. 2019. Safety assessment of Gossence™(galactooligosaccharides): Genotoxicity and general toxicity studies in Sprague Dawley rats. *Toxicology Research and Application*, 3, 2397847319860375.
- JENAB, E., OMIDGHANE, M., MUSSONE, P., ARMADA, D. H., CARTMELL, J. & MONTEMAGNO, C. 2018. Enzymatic conversion of lactose into galacto-oligosaccharides: The effect of process parameters, kinetics, foam architecture, and product characterization. *Journal of Food Engineering*, 222, 63-72.
- JOVANOVIC-MALINOVSKA, R., FERNANDES, P., WINKELHAUSEN, E. & FONSECA, L. 2012. Galacto-oligosaccharides synthesis from lactose and whey by β -galactosidase immobilized in PVA. *Applied Biochemistry and Biotechnology*, 168, 1197-1211.
- KAMPMAYER, C. 2022. Generally Recognized As Safe Determination for the Use of VITAGOS™ IF in Non-Exempt Term Infant Formula and Selected Conventional Foods *In*: INC., V. N. (ed.). FDA, GRAS Notice (GRN) No. 1076.
- KASCHE, V. 1986. Mechanism and yields in enzyme catalysed equilibrium and kinetically controlled synthesis of β -lactam antibiotics, peptides and other condensation products. *Enzyme and Microbial Technology*, 8, 4-16.
- KERRY, R. G., PATRA, J. K., GOUDA, S., PARK, Y., SHIN, H.-S. & DAS, G. 2018. Benefaction of probiotics for human health: A review. *Journal of Food and Drug Analysis*, 26, 927-939.
- KHAN, A., ALI, J., JAMIL, S. U. U., ZAHRA, N., TAYABA, T., IQBAL, M. J. & WASEEM, H. 2022. Removal of micropollutants. *Environmental Micropollutants*. Elsevier.
- KIM, C., JI, E. S. & OH, D. K. 2004a. Characterization of a thermostable recombinant β -galactosidase from *Thermotoga maritima*. *Journal of Applied Microbiology*, 97, 1006-1014.
- KIM, C. S., JI, E.-S. & OH, D.-K. 2004b. A new kinetic model of recombinant β -galactosidase from *Kluyveromyces lactis* for both hydrolysis and transgalactosylation reactions. *Biochemical and Biophysical Research Communications*, 316, 738-743.
- KOVÁCS, Z., BENJAMINS, E., GRAU, K., UR REHMAN, A., EBRAHIMI, M. & CZERMAK, P. 2013. Recent developments in manufacturing oligosaccharides with prebiotic functions. *Biotechnology of Food and Feed Additives*, 257-295.
- LADERO, M., SANTOS, A., GARCÍA, J., CARRASCOSA, A., PESSELA, B. & GARCÍA-OCHOA, F. 2002. Studies on the activity and the stability of β -galactosidases from *Thermus* sp strain T2 and from *Kluyveromyces fragilis*. *Enzyme and Microbial Technology*, 30, 392-405.
- LAMSAL, B. P. 2012. Production, health aspects and potential food uses of dairy prebiotic galactooligosaccharides. *Journal of the Science of Food and Agriculture*, 92, 2020-2028.

- MA, S., KASSINOS, S. C. & KASSINOS, D. 2009. Direct simulation of the limiting flux: I. Interpretation of the experimental results. *Journal of Membrane Science*, 337, 81-91.
- MACFARLANE, G. T., STEED, H. & MACFARLANE, S. 2008. Bacterial metabolism and health-related effects of galacto-oligosaccharides and other prebiotics. *Journal of Applied Microbiology*, 104, 305-344.
- MADANI, R., ZARIF-FARD, M. & GOLCHIN-FAR, F. 1999. Effect of activators and inhibitors on lactase activities to determine its kinetic model. *Archives of Razi Institute*, 50, 93-98.
- MAKSIMAINEN, M., PAAVILAINEN, S., HAKULINEN, N. & ROUVINEN, J. 2012. Structural analysis, enzymatic characterization, and catalytic mechanisms of β -galactosidase from *Bacillus circulans* sp. *alkalophilus*. *The FEBS Journal*, 279, 1788-1798.
- MARTÍN, M. M. 2016. *Industrial chemical process analysis and design*, Elsevier.
- MARTÍNEZ-VILLALUENGA, C., CARDELLE-COBAS, A., CORZO, N., OLANO, A. & VILLAMIEL, M. 2008. Optimization of conditions for galactooligosaccharide synthesis during lactose hydrolysis by β -galactosidase from *Kluyveromyces lactis* (Lactozym 3000 L HP G). *Food Chemistry*, 107, 258-264.
- MARWAHA, S. & KENNEDY, J. 1988. Whey—pollution problem and potential utilization. *International Journal of Food Science and Technology*, 23, 323-336.
- MATELLA, N., DOLAN, K. & LEE, Y. 2006. Comparison of galactooligosaccharide production in free-enzyme ultrafiltration and in immobilized-enzyme systems. *Journal of Food Science*, 71, C363-C368.
- MATEO, C., MONTI, R., PESSELA, B. C., FUENTES, M., TORRES, R., MANUEL GUISÁN, J. & FERNÁNDEZ-LAFUENTE, R. 2004. Immobilization of lactase from *Kluyveromyces lactis* greatly reduces the inhibition promoted by glucose. Full hydrolysis of lactose in milk. *Biotechnology Progress*, 20, 1259-1262.
- MATLAB R2015a. MATLAB. R2015a ed. Natick, MA: MathWorks.
- MEI, Z., YUAN, J. & LI, D. 2022. Biological activity of galacto-oligosaccharides: A review. *Frontiers in Microbiology*, 13.
- MITMESSER, S. & COMBS, M. 2017. Chapter 23-Prebiotics: inulin and other oligosaccharides A2. *The Microbiota in Gastrointestinal Pathophysiology*.
- MOZAFFAR, Z., NAKANISHI, K. & MATSUNO, R. 1985. Formation of oligosaccharides during hydrolysis of lactose in milk using β -galactosidase from *Bacillus circulans*. *Journal of Food Science*, 50, 1602-1606.
- MOZAFFAR, Z., NAKANISHI, K., MATSUNO, R. & KAMIKUBO, T. 1984. Purification and properties of β -galactosidases from *Bacillus circulans*. *Agricultural and Biological Chemistry*, 48, 3053-3061.
- NAKAKUKI, T. 2002. Present status and future of functional oligosaccharide development in Japan. *Pure and Applied Chemistry*, 74, 1245-1251.

- NATH, A., BHATTACHARJEE, C. & CHOWDHURY, R. 2013. Synthesis and separation of galacto-oligosaccharides using membrane bioreactor. *Desalination*, 316, 31-41.
- NATH, A., HAKTANIRLAR, G., VARGA, Á., MOLNÁR, M. A., ALBERT, K., GALAMBOS, I., KORIS, A. & VATAI, G. 2018a. Biological activities of lactose-derived prebiotics and symbiotic with probiotics on gastrointestinal system. *Medicina*, 54, 18.
- NATH, A., MOLNÁR, M. A., CSIGHY, A., KŐSZEGI, K., GALAMBOS, I., HUSZÁR, K. P., KORIS, A. & VATAI, G. 2018b. Biological activities of lactose-based prebiotics and symbiosis with probiotics on controlling osteoporosis, blood-lipid and glucose levels. *Medicina*, 54, 98.
- NATH, A., VERASZTÓ, B., BASAK, S., KORIS, A., KOVÁCS, Z. & VATAI, G. 2016. Synthesis of lactose-derived nutraceuticals from dairy waste whey—A review. *Food and Bioprocess Technology*, 9, 16-48.
- NERI, D. F., BALCÃO, V. M., COSTA, R. S., ROCHA, I. C., FERREIRA, E. M., TORRES, D. P., RODRIGUES, L. R., CARVALHO JR, L. B. & TEIXEIRA, J. A. 2009. Galacto-oligosaccharides production during lactose hydrolysis by free *Aspergillus oryzae* β -galactosidase and immobilized on magnetic polysiloxane-polyvinyl alcohol. *Food Chemistry*, 115, 92-99.
- ONISZCZUK, A., ONISZCZUK, T., GANCARZ, M. & SZYMAŃSKA, J. 2021. Role of gut microbiota, probiotics and prebiotics in the cardiovascular diseases. *Molecules*, 26, 1172.
- OSMAN, A., TZORTZIS, G., RASTALL, R. A. & CHARALAMPOPOULOS, D. 2010. A comprehensive investigation of the synthesis of prebiotic galactooligosaccharides by whole cells of *Bifidobacterium bifidum* NCIMB 41171. *Journal of Biotechnology*, 150, 140-148.
- OTIENO, D. O. 2010. Synthesis of β -galactooligosaccharides from lactose using microbial β -galactosidases. *Comprehensive Reviews in Food Science and Food Safety*, 9, 471-482.
- P. CZERMAK, D. NEHRING & EBRAHIMI., M. 2005. *Method for the continuous production of galactosyl oligosaccharides*.
- PALAI, T., MITRA, S. & BHATTACHARYA, P. K. 2012. Kinetics and design relation for enzymatic conversion of lactose into galacto-oligosaccharides using commercial grade β -galactosidase. *Journal of Bioscience and Bioengineering*, 114, 418-423.
- PAPAYANNAKOS, N., MARKAS, G. & KEKOS, D. 1993. Studies on modelling and simulation of lactose hydrolysis by free and immobilized β -galactosidase from *Aspergillus niger*. *The Chemical Engineering Journal*, 52, B1-B12.
- PARK, A.-R. & OH, D.-K. 2010. Galacto-oligosaccharide production using microbial β -galactosidase: current state and perspectives. *Applied Microbiology and Biotechnology*, 85, 1279-1286.
- PATEL, S. & GOYAL, A. 2011. Functional oligosaccharides: production, properties and applications. *World Journal of Microbiology and Biotechnology*, 27, 1119-1128.
- PATERSON, A. H. 2022. Production and uses of lactose. *Advanced dairy chemistry*. Springer.
- PAULEN, R., FOLEY, G., FIKAR, M., KOVÁCS, Z. & CZERMAK, P. 2011. Minimizing the process time

- for ultrafiltration/diafiltration under gel polarization conditions. *Journal of Membrane Science*, 380, 148-154.
- PÁZMÁNDI, M., KOVÁCS, Z., BALGA, E., KOVÁCS, M. & MARÁZ, A. 2020. Production of high-purity galacto-oligosaccharides by depleting glucose and lactose from galacto-oligosaccharide syrup with yeasts. *Yeast*, 37, 515-530.
- PÁZMÁNDI, M., MARÁZ, A., LADÁNYI, M. & KOVÁCS, Z. 2018. The impact of membrane pretreatment on the enzymatic production of whey-derived galacto-oligosaccharides. *Journal of Food Process Engineering*, 41, e12649.
- PETZELBAUER, I., SPLECHTNA, B. & NIDETZKY, B. 2002. Development of an ultrahigh-temperature process for the enzymatic hydrolysis of lactose. III. Utilization of two thermostable β -glycosidases in a continuous ultrafiltration membrane reactor and galacto-oligosaccharide formation under steady-state conditions. *Biotechnology and Bioengineering*, 77, 394-404.
- PETZELBAUER, I., ZELENY, R., REITER, A., KULBE, K. D. & NIDETZKY, B. 2000. Development of an ultra-high-temperature process for the enzymatic hydrolysis of lactose: II. Oligosaccharide formation by two thermostable β -glycosidases. *Biotechnology and Bioengineering*, 69, 140-149.
- PIRES, A. F., MARNOTES, N. G., RUBIO, O. D., GARCIA, A. C. & PEREIRA, C. D. 2021. Dairy by-products: A review on the valorization of whey and second cheese whey. *Foods*, 10, 1067.
- PLOU, F. J., SEGURA, A. G. D. & BALLESTEROS, A. 2007. Application of glycosidases and transglycosidases in the synthesis of oligosaccharides. *Industrial enzymes: structure, function and applications*. Springer.
- POCEDIČOVÁ, K., ČURDA, L., MIŠÚN, D., DRYÁKOVÁ, A. & DIBLÍKOVÁ, L. 2010. Preparation of galacto-oligosaccharides using membrane reactor. *Journal of Food Engineering*, 99, 479-484.
- QIANG, X., YONGLIE, C. & QIANBING, W. 2009. Health benefit application of functional oligosaccharides. *Carbohydrate Polymers*, 77, 435-441.
- RAMANA RAO, M. & DUTTA, S. 1978. Lactase activity of microorganisms. *Folia Microbiologica*, 23, 210-215.
- REN, H., FEI, J., SHI, X., ZHAO, T., CHENG, H., ZHAO, N., CHEN, Y. & YING, H. 2015. Continuous ultrafiltration membrane reactor coupled with nanofiltration for the enzymatic synthesis and purification of galactosyl-oligosaccharides. *Separation and Purification Technology*, 144, 70-79.
- RESEARCH, P. 2022. *Prebiotic Ingredients Market- Global Industry Analysis, Size, Share, Growth, Trends, Regional Outlook, and Forecast 2022 – 2030* [Online]. PRECEDENCE RESEARCH. Available: <https://www.precedenceresearch.com/prebiotic-ingredients-market> [Accessed].
- RICO-RODRÍGUEZ, F., NORIEGA, M., LANCHEROS, R. & SERRATO-BERMÚDEZ, J. 2021. Kinetics of galactooligosaccharide (GOS) production with two β -galactosidases combined: Mathematical model and raw material effects. *International Dairy Journal*, 118, 105015.
- ROCHA, J. M. & GUERRA, A. 2020. On the valorization of lactose and its derivatives from cheese whey

- as a dairy industry by-product: an overview. *European Food Research and Technology*, 246, 2161-2174.
- ROSENBERG, Z. M.-M. 2006. Current trends of β -galactosidase application in food technology. *Journal of Food and Nutrition Research*, 45, 47-54.
- ROY, I. & GUPTA, M. N. 2003. Lactose hydrolysis by Lactozym™ immobilized on cellulose beads in batch and fluidized bed modes. *Process Biochemistry*, 39, 325-332.
- SADANA, A. & HENLEY, J. P. 1987. Single-step unimolecular non-first-order enzyme deactivation kinetics. *Biotechnology and Bioengineering*, 30, 717-723.
- SANGWAN, V., TOMAR, S., SINGH, R., SINGH, A. & ALI, B. J. J. O. F. S. 2011. Galactooligosaccharides: novel components of designer foods. 76, R103-R111.
- SAQIB, S., AKRAM, A., HALIM, S. A. & TASSADUQ, R. 2017. Sources of β -galactosidase and its applications in food industry. *3 Biotech*, 7, 1-7.
- SCHLEY, P. & FIELD, C. 2002. The immune-enhancing effects of dietary fibres and prebiotics. *British Journal of Nutrition*, 87, S221-S230.
- SCHMIDT, M. & STOUGAARD, P. 2010. Identification, cloning and expression of a cold-active β -galactosidase from a novel Arctic bacterium, *Alkalilactibacillus ikkense*. *Environmental technology*, 31, 1107-1114.
- SCHULTZ, G., ALEXANDER, R., LIMA, F. V., GIORDANO, R. C. & RIBEIRO, M. P. 2021. Kinetic modeling of the enzymatic synthesis of galacto-oligosaccharides: describing galactobiose formation. *Food and Bioproducts Processing*, 127, 1-13.
- SCOTT, F., VERA, C. & CONEJEROS, R. 2016. Technical and economic analysis of industrial production of lactose-derived prebiotics with focus on galacto-oligosaccharides. *Lactose-derived prebiotics: A process perspective*. Elsevier Inc.
- SEN, P., NATH, A., BHATTACHARJEE, C., CHOWDHURY, R. & BHATTACHARYA, P. 2014. Process engineering studies of free and micro-encapsulated β -galactosidase in batch and packed bed bioreactors for production of galactooligosaccharides. *Biochemical Engineering Journal*, 90, 59-72.
- SMITH, D. L. & GROSS, K. C. 2000. A family of at least seven β -galactosidase genes is expressed during tomato fruit development. *Plant Physiology*, 123, 1173-1184.
- SONG, J., ABE, K., IMANAKA, H., IMAMURA, K., MINODA, M., YAMAGUCHI, S. & NAKANISHI, K. 2011. Causes of the production of multiple forms of β -galactosidase by *Bacillus circulans*. *Bioscience, Biotechnology & Biochemistry*, 75, 268-278.
- SU, Z., LUO, J., LI, X. & PINELO, M. 2020. Enzyme membrane reactors for production of oligosaccharides: A review on the interdependence between enzyme reaction and membrane separation. *Separation and Purification Technology*, 243, 116840.

- TORRES, D. P., GONÇALVES, M. D. P. F., TEIXEIRA, J. A. & RODRIGUES, L. R. 2010. Galacto-oligosaccharides: production, properties, applications, and significance as prebiotics. *Comprehensive Reviews in Food Science and Food Safety*, 9, 438-454.
- TORRES, P. & BATISTA-VIERA, F. 2012. Improved biocatalysts based on *Bacillus circulans* β -galactosidase immobilized onto epoxy-activated acrylic supports: Applications in whey processing. *Journal of Molecular Catalysis B: Enzymatic*, 83, 57-64.
- TUOHY, K. M., PROBERT, H. M., SMEJKAL, C. W. & GIBSON, G. R. 2003. Using probiotics and prebiotics to improve gut health. *Drug Discovery Today*, 8, 692-700.
- URRUTIA, P., MATEO, C., GUISÁN, J. M., WILSON, L. & ILLANES, A. 2013a. Immobilization of *Bacillus circulans* β -galactosidase and its application in the synthesis of galacto-oligosaccharides under repeated-batch operation. *Biochemical engineering journal*, 77, 41-48.
- URRUTIA, P., RODRIGUEZ-COLINAS, B., FERNANDEZ-ARROJO, L., BALLESTEROS, A. O., WILSON, L., ILLANES, A. & PLOU, F. J. 2013b. Detailed analysis of galactooligosaccharides synthesis with β -galactosidase from *Aspergillus oryzae*. *Journal of Agricultural and Food Chemistry*, 61, 1081-1087.
- VERA, C., CORDOVA, A., ABURTO, C., GUERRERO, C., SUÁREZ, S. & ILLANES, A. 2016. Synthesis and purification of galacto-oligosaccharides: state of the art. *World Journal of Microbiology and Biotechnology*, 32, 1-20.
- VERA, C., GUERRERO, C., ILLANES, A. & CONEJEROS, R. 2011. A pseudo steady-state model for galacto-oligosaccharides synthesis with β -galactosidase from *Aspergillus oryzae*. *Biotechnology and Bioengineering*, 108, 2270-2279.
- VETERE, A. & PAOLETTI, S. 1998. Separation and characterization of three β -galactosidases from *Bacillus circulans*. *Biochimica et Biophysica Acta -General Subjects*, 1380, 223-231.
- WAN, M. L. Y., FORSYTHE, S. J. & EL-NEZAMI, H. 2019. Probiotics interaction with foodborne pathogens: a potential alternative to antibiotics and future challenges. *Critical Reviews in Food Science Nutrition*, 59, 3320-3333.
- WARMERDAM, A. 2013. *Synthesis of galacto-oligosaccharides with β -galactosidases*, Wageningen University and Research.
- WARMERDAM, A., BOOM, R. M. & JANSSEN, A. E. 2013. β -galactosidase stability at high substrate concentrations. *SpringerPlus*, 2, 1-8.
- WARMERDAM, A., ZISOPOULOS, F. K., BOOM, R. M. & JANSSEN, A. E. 2014. Kinetic characterization of galacto-oligosaccharide (GOS) synthesis by three commercially important β -galactosidases. *Biotechnology Progress*, 30, 38-47.
- WEIJERS, C. A., FRANSSEN, M. C. & VISSER, G. M. 2008. Glycosyltransferase-catalyzed synthesis of bioactive oligosaccharides. *Biotechnology Advances*, 26, 436-456.
- WILSON, B. & WHELAN, K. 2017. Prebiotic inulin-type fructans and galacto-oligosaccharides: definition,

specificity, function, and application in gastrointestinal disorders. *Journal of Gastroenterology and Hepatology*, 32, 64-68.

YAN, Y., GUAN, W., LI, X., GAO, K., XU, X., LIU, B., ZHANG, W. & ZHANG, Y. 2021. β -galactosidase GALA from *Bacillus circulans* with high transgalactosylation activity. *Bioengineered*, 12, 8908-8919.

YAZDANSHENAS, M., TABATABAEENEZHAD, A., ROOSTAAZAD, R. & KHOSHFETRAT, A. 2005. Full scale analysis of apple juice ultrafiltration and optimization of diafiltration. *Separation and Purification Technology*, 47, 52-57.

YU, L. & O'SULLIVAN, D. 2014. Production of galactooligosaccharides using a hyperthermophilic β -galactosidase in permeabilized whole cells of *Lactococcus lactis*. *Journal of Dairy Science*, 97, 694-703.

A2. Additional information

Table 10. Summary of investigations on enzyme membrane reactors for production of galacto-oligosaccharides by utilizing free enzymes.

Enzyme/source	Reactor volume /Total run	Membrane/Module/ Cut-off/Area	Recirculation pump /Crossflow velocity	Transmembrane pressure (TMP) /Temperature	pH/Buffer	Enzyme concentration	Residence time	Residence time control	Lactose feed	Max. GOS yield	Lactose conversion	Half-life	Ref.
Maxilact L 2000 (Gist-Brocades, Holland) / <i>Kluyveromyces lactis</i>	0.3 L, 11 L /4 h	polysulfone/ hollow-fiber/ 10 kDa/ 41.8 cm ² , 0.5 m ²	n.r. ^{a)} /0.072 L·h ⁻¹ , 2.75 L·h ⁻¹	1.5 bar /45 °C	pH 7 /NaOH	0.5% v·v ⁻¹	4 h	Regulating TMP	~200 g/L (whey permeate)	31% w/w	87%	n.r. ^{a)}	(Foda and Lopez-Leiva, 2000)
Maxilact L2000 (Gist-Brocades, Holland) / <i>Kluyveromyces lactis</i>	<2 L /2.5 h	ceramic/ tubular/ 20 kDa/ 0.1 m ²	n.r. ^{a)} /n.r. ^{a)}	1.2-2.4 bar /40 °C	pH 6.7-7.5 /phosphate buffer	n.r. ^{a)}	1 h	n.r. ^{a)}	310 g·L ⁻¹	40% w·w ⁻¹	n.r. ^{a)}	n.r. ^{a)}	(Czermak et al., 2004, P. Czermak et al., 2005, Gonzalez et al., 2009)
Maxilact L2000 (Gist-Brocades, Holland) / <i>Kluyveromyces lactis</i>	0.1 L /3 h	ceramic/ tubular/ 20 kDa/ M1:13.5*10 ⁻³ m ² , M2: 20.1*10 ⁻³ m ²	peristaltic pump /n.r. ^{a)}	2 bar /40 °C	pH 6.7 /phosphate buffer	2.5% w·w ⁻¹	24 min	n.r. ^{a)}	30% w·w ⁻¹	38% w·w ⁻¹	n.r. ^{a)}	n.r. ^{a)}	(Ebrahimi et al., 2010)
Maxilact L200 (DSM, U.K.) / <i>Kluyveromyces lactis</i>	0.2 L /4 h	cellulose acetate/ n.r. ^{a)} / 10 kDa/ 50 cm ²	diaphragm pump /n.r. ^{a)}	2.75 bar /40 °C	pH 7 /phosphate buffer	8 U·mL ^{-1 d)}	52 min	n.r. ^{a)}	250 g·L ⁻¹	19% w·w ⁻¹	69%	no loss of activity.	(Chockchaisa wasdee et al., 2005)
Lactozym Pure 6500L (Novozymes, Denmark) / <i>Kluyveromyces lactis</i>	0.8L /4 h	composite regenerated cellulose/ tubular/ 50 kDa/ 0.12 m ²	diaphragm pump /n.r. ^{a)}	0.75-2.75 bar /25 °C	pH 6.5 /phosphate buffer	1 U·mL ^{-1 b)}	66 min	n.r. ^{a)}	300 g·L ⁻¹	34% w·w ⁻¹	75%	no loss of activity	(Ren et al., 2015)
Maxilact LX5000 (Gist-Brocades, Holland) / <i>Kluyveromyces lactis</i>	2 L, 11 L /2.5 h	ceramic/ tubular/ 20 kDa/ 0.1 m ²	n.r. ^{a)} /5 m/s	0.5 bar /40 °C	pH 7.5 /phosphate buffer	n.r. ^{a)}	0.5 h	Regulating TMP	20% w·w ⁻¹	24% w·w ⁻¹	n.r. ^{a)}	some loss of enzyme through the membrane	(Czermak et al., 2004)
Maxilact LX 5000 (DSM, The Netherlands) / <i>Kluyveromyces lactis</i>	1.5 kg /1.3 h	ceramic/tubular/ 150 kDa/ n.r. ^{a)}	n.r. ^{a)} /11.8 g·min ⁻¹	n.r. ^{a)} /37 °C	pH 6.75 /phosphate buffer	6 U·mL ^{-1 c)}	127 min	n.r. ^{a)}	200 g·L ⁻¹ (recombined whey)	21 g·L ⁻¹ (11% w·w ⁻¹)	50%	n.r. ^{a)}	(Pocedičová et al., 2010)

β -galactosidase (Sigma, St. Louis, Mo., U.S.A.) <i>Aspergillus oryzae</i>	4 L / 1.5 h	polyethersulfone/ 2 tubular / 4 kDa/ 0.024 m ²	n.r. ^{a)} /18.9 L·min ⁻¹	7 bar /40 °C	pH 4.5 /0.1 M acetate buffer	4.5 g·L ⁻¹	n.r. ^{a)}	n.r. ^{a)}	270 g·L ⁻¹	22% w·w ⁻¹	45%	n.r. ^{a)}	(Matella et al., 2006)
Enzeco (Enzyme Development Corporation, USA) <i>Aspergillus oryzae</i>	2.5L /12.5 h	ceramic/ tubular/ 50 kDa / 0.0047 m ²	positive displacement pump /7.35 m ³ ·s ⁻¹	4.38 bar /53.1 °C	pH 4.5 /30 mM citrate	50 IU·g ⁻¹ ^{e)}	6.3 h	n.r. ^{a)}	400 g·L ⁻¹	30% w·w ⁻¹	50%	231 h	(Córdova et al., 2016c)
Biolacta FN5 (Daiwa Kasei, Japan) <i>Bacillus circulans</i>	n.r. ^{a)} /5 h	polyethersulphone / crossflow/ 10 kDa/ 0.02 m ²	peristaltic pump / 2 × 10 ⁻⁸ m ³ ·s ⁻¹	1.5 bar /24 °C	pH 6.6 /potassium phosphate buffer	0.5 % w·v ⁻¹	n.r. ^{a)}	n.r. ^{a)}	50 g/L (UF whey permeate origin)	64% w·w ⁻¹	72%	12 h	(Das et al., 2011)
Biolacta N5 (Amano Enzyme Inc., Japan) <i>Bacillus circulans</i>	2 L, 4 L /120 h	polyethersulfone/ spiral-wound/ 50 kDa/ 0.37 m ²	diaphragm pump / 0.18 m ³ ·h ⁻¹	1.0 bar /50 °C	pH 6.0 /DI water	46150 U·kg ⁻¹ ^{f)}	1.8 h	Self-adjusted by pump	300 g·L ⁻¹	33% w·w ⁻¹	42%	Negligible enzyme activity losses (120h)	(Cao et al., 2020)
<i>Sulfolobus solfataricus</i> (SsβGly) & <i>Pyrococcus furiosus</i> (CelB)	0.11L /200 h	polyethersulfone/ spiral-wound/ 10 kDa/ 0.05 m ²	peristaltic /25 mL·min ⁻¹	n.r. ^{a)} /70 °C	pH 5.5 /sodium citrate buffer	CelB: 1.2 U·L ⁻¹ , SsβGly: 0.4 U·L ⁻¹ ^{g)}	10 h average	n.r. ^{a)}	170 g·L ⁻¹ (500 mM)	CelB: 98 mM (20% w·w ⁻¹), SsβGly: 90 mM (18% w·w ⁻¹)	~80%	5-7 days	(Petzelbauer et al., 2002)

a) n.r. : not reported.

b) One NLU is defined as that quantity of enzyme which will liberate 1.0 μmol O-nitrophenol per min under the conditions of 40°C, pH 7.

c) One unit of enzyme activity was defined as the amount of enzyme necessary to release 1 μmol o-nitrophenol/min at 30°C, pH 6.75.

d) One enzyme unit (U) is defined as 1 μmol of glucose released per mL per minute at 40°C, pH 7.

e) One international unit of activity (IU) was defined as the amount of enzyme hydrolyzing 1 μmol of o-NPG per minute at pH 4.5, 40°C and 45 mM.

f) 1LU is defined as amount of enzyme, which liberates 1 μmol of glucose per minute from lactose under the conditions of 30% w·w⁻¹ lactose, 50°C, pH 6.0.

g) One unit of enzyme activity (U) was defined as the amount of crude enzyme that converts 1 μmol of DP2 per minute under 80°C, pH 5.5.

Table 11. Summarized enzyme deactivation model.

Enzyme/ microorganism	Reactor configuration	Reaction conditions			Half-life (h)	Activity Measurement method	Deactivation Model	Ref.
		Lactose conc.	pH	Temp. (°C)				
β -galactosidase / <i>Aspergillus oryzae</i>	Batch (FE)	0 g·L ⁻¹	4.5	40	399	DM	Eq. 10.9.2-6	(Albayrak and Yang, 2002)
				50	49			
				60	2			
	Continuous (IE)	200 g·L ⁻¹	4.5	40	10040			
				50	1155			
				60	49			
β -galactosidase / <i>Aspergillus oryzae</i>	Batch (FE)	0.1 g·L ⁻¹	4.5	50	42	oNPG	Eq. 10.9.2-2	(Huerta et al., 2011)
				55	7.4			
				60	0.8			
	Batch (IE)	2% w·v ⁻¹	4.5	50	163–166			
				55	9.3–20.5			
				60	0.9–1.9			
Biolacta N5 / <i>Bacillus circulans</i>	Batch (FE)	30% w·w ⁻¹	6	25	29	oNPG	Eq. 10.9.2-6	(Warmerdam et al., 2013)
				40	29			
				60	16			
Biolacta N5 / <i>Bacillus circulans</i>	Batch (FE)	4.6% w·w ⁻¹	6	50	12	oNPG	Eq. 10.9.2-5	(Torres and Batista- Viera, 2012)
	Batch (IE)				21–387			
Biolactasa-NTL X2 / <i>Bacillus circulans</i>	CONC Batch (FE)	0 g·L ⁻¹	6	60	~ 0.05	oNPG	Eq. 10.9.2-3	(Urrutia et al., 2013a)
	Batch (IE)				0.25–3			
β -galactosidase / <i>Klebsiella</i> ZJUH1705	oxytoca	40% w·w ⁻¹	7	30	141.67	oNPG	Eq. 10.9.2-6	(Huang et al., 2020)
				40	18.33			
				50	0.04			
				60	0.01			
				30	88.33			
				40	1.17			
				50	0.17			
				60	0.01			

* DM: direct method defining one unit of enzyme activity as the amount of enzyme producing 1 μ mol of glucose from lactose under defined conditions;
FE: free enzyme; IE: immobilized enzyme.

11. ACKNOWLEDGEMENT

My deepest and sincerest gratitude goes to my supervisor, Prof. Zoltán Kovács, for his consistently supportive and helpful guidance throughout my Ph.D. studies. It is a great honor and privilege that I was given the opportunity to work under his supervision. I would like to express my gratitude and appreciation for his patience, help, empathy, and academic reputation. He provided me with excellent opportunities and advice for writing research papers and provided many resources for me to participate in international conferences and academic communications. I greatly appreciate the time he spent reviewing my papers and providing me with constructive feedback in order to help me improve my work. I consider myself one of the luckiest people who benefited from Professor Zoltán Kovács's knowledge and character.

Furthermore, I would like to express my heartfelt gratitude and extend a sincere thank you to Dr. Arijit Nath, my co-supervisor, for his invaluable support and guidance throughout the thesis revision, review paper revision, and defense processes. Dr. Nath's expertise, dedication, and meticulous attention to detail have been instrumental in shaping the final outcome of my research. His insightful feedback, constructive criticism, and unwavering belief in my abilities have not only enhanced the quality of my work but also bolstered my confidence as a researcher. I am truly grateful for his mentorship, which has undoubtedly played a significant role in my academic and personal growth.

My gratitude to Professor Márta Ladányi for her support and guidance in the analysis and processing of the data. Her professional, patient, and attentive guidance enabled me to grasp the main points and make progress quickly. In addition, I am also thankful to the academics and colleagues in the Faculty of Food Process Engineering at Hungarian University of Agriculture and Life Sciences. I would gratefully acknowledge the support of my dearest friends and research group mates for their encouragement, friendship and support since the beginning of my study. I am extremely grateful to my parents for their motivation, patience, love and care during my education and life journey.

Additionally, I appreciated the support from the Food Science Doctoral School of the Hungarian University of Agriculture and Life Sciences, Chinese government scholarships and the Tempus Public Foundation for the Stipendium Hungaricum Scholarship.

Lastly, I would like to express my gratitude to all those who have directly or indirectly assisted me in the completion of my thesis. With sincere wishes for your well-being, may you experience it all in a pleasant way.